The prospectivity of the Barents Sea: Ice ages, erosion and tilting of traps

Eiliv Larsen[1], Karin Andreassen[2], Lena Charlotte Nilssen[2] and Ståle Raunholm[1]

[1] Geological Survey of Norway, N-7491 Trondheim, Norway
[2] Department of geology, University of Tromsø, Dramsveien 201, N-9037 Tromsø

December 2003

Contract no. Geological Survey of Norway: **5223807**
Contract no. University of Tromsø: **5223117**

Geological Survey of Norway report number: 2003.102

Geological Survey of Norway
N-7441 Trondheim, Norway
Tel.: 47 73 90 40 00
Telefax 47 73 92 16 20

REPORT

Report no.: 2003.102 | ISSN 0800-3416 | Grading: Restricted until December 15, 2005

Title:
The prospectivity of the Barents Sea: Ice ages, erosion and tilting of traps

Authors:
Eiliv Larsen, Karin Andreassen,
Lena C. Nilssen and Ståle Raunholm

Client:
Norsk Hydro AS

County:

Commune:

Map-sheet name (M=1:250.000)

Map-sheet no. and -name (M=1:50.000)

Deposit name and grid-reference:

Number of pages: 60 Price (NOK):
Map enclosures:

Fieldwork carried out:

Date of report:
December 12, 2003

Project no.:
303600

Person responsible:
Bjørn Bergstrøm

Summary:

A three-phase conceptual glacial geological model for the Late Pliocene and entire Pleistocene period has been developed. The model explains variations in erosion in the Barents Sea in space and time and shows:

- The first phase (until ca. 1.5 mill. years) was characterized by glacial erosion over the present land areas of Svalbard and Norway. Minimal, if any, erosion over present shelf areas.
- A transition phase (ca. 1.5 – ca. 0.5 mill. years) with glacial erosion over restricted areas. In the Norwegian sector glacial erosion was active from Svalbard down to the Bear Island Trough. Little, if any, glacial erosion south of the Bear Island Trough.
- The last phase (ca. 0.5 mill. years – present) is characterized by glaciations covering the entire shelf areas. This seems to be the only period when repeated glaciations eroded in the southwestern Barents Sea shelf, i.e. in the areas of petroleum prospecting.

The three-phase glacial erosion model is supported by data on climate change over the period, by modelled change in topography, and by glacial geological data, especially from the Barents Sea. The approach and data also show that there is a great potential to *test and refine the model to make it applicable to erosion estimates.*

Keywords:	Barents Sea	Hydrocarbon potential
Glacial erosion	Glacially induced tilting	Glacial history

Content

Summary

A three-phase conceptual glacial geological model for the Late Pliocene and entire Pleistocene period has been developed. The model explains variations in erosion in the Barents Sea in space and time and shows:

- The first phase (until ca. 1.5 mill. years) was characterized by glacial erosion over the present land areas of Svalbard and Norway. Minimal, if any, erosion over present shelf areas.
- A transition phase (ca. 1.5 – ca. 0.5 mill. years) with glacial erosion over restricted areas. In the Norwegian sector glacial erosion was active from Svalbard down to the Bear Island Trough. Little, if any, glacial erosion south of the Bear Island Trough.
- The last phase (ca. 0.5 mill. years – present) is characterized by glaciations covering the entire shelf areas. This seems to be the only period when repeated glaciations eroded in the southwestern Barents Sea shelf, i.e. in the areas of petroleum prospecting.

The three-phase glacial erosion model is supported by data on climate change over the period, by modelled change in topography, and by glacial geological data, especially from the Barents Sea. The approach and data also show that there is a great potential to *test and refine the model to make it applicable to erosion estimates.*

1. Background and objectives

1.1. About the project and the report

This collaborative project between the Geological Survey of Norway, the University of Tromsø, and Norsk Hydro AS started April 1, 2003. Since then we have:

- Gathered published and unpublished data.
- Interpreted new onshore stratigraphical and offshore 3D seismic data.
- Synthesized/developed new models for glaciations from the Plio-/Pleistocene to the present.

The Last Glaciation (the Weichselian, ca. 115-10 ka) can be reconstructed with fairly high degree of precision. Thus, this period serves as a model for the way the system works under the present type of boundary conditions. This information together with the more sparse information about older glaciations and models for erosion and uplift is used to, for the first time, to put together a model for the style of glaciations for the entire Pliocene – Pleistocene period.

Chapter 1 of the report contains the background and objectives of the project. In Chapter 2 a new glacial geological model explaining variations in erosion in the Barents Sea in space and time is presented. Chapter 3 summarizes present understanding of erosion and uplift in the Barents Sea. A synthesis of our present understanding of glaciations for the entire Barents/Kara Sea region is given in Chapter 4. Chapter 5 gives a more in depth evaluation by areas in the region. The final chapter discusses some further steps that should be taken to refine the models presented in this report.

1.2. Dry wells related to glacial history?

Hydrocarbon traps in the south-western Barents Sea seem to have experienced partial or complete drainage of hydrocarbons. Up to 3000 m of sedimentary overburden have been removed from the Barents Shelf since the opening of the Norwegian-Greenland Sea around 50 mill years ago. This is widely held responsible for the negative results in petroleum exploration. Negative effects include spillage of hydrocarbons, phase transition from oil to gas, expansion of gas, potential for seal failure and cooling of source rocks (Doré & Jensen 1996), cf. Figure 1.1. Further east (Russian sector) this seems to be less of a problem. Two-thirds of the erosion took place during the late Cenozoic, and the Plio-Pleistocene erosion is assumed to be largely of glacial origin (Fjeldskaar 2001). Thus, as Late Tertiary and Quaternary regional uplift and erosion seems to be a common denominator for areas with partial or complete drainage (Nils Tælnes in Murmansk 2002), the question has been raised whether the leaking of hydrocarbons is caused by Quaternary glaciations.

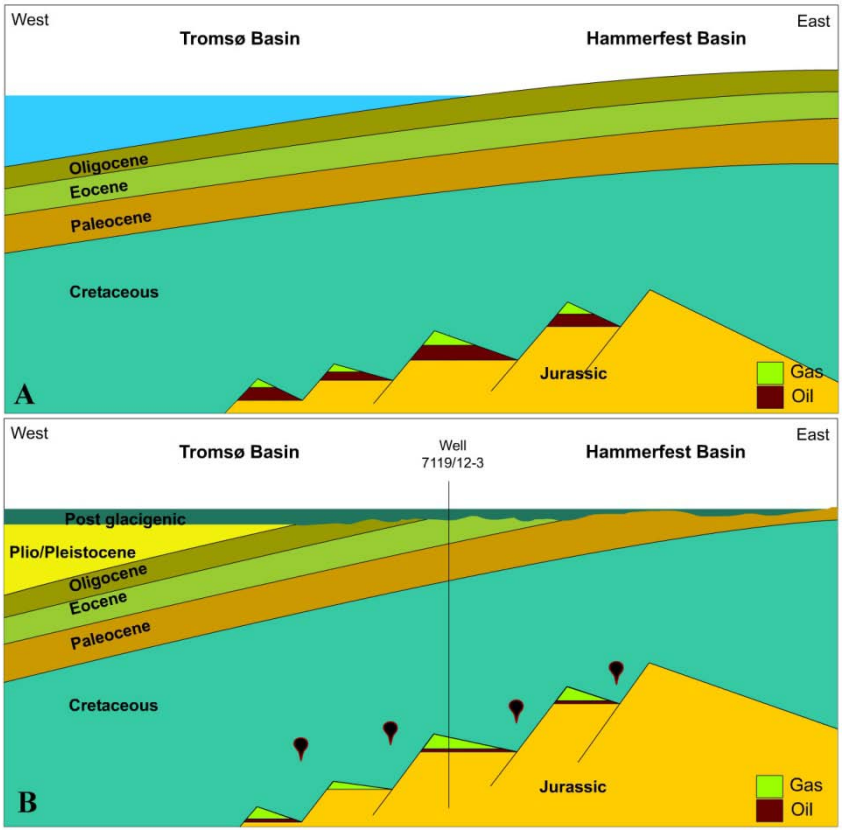

Figure 1.1. Uplift and tilting of the Barents Sea region. **A)** configuration prior to glacial erosion, **B)** Erosion that gives reduced pressure and results in increased gas volumes by gas expansion and by phase transition from oil to gas, breaching of trap seals and to tilting of the hydrocarbon traps as erosion is compensated by oblique uplift.

Main structural elements in the Barents Sea and location of 3D surveys are shown in Figure 1.2. This is an area repeatedly affected by Quaternary glaciations centered over Svalbard and Scandinavia. As the report shows, there are systematic variations in these glaciations throughout the Quaternary.

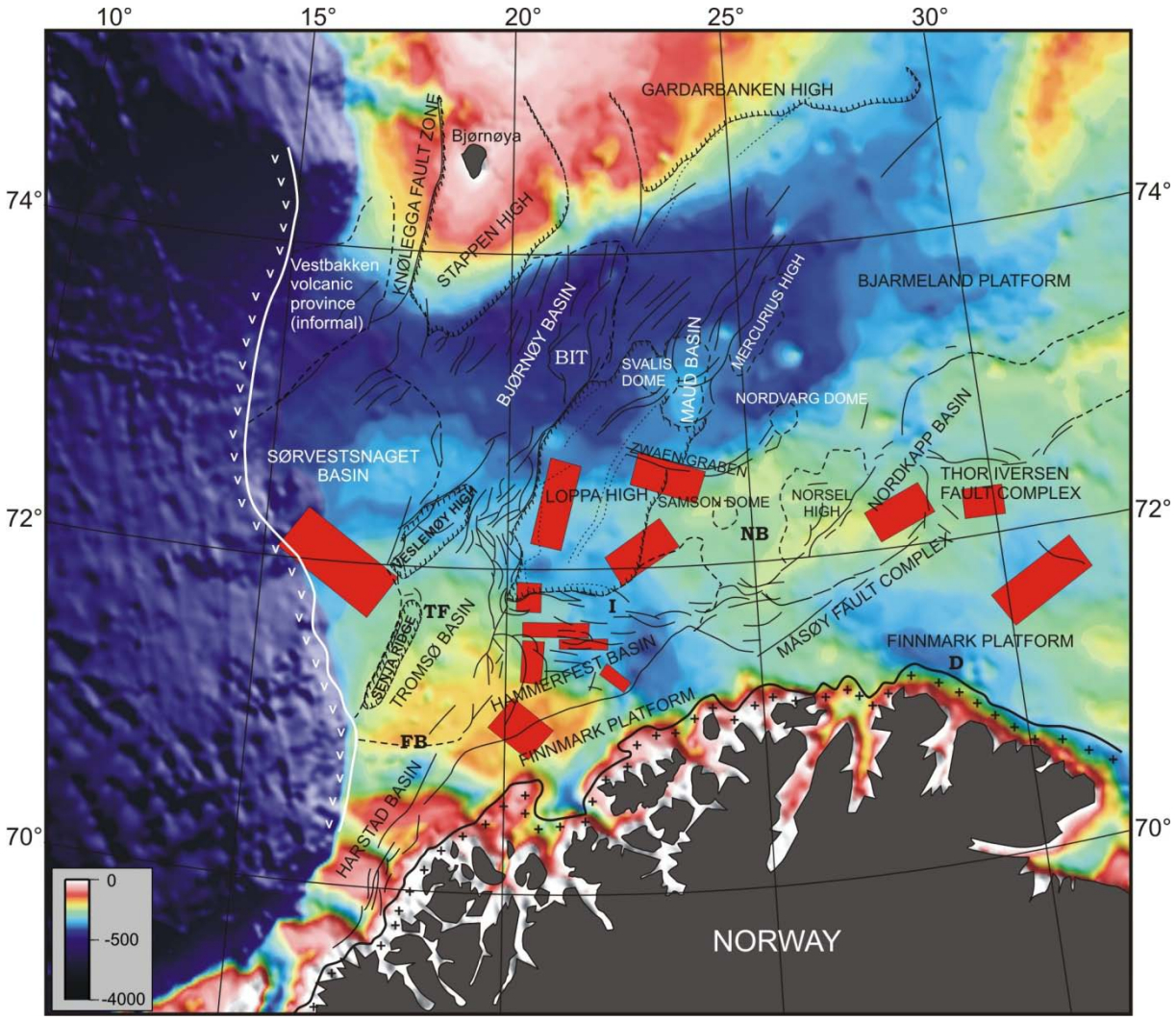

Figure 1.2. Barents Sea; main structural elements (after Gabrielsen *et al.* 1990). Red boxes indicate location of the 3D seismic data used in this project. FB: Fugløybanken; TF: Tromsøflaket; BIT: Bear Island Trough; I: Ingøydjupet; NB: Nordkappbanken and D: Djuprenna.

1.3. Up-to-date overview of glacial history

The primary objective of this project is to present a state of the art glaciation model for the last glaciation. This objective has been met with the synthesis presented in Chapter 4 of the report. The last glaciation only covers a short period of the time relevant to understand Pliocene – Pleistocene erosion and uplift, but is the only period that can be synthesised in some detail. Nevertheless, we have put together a conceptual model also including the older glaciations (Chapter 2). This model gives insights into how Pliocene – Pleistocene glaciations may have changed with time and affected increasingly larger areas towards the present time. This information can provide a background for glacidynamic modelling as well as flexural and isostatic modelling that is suggested as follow-up studies.

The new glaciation models are made possible by combining research that the parties have undertaken in the southwestern Barents Sea and northwestern Russia over the last years with a broad synthesis of available data from the entire region affected by glaciations. The University of Tromsø has during the last few years been using industry 3D-seismic data from the southwestern Barents Sea (Fig. 1.3; red boxes). These data are crucial for understanding older glaciations and provide flow directions of former ice streams. The Geological Survey of Norway has carried out field investigations onshore northwestern Russia (Fig. 1.3: large rectangle). This is critical for constructing models of the last glaciation since this part of

Russia was a confluence area of the Barents Sea, the Kara Sea and the Scandinavian Ice Sheets.

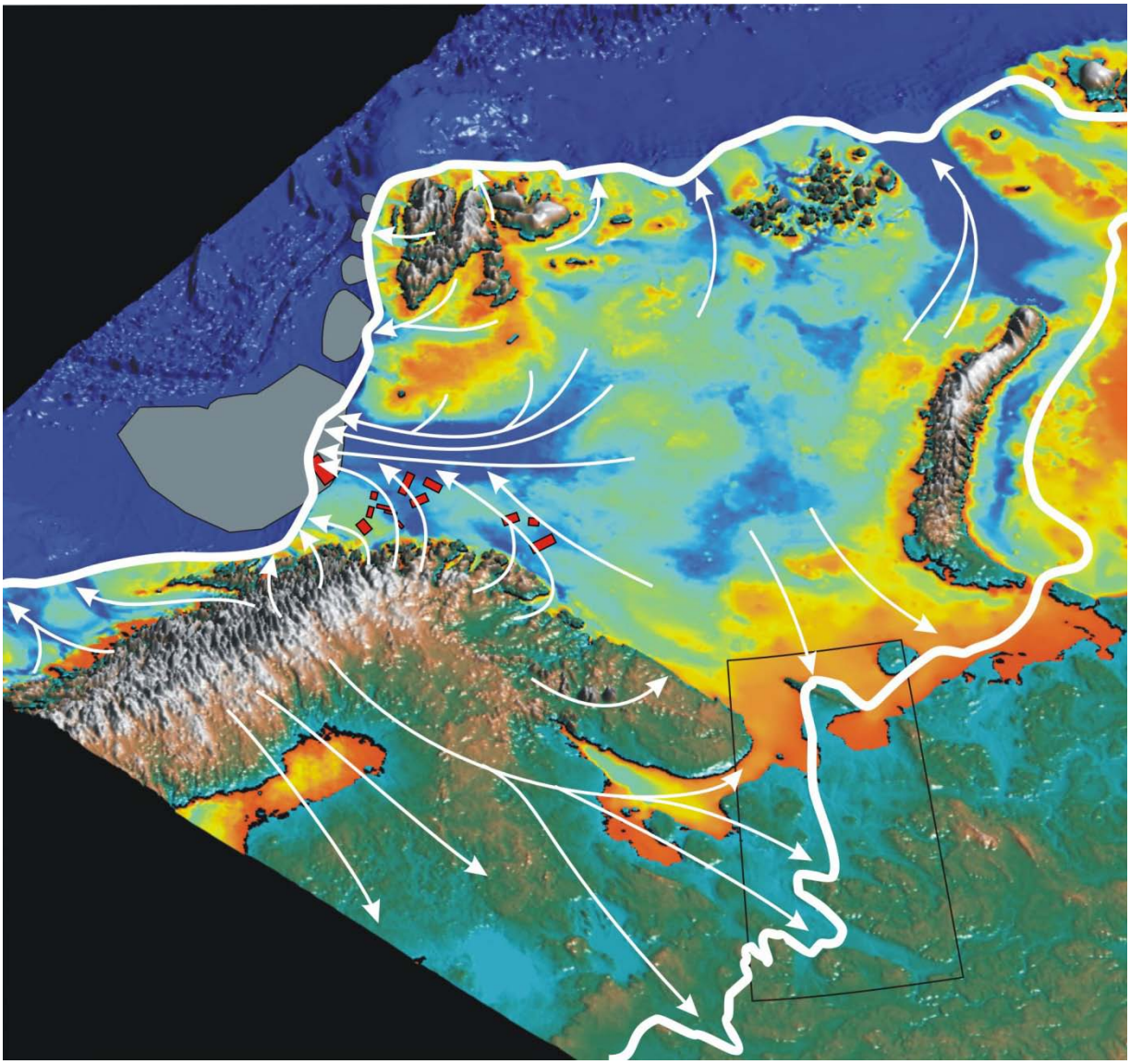

Figure 1.3. 3D seismic datasets in the southern Barents Sea (red boxes) and study area on land in north-western Russia (open rectangle). Ice extent (white line) and large-scale ice-flow directions (arrows) during the Last Glacial Maximum are indicated.

2. Glaciation models (ca. 2.5 mill. years - present) and significance for erosion

Relatively little is known about glaciations older than the Saalian (before ca. 200 ka), especially about their distribution in space and time. Corings in subciding areas in Holland has, however, provided a Quaternary framework for western Europe for the entire Quaternary showing the variations between glacial and non-glacial periods (Fig. 2.1).

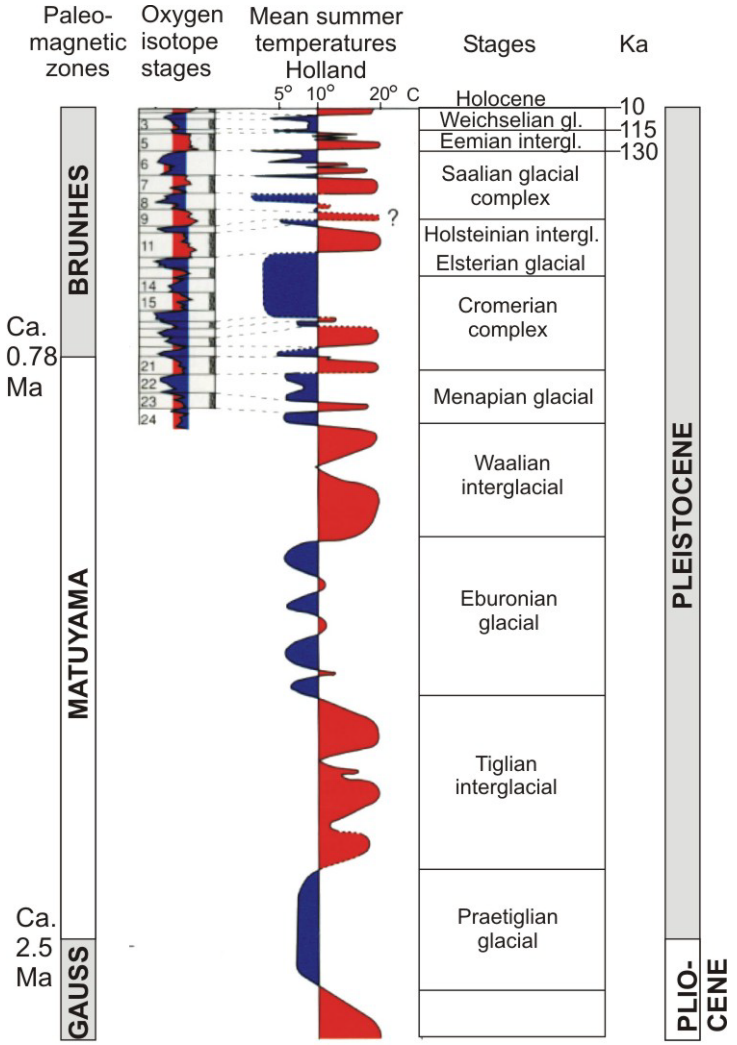

Figure 2.1. Subdivision of the Quaternary showing paleomagnetic zones, oxygen isotopes, temperature estimates from Holland, and glacial and interglacial stages as used in western European stratigraphy. Modified from Andersen & Borns (1997).

In the Barents Sea region a comprehensive stratigraphy and glacial history for the entire Quaternary is still premature. Some interesting accounts can, however, be given with reference to preglacial topography and global ice volume curves (Fig. 2.2). In preglacial time the present Svalbard area and northern Barents shelf was a highland with elevations up to some 1500 meters. Except for the northern part, most of the Barents Sea area was lowland around present sea level. Thus one might infer that glaciations were initiated as mountain glaciations over the Svalbard region. As global temperatures reached lower levels during

Middle Pleistocene time, the glaciations could expand further in the Svalbard region, but larger parts of the Barents Sea area might still have been ice-free. Only in the later part of the Pleistocene (the last ca. 500 ka), one can assume glaciations of magnitudes comparable to the youngest glaciations.

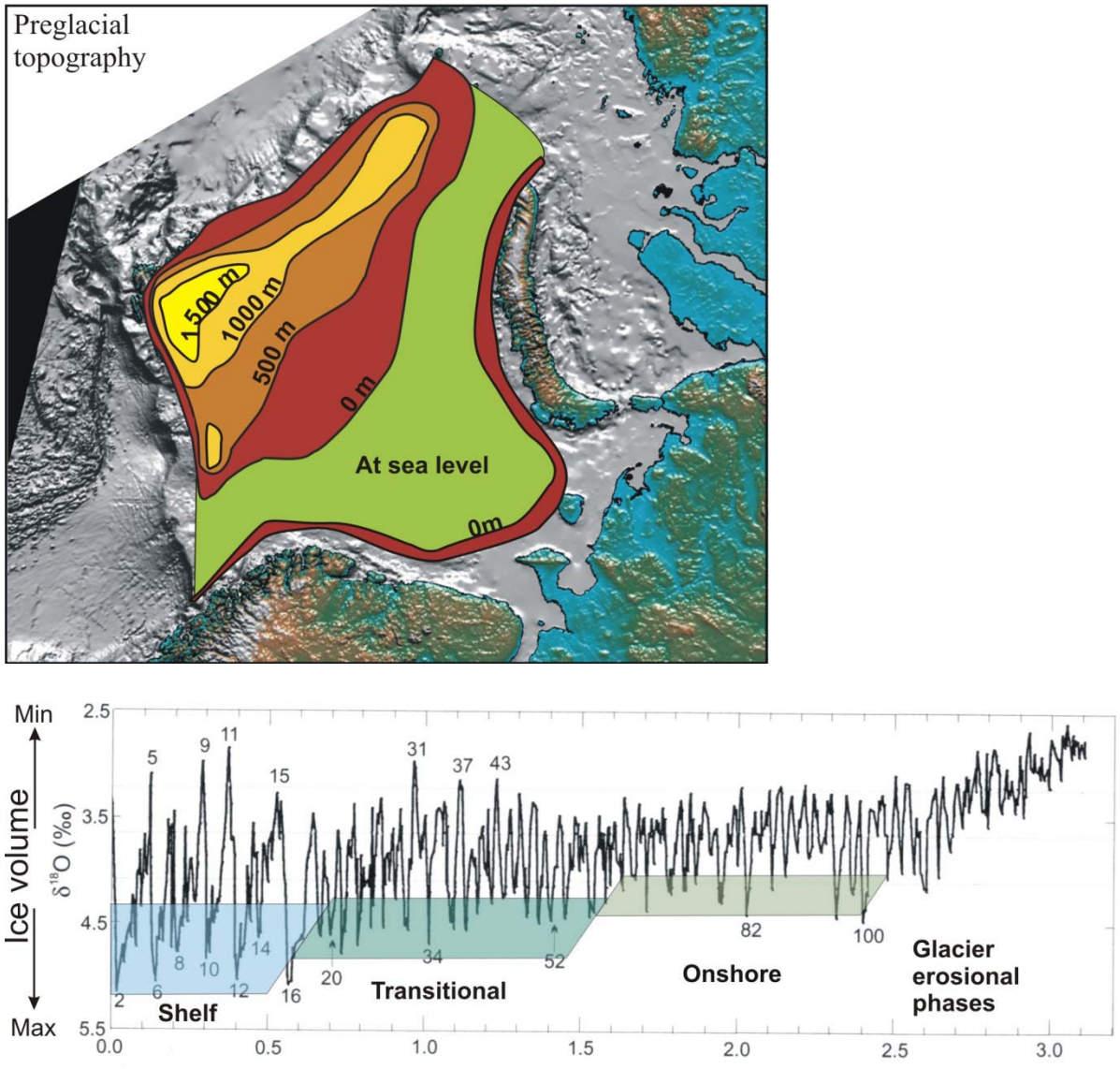

Figure 2.2. Upper part: Reconstructed preglacial relief of the Barents Shelf. Modified from Rasmussen & Fjeldskaar (1996). Lower part: Oxygen isotope curve indicating global ice volume. Modified from Raymo (1992). Three glacier erosional phases in the evolution of the Barents Sea area are indicated: An onshore phase (up to ca. 1.5 Ma), a transitional phase (ca. 1.5-0.5 Ma), and a shelf phase (ca. 0.5 Ma-present). Modified from Butt *et al.* (2002).

By combining data about the youngest glaciations and 2D and 3D seismic data (Fig. 2.3) with the topographic and climate data (Fig. 2.2), it has been possible, for the first time, to construct a model for the style of glaciations for the Late Pliocene to the present. This new model is shown as Figure 2.4. One important aspect of the model is that even in periods with limited ice extent (Fig. 2.4A, B), glaciers reach the shelf break in some areas. The deep water below the western Barents Sea shelf edge is a topographic barrier to further ice growth, and the potential for growth to maximum style glaciation (Fig. 2.4C) is by expansion towards the east and south.

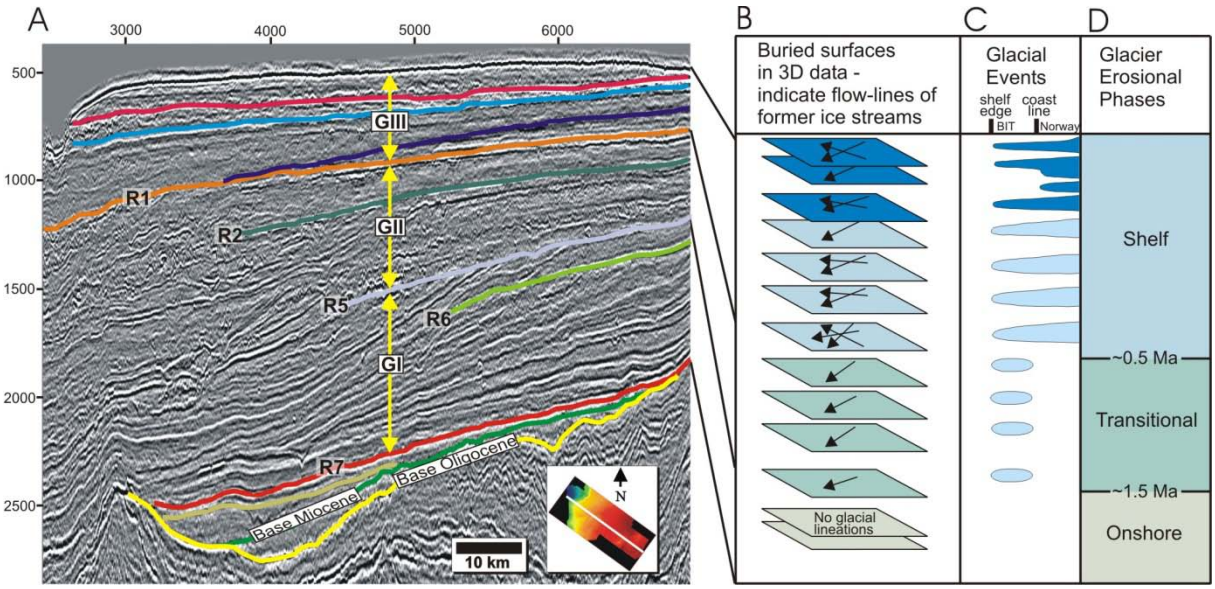

Figure 2.3. Composite diagram showing: **A)** Interpreted seismic profile through the Sørvestsnaget 3D. **B)** Sketch of buried surfaces in the 3D indicating glacial events and flow directions of ice streams. Inferred ice streams in sequence GII drained from northeast to the Bear Island Trough (BIT) shelf edge, probably from a Svalbard/Barents Sea ice sheet. Ice streams in sequence GIII also drained from southeast, from a Scandinavian Ice Sheet. **C)** Suggested glaciation curve for the Western Barents Sea Margin composed from a glacier variation curve after Svendsen *et al.*(in press) and the buried 3D surfaces. BIT denotes Bear Island Trough. **D)** Inferred glacier erosional phases are indicated.

The first glaciations (until 1.5 mill. years ago) were probably limited to onshore Scandinavia, the Svalbard area and other arctic highlands (Fig. 2.4A). It is important to note that even with this limited ice extent, the glaciers might have reached the western/northern shelf edges. Most of the Barents Sea area was ice-free. Between ca. 1.5 and 0.5 mill. years ago, climate had cooled and the glaciers could expand further (Fig. 2.4B). Probably there was no contact between the Scandinavian and the Barents Sea ice sheets, and parts of the southern Barents Sea area were ice-free. The north and west extent of glaciations probably was very similar to the youngest period. In the youngest period (ca. 0.5 mill. years to present) glaciers grew to the maximum Quaternary size (Fig. 2.4D). Compared with the older glaciations, practically all of this expansion took place in the east and south. This is because the deep water at the shelf break is a barrier towards further north- and westwards expansion.

Based on this hypothesis it can be inferred that very limited areas in the Barents Sea were subject to glacial erosion in the oldest of the three periods (Fig. 2.4A). In the intermediate period, larger areas, mainly in the north were subject to glacial erosion (Fig. 2.4B). Only during the youngest period glaciers could erode over an area as illustrated in Figure 2.4C. The main erosion in the southwestern Barents Sea probably took place in this period. Thus south- and eastwards expansion of glaciers was accompanied by a similar expansion of glacial erosion.

Erosion (and deposition) will not be evenly distributed under an ice sheet. Generally speaking, both erosion and deposition will be largest in near ice-marginal areas. Within each of the periods (Fig. 2.4A-C), ice-margins shifted during growth and decay. Thus erosion potential has shifted several times during each glaciation. Nevertheless, the western and northern Barents Sea margins were at or near the ice margin for a very long period of time (Fig. 2.4A-C) suggesting that this area has been more subject to glacial erosion and deposition than any other area.

Change in ice load and resulting glacioisostatic depression will follow a similar pattern over time as glaciation style and erosion. Thus it is suggested that the northern and western areas of Figure 2.4 have been subject to many more glacioisostatic adjustments than the eastern and southern areas.

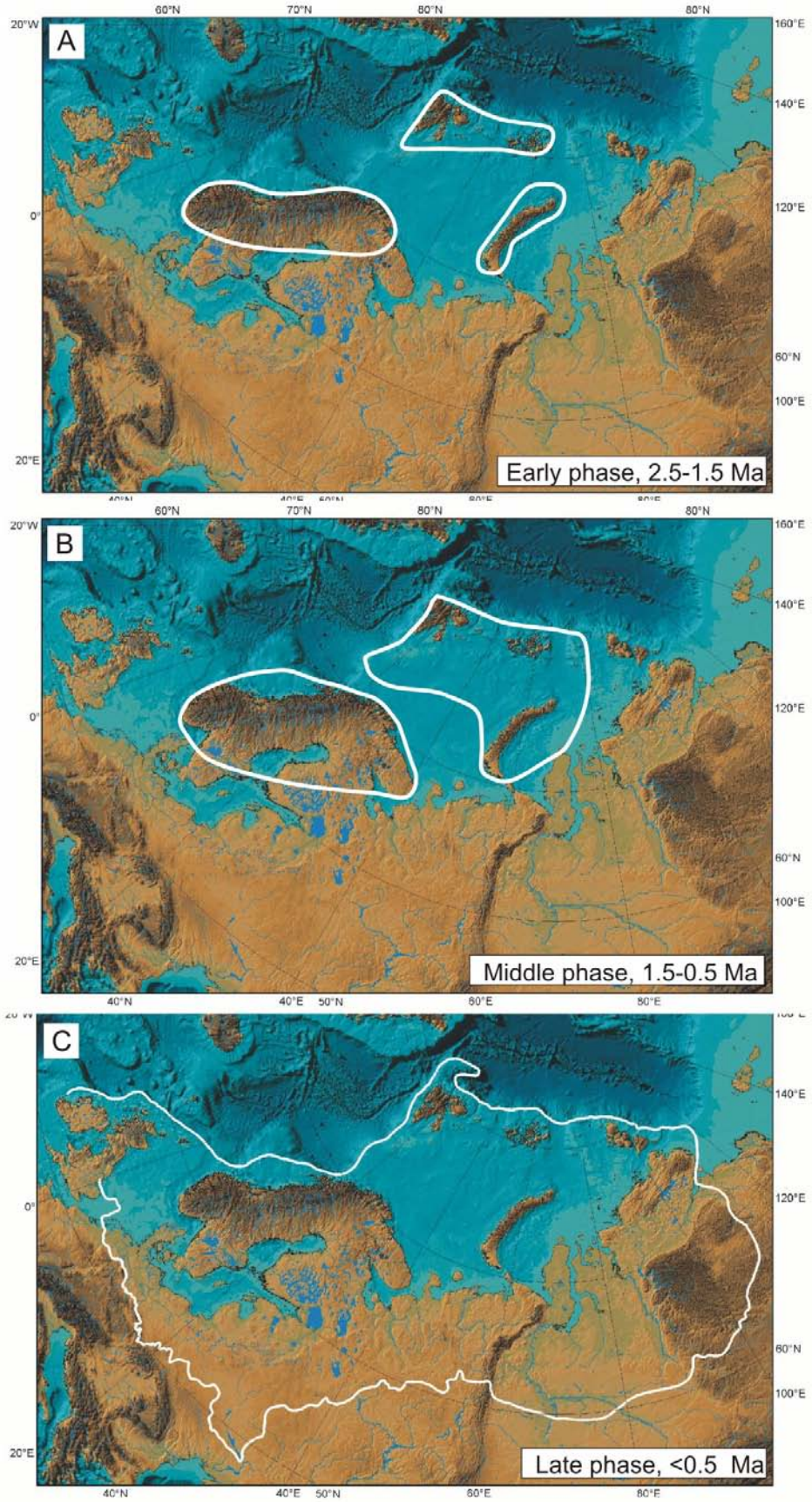

Figure 2.4. Style of maximum type glaciations within three periods of the Plio-Pleistocene. The oldest two are conceptual based on data and reasoning discussed in the text. The youngest style of glaciation is represented by the reconstructed Saalian maximum glaciation (Svendsen *et al.* in press). Within each of the three phases glaciers have varied several times between being almost completely absent to acquiring the respective maximum size.

3. Erosion and uplift of the Barents Sea region

3.1. Present models for Plio-Pleistocene erosion and uplift

Since the opening of the Norwegian-Greenland Sea around 50 Ma ago, the Barents Sea has experienced considerable uplift. Nyland *et al.* (1992) postulated uplift and erosion for the southwestern Barents Sea based on vitrinite reflectance profiles as shown in Fig. 3.1. A main part of this erosion is now assumed to have taken place during the glacial periods. A newer study of the Late Tertiary and Quaternary uplift and erosion performed by Statoil (Fig. 3.2) shows the same trends as those of Fig. 3.1, with the lowest values (<500 m) in southwest, in the Tromsø Basin, and increasing magnitude of uplift and erosion towards the north and northwest (>2000 m) on the Stappen High and Bjørnøya. Other investigations have shown similar values (Doré & Jensen 1996; Hjelstuen *et al.* 1996; Rasmussen & Fjeldskaar 1996; Dimakis *et al.* 1998). Also the eastern parts of the Barents Sea region experienced considerable uplift in Oligocene-Miocene times, which has resulted in up to 3000 m erosion in this area (Musatov & Romashchenko 2003, Fig. 3.3).

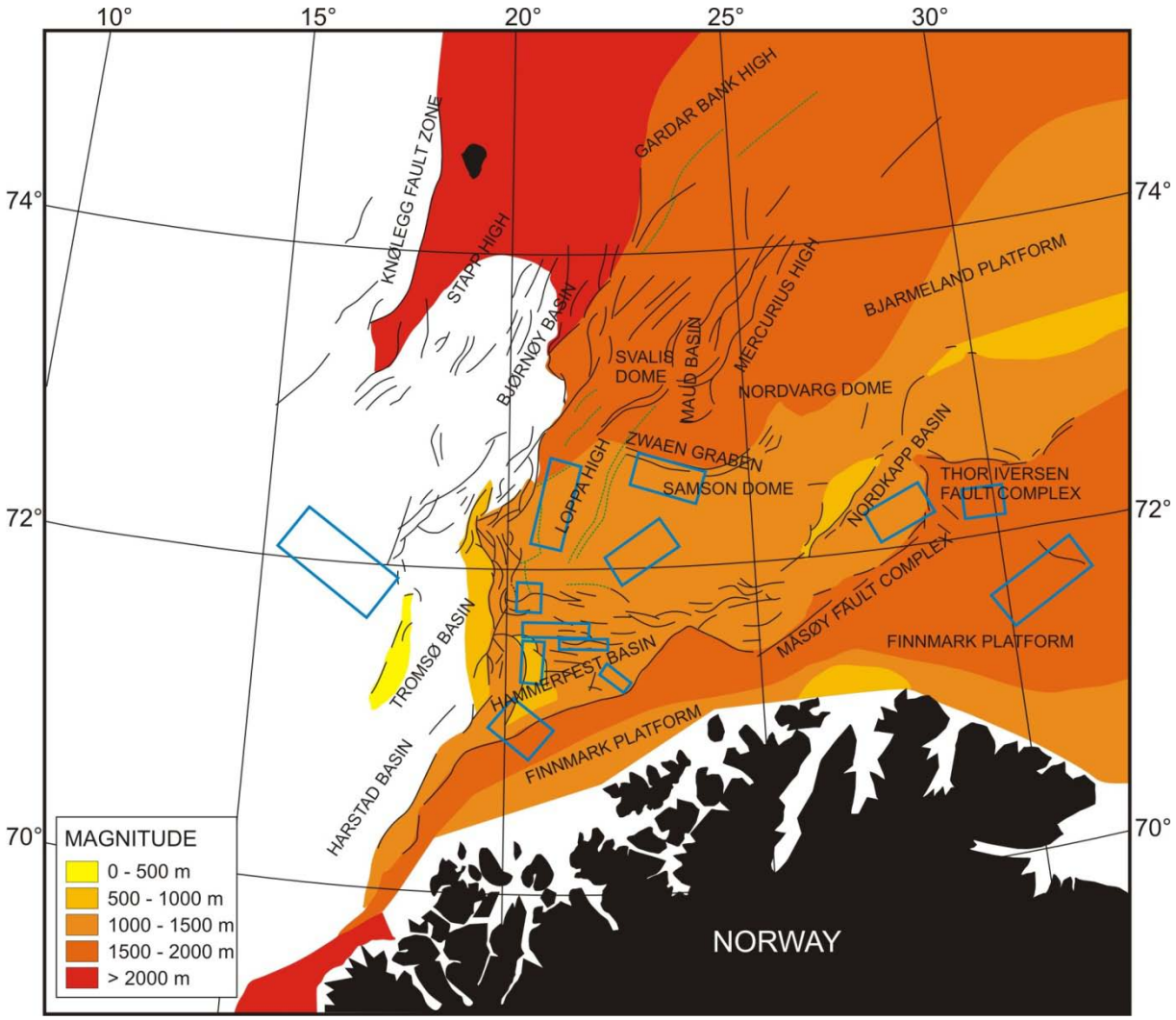

Figure 3.1. Postulated uplift and erosion. Based on vitrinite reflectance profiles. From Nyland *et al.* (1992). The boxes indicate location of 3D seismic surveys that are being studied in this project.

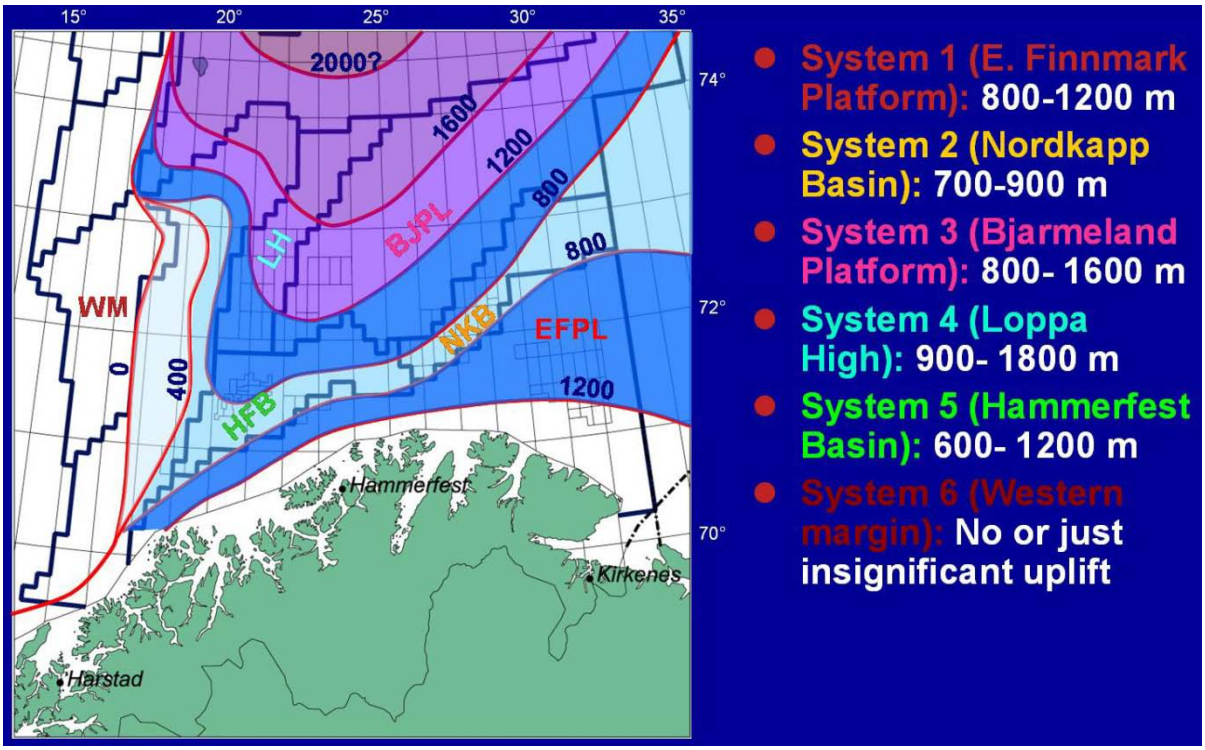

Figure 3.2. Magnitude of Late Tertiary and Quaternary uplift and erosion. From Statoil study 2003 (PL202). Petroleum systems are from Telnæs *et al.*(2002).

The age of the erosion has been subject to considerable discussion, and is an important factor controlling the generation and migration of hydrocarbons. Based on datings from exploration wells and a regional seismic stratigraphic framework (Faleide *et al.* 1996), Rasmussen & Fjeldskaar (1996) divide the Tertiary erosional history of the Barents Shelf into two different episodes:

1) An Early Tertiary phase after continental rifting in the North Atlantic, involving tectonic uplift of the whole north-western Barents Shelf (Fig. 3.4A), with subsequent subaerial erosion and deposition of erosional products along the shelf margins and filling of sedimentary basins on the southern and south-eastern Barents Shelf (Fig. 3.4B). These volumes of sediments are believed to derive from provenance areas on the north-western tectonically uplifted shelf, possibly with minor contribution also from the Fennoscandian and Uralian areas. The Tertiary sediments located on the southern and south-eastern Barents shelf were later removed by glacial erosion. The present day thickness of Paleocene-Miocene sediments on the Barents Shelf is shown in Fig. 3.4C.
2) A second Plio-Pleistocene phase characterised by glacial erosion on the whole shelf area with transport of erosional products to the present day margins (Fig. 3.5B), and with subsequent isostatic uplift of the eroded area. A regional map displaying the estimated glacial erosion is shown in Figure 3.6.

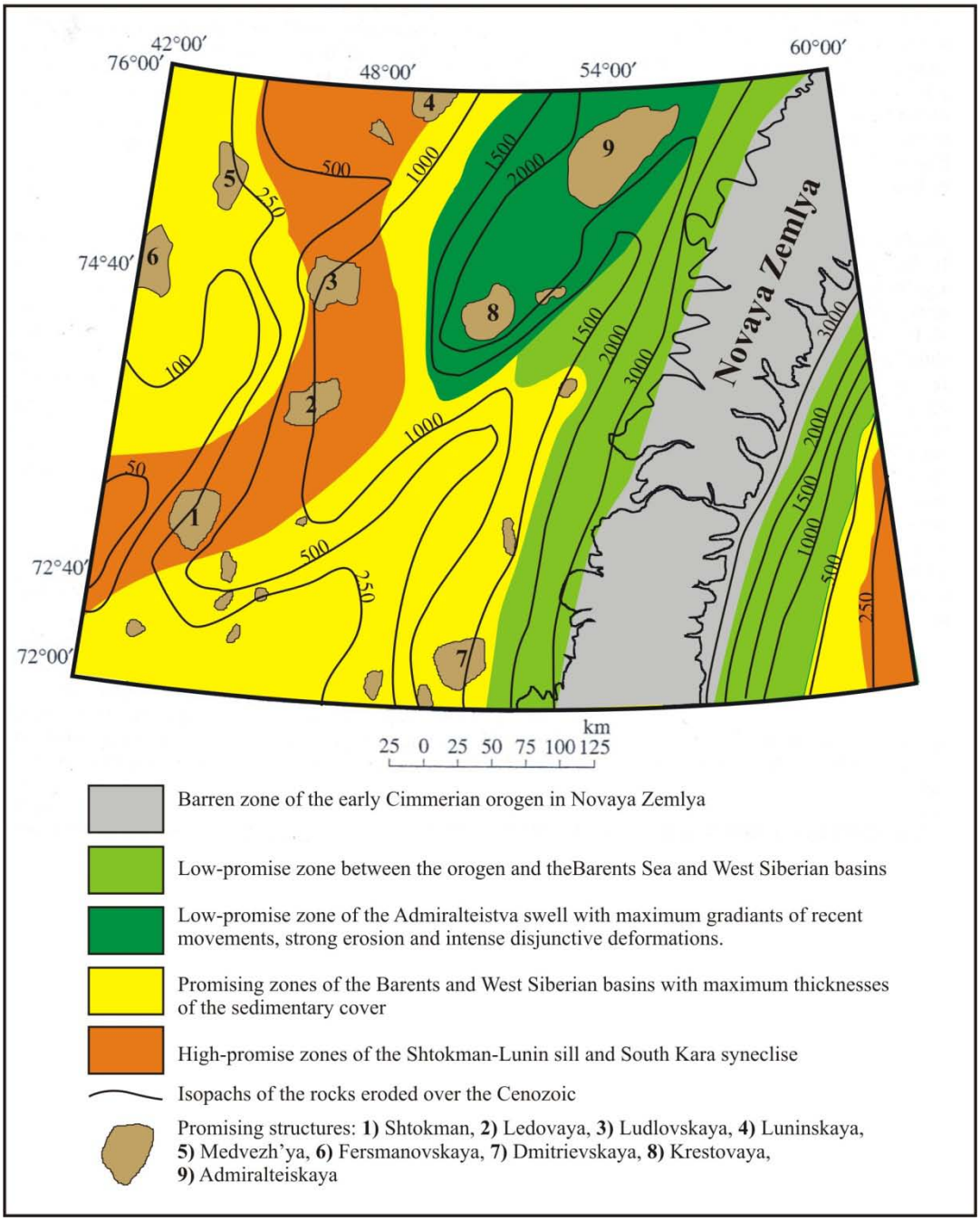

Figure 3.3. Erosional estimate in the eastern Barents Sea, also showing oil-gas-bearing prospects in the Novaya Zemlya region based on geomorphological and neotectonic analyses. Modified from Musatov & Romashchenko (2003).

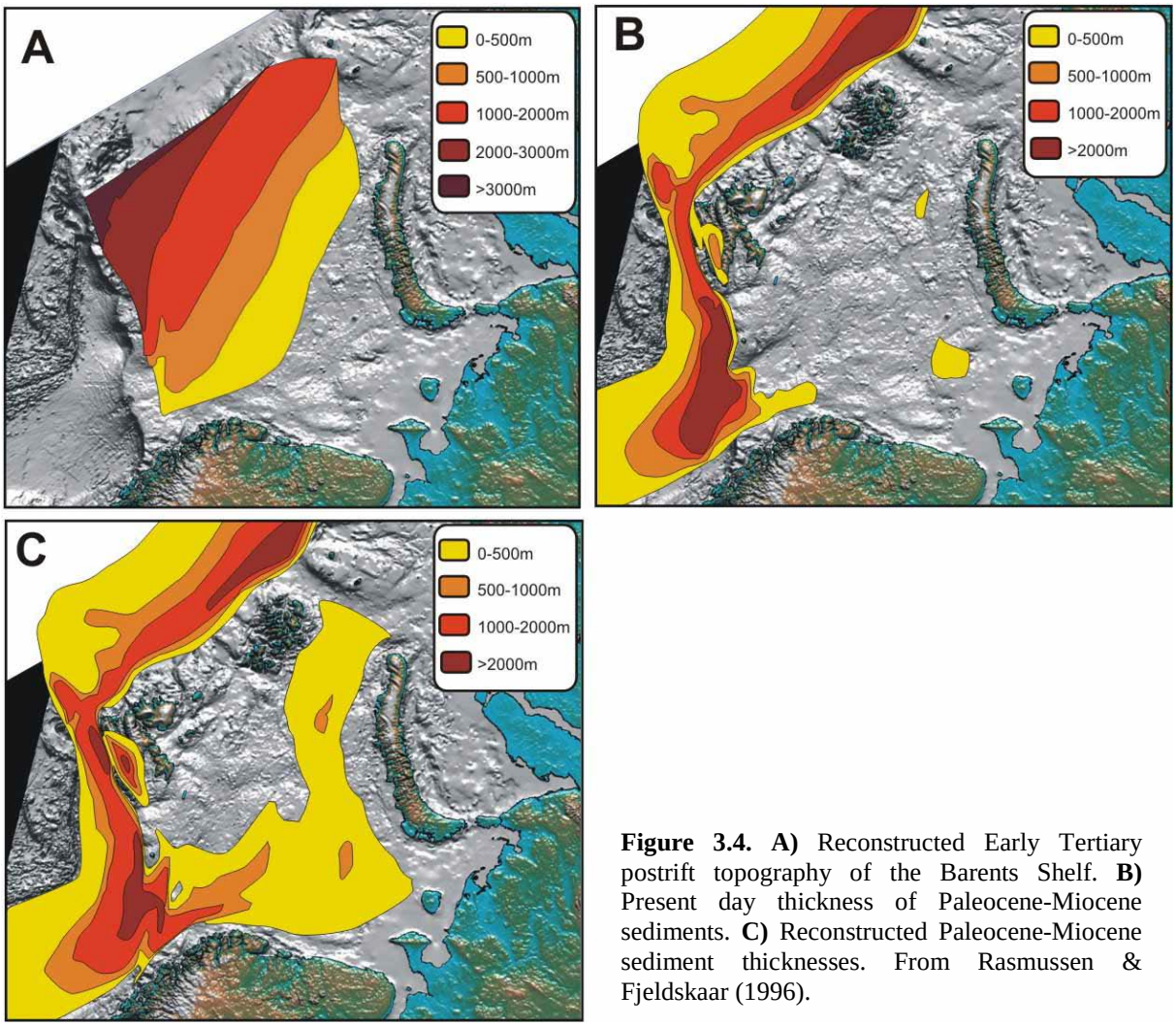

Figure 3.4. A) Reconstructed Early Tertiary postrift topography of the Barents Shelf. **B)** Present day thickness of Paleocene-Miocene sediments. **C)** Reconstructed Paleocene-Miocene sediment thicknesses. From Rasmussen & Fjeldskaar (1996).

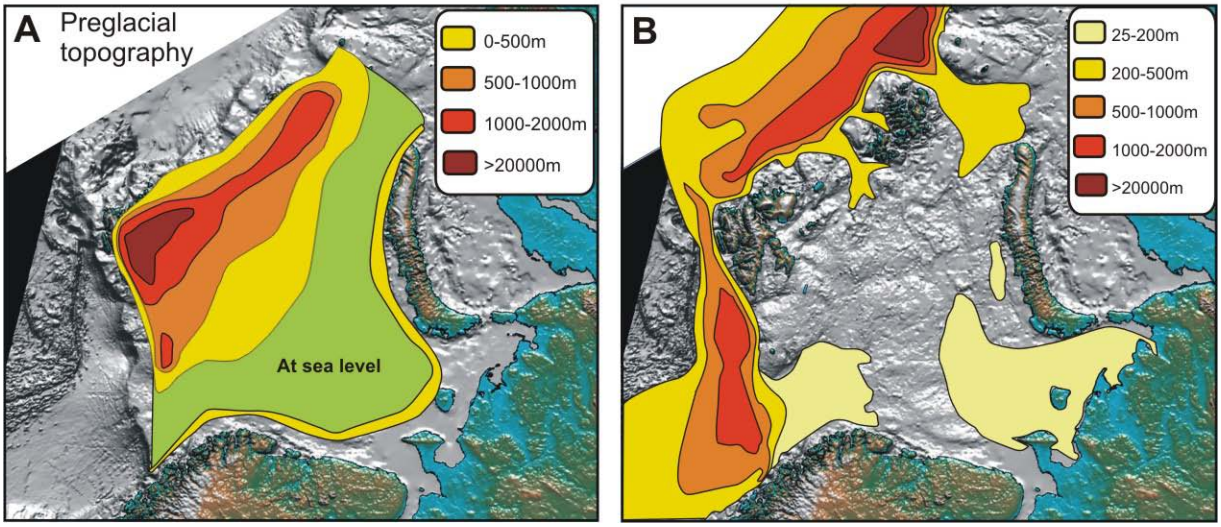

Figure 3.5. A) Reconstructed preglacial relief of the Barents Shelf. **B)** Pliocene-Pleistocene sediment thickness on the Barents Shelf and margins. From Rasmussen & Fjeldskaar (1996).

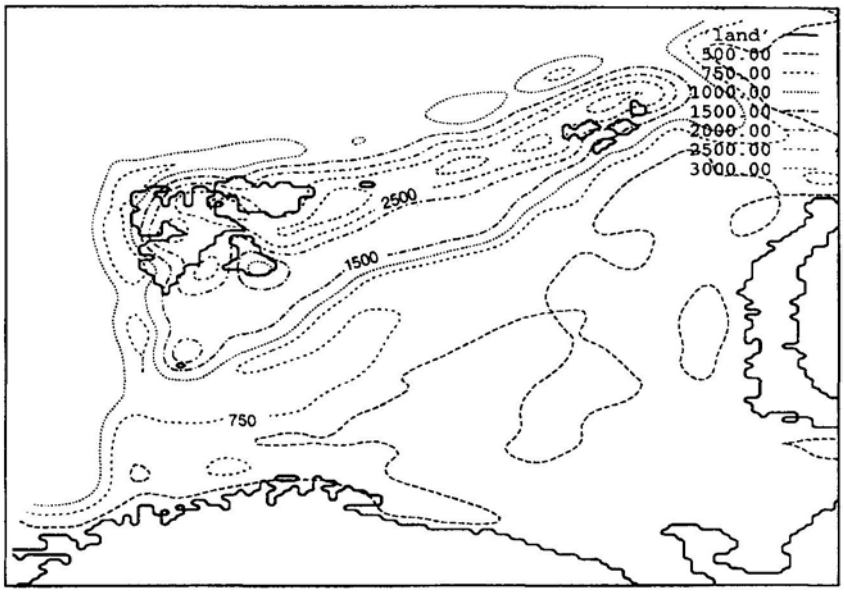

Figure 3.6. Estimated amount of glacially eroded Pre-Quaternary sediments using an elastic lithosphere thickness te = 10 km. For a thick lithosphere (te = 50 km) the pattern of the estimated erosion is more smeared out, with gradually increasing values from south to north, without any local maximum in the Bear Island Trough. From Rasmussen & Fjeldskaar (1996).

3.2. Consequences of new glaciation model

The models that we have suggested for glaciations in the Barents Sea area, as described in chapters 2 and 4, have consequences for the timing and spatial distribution of glacial erosion. We propose that the glaciations and erosion should be divided into three phases:

1) An onshore phase (ca. 2.5-1.5 mill. years ago), with glaciers limited to Scandinavia, Svalbard and other arctic uplands, where main glacial erosion took place (Fig. 2.4; Early Phase). Most of the Barents Sea was ice-free, large parts may have been emergent, and fluvial erosions may have been important.
2) A transitional phase (ca. 1.5-0.5 mill. years ago) where glaciers expanded further under a cooling climate (Fig. 2.4; Middle Phase). Ice streams from the Svalbard ice sheet seem to have reached the shelf edge at the mouth of the Bear Island Trough several times during this phase (Fig. 2.3), causing glacial erosion of the areas north/northeast of the Bear Island. Erosion from the Scandinavian Ice Sheet may have taken place just off the coast of Scandinavia. Erosional products in the Bear Island Fan (sediment package GII) suggest that this phase had the highest erosion and sedimentation rates.
3) A shelf phase (Fig. 2.4) with extensive ice sheet drainage to the shelf edge, also from the Scandinavian mainland, seems to have taken place from around 0.5 Ma. During this phase the whole Barents Shelf was subject to glacial erosion.

4. Glaciation models (ca. 0.2 mill. years - present)

Several ice sheets with different dynamic behaviour influence the glaciation history of the Barents Sea area. These are the terrestrially based Scandinavian and Svalbard ice sheets, and the marine based Barents and Kara Sea ice sheets. During the last ca. 0.5 mill years these ice sheets have coalesced several times to form an ice sheet covering the entire shelf areas. This section contains a brief summary of the present understanding of the variations of these ice sheets during the last ca. 200,000 years.

4.1 Previous glaciation models – Last glaciation (at ca. 20 ka)

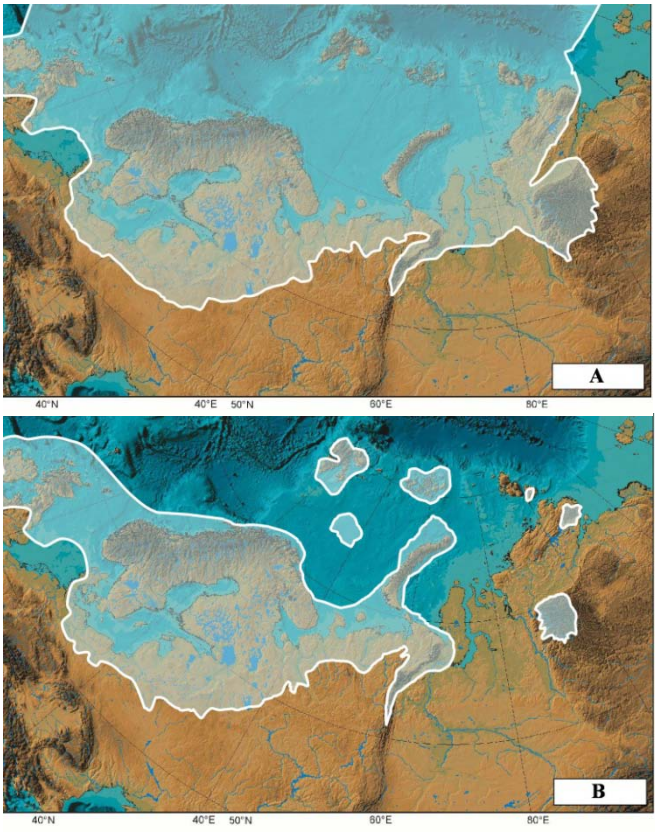

Figure 4.1. Glaciation models for the Last Glacial Maximum around 20 ka. **A)** Maximum model modified from Grosswald (1980). **B)** Minimum model modified from Velichko (1987).

Various glaciation models have been proposed for the Barents Sea area during the Late Glacial Maximum, ranging from very restricted ice (Velichko 1987, Fig. 4.1B), to a large ice sheet covering the whole Barents Sea as well as the polar ocean (Grosswald 1980), Fig. 4.1A). Given this range of disagreement notably over the Barents Sea area, the effects of glaciations over the shelf areas could hardly be evaluated.

4.2. Current glaciation models

4.2.1. The Saalian glaciation (ca. 200 – 130 ka)

Little is known about variations through time during the Saalian glaciation. It is, however, evident that the maximum Saalian glaciation (Fig. 4.2) was much larger than any of the subsequent Weichselian glaciations (cf. Fig. 4.3). At its maximum the Saalian glaciation covered the entire Barents and Kara seas to their continental margins, and was continuous over Britain, the North Sea, Scandinavia, and far south into Russia.

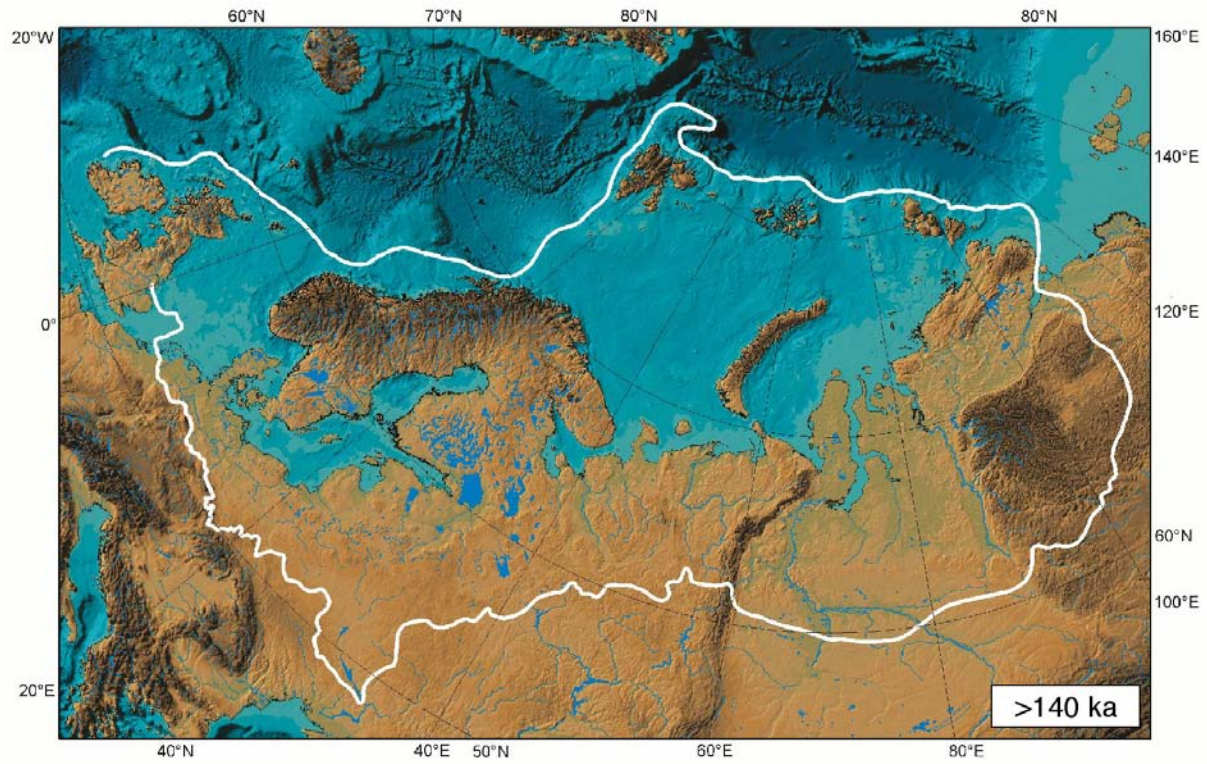

Figure 4.2. Maximum ice configurations during the Late Saalian glaciation around 160-140 ka (Svendsen *et al.* in press).

4.2.2. Reconstruction of the Weichselian glaciations (115-10 ka)

The maps below (Fig. 4.3) show ice limits during three main glacial phases of the Weichselian (Svendsen *et al.* in press). These maps only show reconstructed maximum limits for each of the three glacial events. The growth patterns of all three, and the decay patterns of the two oldest are poorly known. The decay pattern of the youngest will be dealt with in a subsequent section. In each of the reconstructions the maximum position is not completely synchronous. For instance it is known that the maximum position of the Scandinavian ice sheet (Fig. 4.3A) is about 10 ka older outside western Norway than it is in NW Russia (Larsen *et al.* 1999b). In these reconstructions the two older glaciations (Fig. 4.3B and C) are portrayed as a merge between the Scandinavian and the Barents Sea ice sheets (Svendsen *et al.* in press). It may be that there was an ice-free corridor between the two at both these stages (Larsen *et al.* in prep.).

The most noteworthy feature of the last glaciation at this scale is the shift in glaciation centre through time. The oldest was largest in the east, whereas the youngest was largest in the southwest. The intermediate in time was also intermediate in size between the two extremes. This has probably to do with temperature evolution and variations in availability of precipitation through time in the Weichselian.

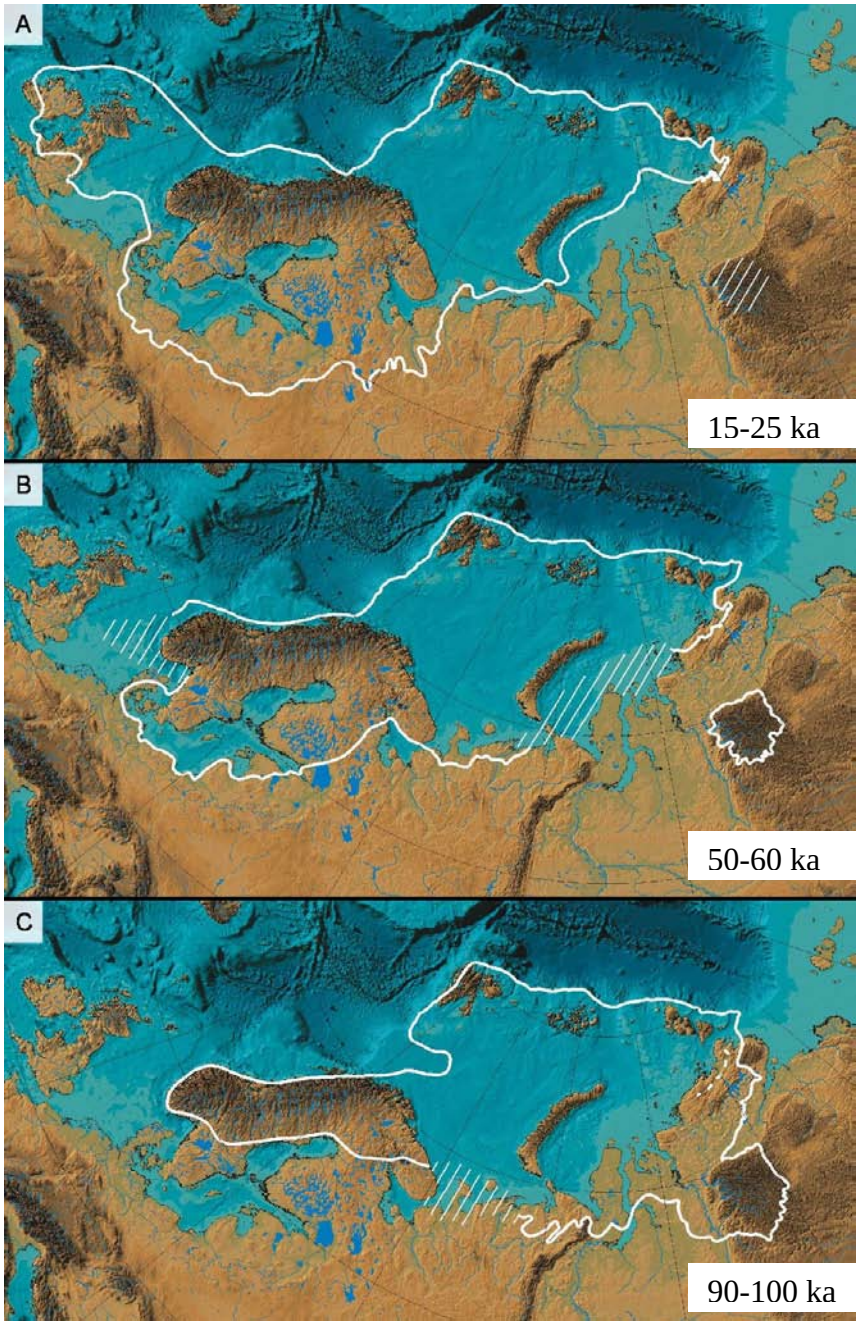

Figure 4.3. Mapped Weichselian ice limits for the Fennoscandian and Barents-Kara Sea ice sheets. **A)** Last Glacial Maximum at ca. 15-25 ka with the Scandinavian Ice Sheet being the dominant in size. **B)** A 50-60 ka intermediate sized ice sheet both over Scandinavia and the Barents-/Kara Sea. **C**) A 90-100 ka ice sheet which was larger than the two younger to the east. From Svendsen *et al.*(in press).

4.2.3 The last glacial maximum (LGM): Reconstructed and modelled

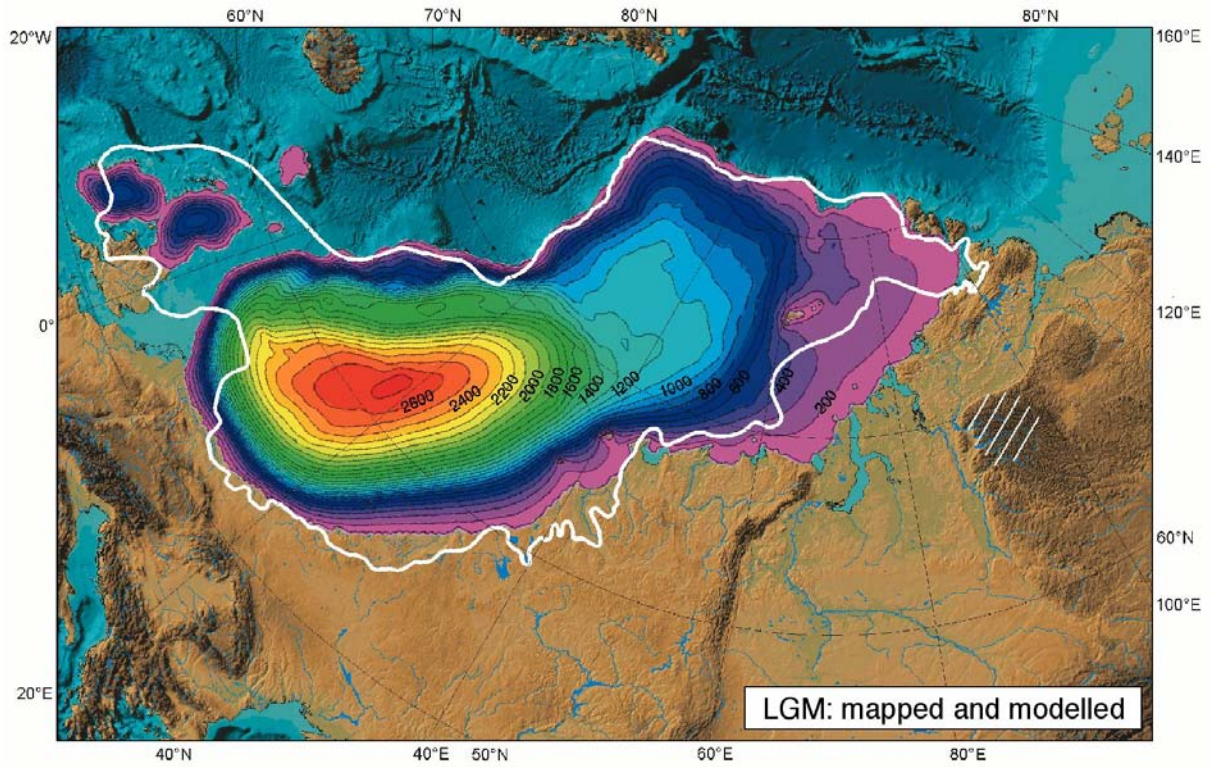

Figure 4.4. Mapped and modelled ice limits during the last glacial maximum. From Svendsen *et al.* (in press).

The map (Fig. 4.4) shows a comparison between glacial geological reconstruction of ice extent during the last glacial maximum (white line, cf. Fig. 4.3A) and numerically modelled ice extent for the same time. In addition, the model result also indicates ice thickness. The model is tuned to the geological observations. This means that it was driven to give a best fit to the reconstructed ice margin. The model suggests a rather single-domed situation with ice thickness over Scandinavia of some 2700 meters. Furthermore it suggests thin ice over the Barents Sea area, which is expected, but probably with a more complex dome configuration.

4.2.4 Deglaciation after the last glacial maximum

This model output (Fig. 4.5) shows a solution for stages in deglaciation from the last glacial maximum persisting until 14 ka, and until 11 ka. Most notably in this result is the separation into individual domes as deglaciation proceeded. This is also reflected in isolines for shore-levels as a result of glacial isostasy (Fig. 4.6). Furthermore, the model also underlines the importance of the Bear Island Channel for rapid disintegration of ice in the central Barents Sea. In general terms this model output can be substantiated by geological data, but it is not known if ice prevailed as long as indicated in the easternmost areas.

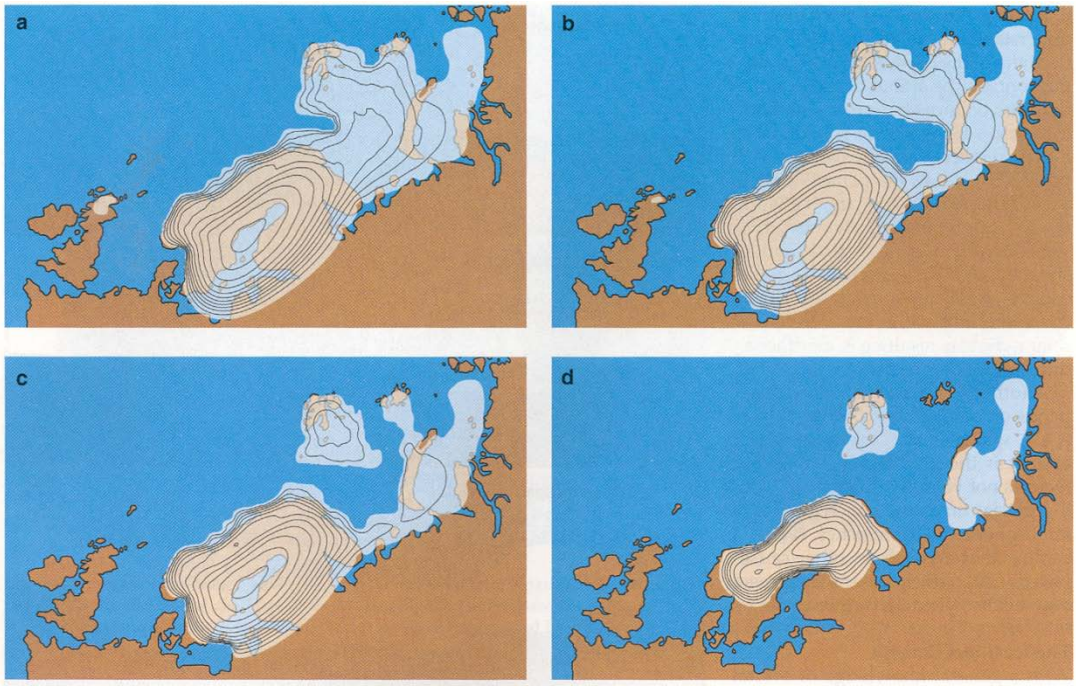

Figure 4.5. Numerical simulation of how the Scandinavian-Barents Sea ice sheet decayed from a maximum thickness of about 2750 m, which persisted until ca. 14 ka (a). By 13 ka, much of the region between Scandinavia and Novaya Zemlya was free of grounded ice (b). By some 12 ka, the ice covering Svalbard separated from the ice sheet that still covered Scandinavia and the Russian Arctic (c). By 11 ka, the ice in the region had further thinned and separated into three disjoint masses (d). Light colours show where the ice sheet was at least 50 m thick. Contour interval of ice thickness is 250 m. From Siegert *et al.* (2002).

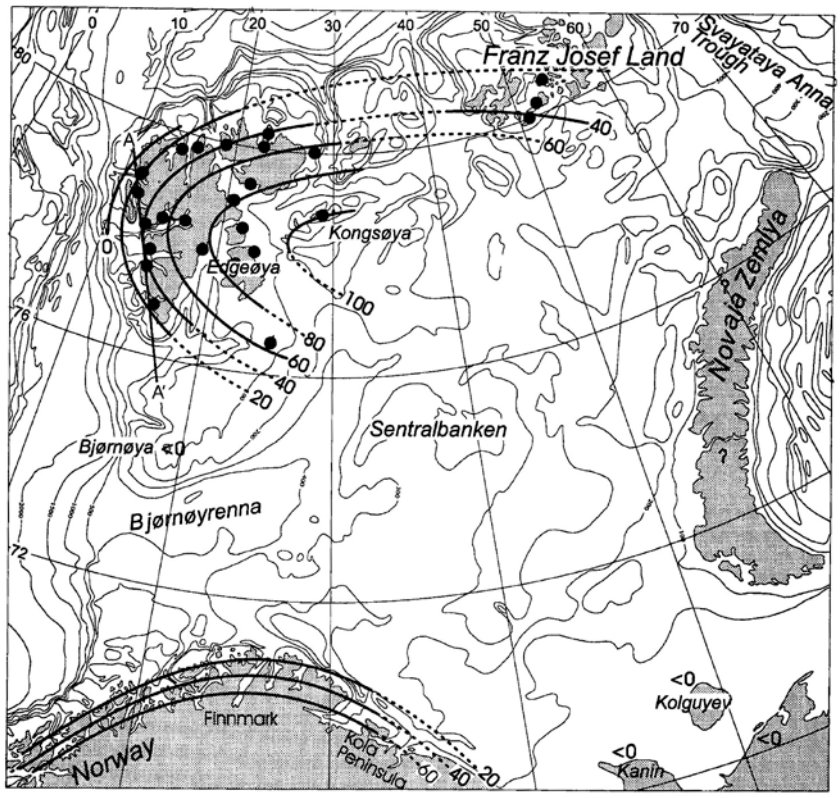

Figure 4.6. The contour lines (m above present sea level) for the 10 ka shoreline show how uplift is centred around Scandinavia and east of Svalbard. This is due to separation into ice domes during the last deglaciation. From Landvik *et al.* (1998).

4.2.5 Modelled ice thickness

Siegert *et al.* (2001) used a numerical ice-sheet model forced by global sea level and solar insolation changes to model the Weichselian glaciations of Scandinavia and the Eurasian Arctic. They used two sets of input giving a maximum and a minimum solution for ice distribution over time (Fig. 4.7). Both experiments result in three periods of glaciation during the Weichselian. The maximum model compares rather well to geological evidence for ice-sheet extent during the Early, Middle and Late Weichselian (cf. Fig. 4.3). Thus the resulting ice thickness for the three periods represents the present best estimate (Fig. 4.7).

Maximum model **Minimum model**

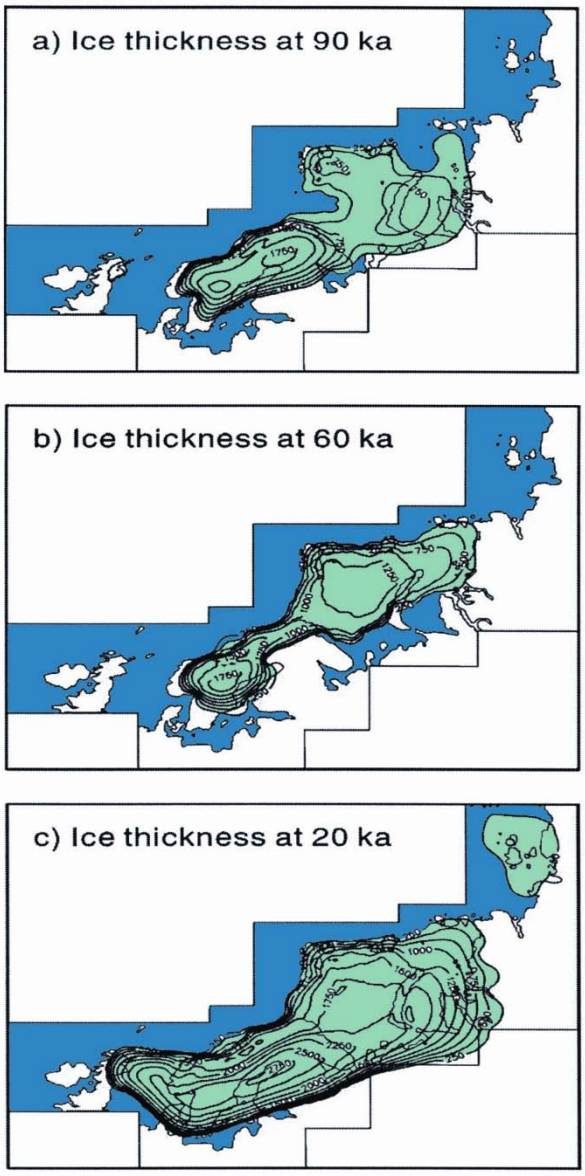
a) Ice thickness at 90 ka
b) Ice thickness at 60 ka
c) Ice thickness at 20 ka

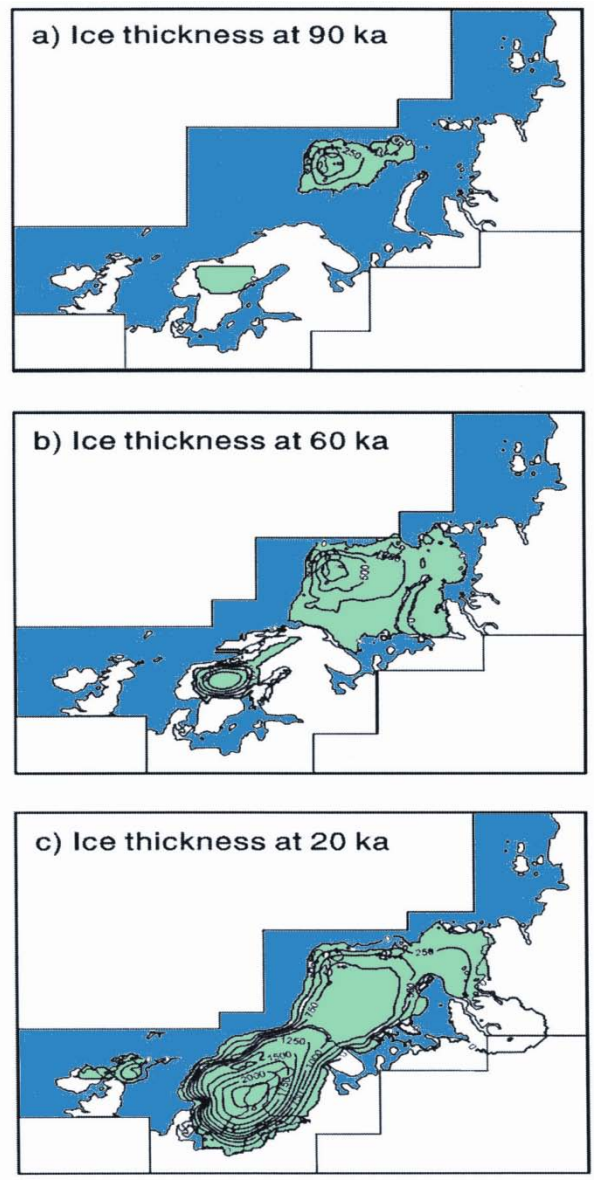

Figure 4.7. Modelled ice sheet thickness for a maximum (left column) and minimum (right column) solution at 90, 60 and 20 ka, respectively. From Siegert *et al.* (2001).

4.3. Towards comprehensive glaciation models

A conceptual model for maximum style glaciations in the three periods ca. 2.5-1.5, ca. 1.5-0.5, and ca. 0.5-present has been developed (Fig. 2.4). According to this model, glaciations will within each of the three periods, have varied several times between being completely absent to acquire a size comparable with the maximum size for each time period (Fig. 2.3). Only for the last glaciation, the Weichselian, a reconstruction of the dimensions for ice sheets at different times can be made (Fig. 4.3: 90 ka, 60 ka and 20 ka). Between each of the Weichselian glacial phases (Fig. 4.3) the ice melted more or less completely away. The background for constructing the Weichselian glacial model are numerous cores, sediment and seismic sections, and morphological mapping which then is synthesized into glacier variation curves for different sections of the ice sheet (Fig. 5.25).

At present it is premature to construct glacier variation curves for long time periods with a similar level of detail. In Figure 2.3 we have plotted a composite sequence of glacial events from the 3D surveys against the glacier variation curve from the western Barents Sea (curve a in Figure 5.25). The sequence of glacial events from the 3D interpretations is very preliminary, and the correlation to the western Barents Sea glaciation curve is tentative.

It is necessary to establish a stratigraphic framework by 2D seismics and cores to ensure correct correlation between the different 3D areas. Nevertheless, Figure 2.3 shows the potential in combining these different type of data, and thus the prospects of being able to establish glacial reconstructions over longer time series. With longer glacial records at hand it might be possible to resolve the conceptual model of glaciations (Fig. 2.4) into time slices of glacier occupation (cf. Fig. 4.3).

5. Background for the new models

5.1. Western Barents Sea - Svalbard Margin

The Barents Sea is today a shallow epicontinental sea characterised by relatively shallow banks separated by deep troughs (Fig. 5.1). It is covering an area of $1.2x10^6$ km^2, and the average water depth is around 230 m. It is bound in the north and west by Tertiary rift and shear margins (Faleide *et al.* 1993). The Novaya Zemlya region forms the eastern boundary whereas the Norwegian coast and the Kola Peninsula mark the southern boundary. The Kara Sea is located to the east of Novaya Zemlya and dominated by a shallow eastern part and a 400 m deep trench parallel to Novaya Zemlya. Large submarine fans, reflected as seaward-convex bulges in the bathymetry, are found at the mouth of each of the troughs that extends to the margins (Fig 5.1). The size of the individual fans reflects both the size of the troughs and their corresponding drainage area, with the Bear Island Trough Fan being by far the largest, and the fans along the Svalbard margin the smallest. The trough mouth fans are depocentres dominated by debris flows accumulated in front of ice streams draining the former large ice sheets (Vorren & Laberg 1997).

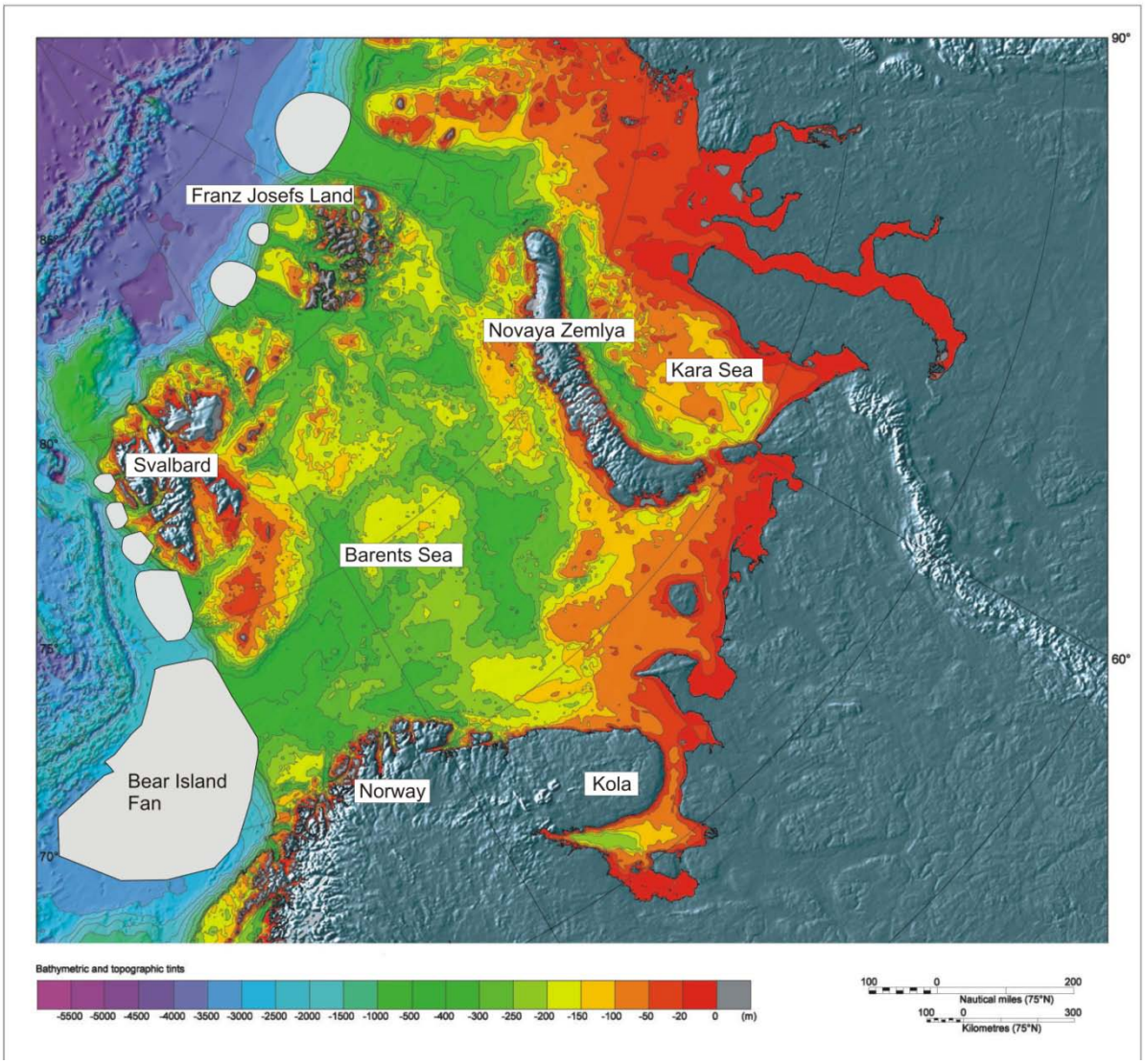

Figure 5.1. Map of the Barents Sea area. Location of trough mouth fans are also shown.

5.1.1. Stratigraphy and chronology

Three main sediment packages (GI, GII, and GIII) and seven regionally correlatable reflectors (R7-R1) have been identified within the Plio-Pleistocene sedimentary succession along western margin of Svalbard and the Barents Sea (Faleide *et al.* 1996, Fig. 5.2). Table 5.1. summarises the age estimates evaluated to be the most reliable for the identified reflectors and units in the area (Fig. 5.2). A more detailed correlation table including correlation between different investigations in the area is, together with a summary of the basis and uncertainties of these age estimates, included in the appendix (Table A1). With reference to Cenozoic formations commonly identified on the Norwegian Shelf by the oil industry, the sediment packages GI-GIII would correspond to the **Naust Formation** of the Nordland Group, when used as a succession of Upper Pliocene to Recent, including glacial and interglacial sequences.

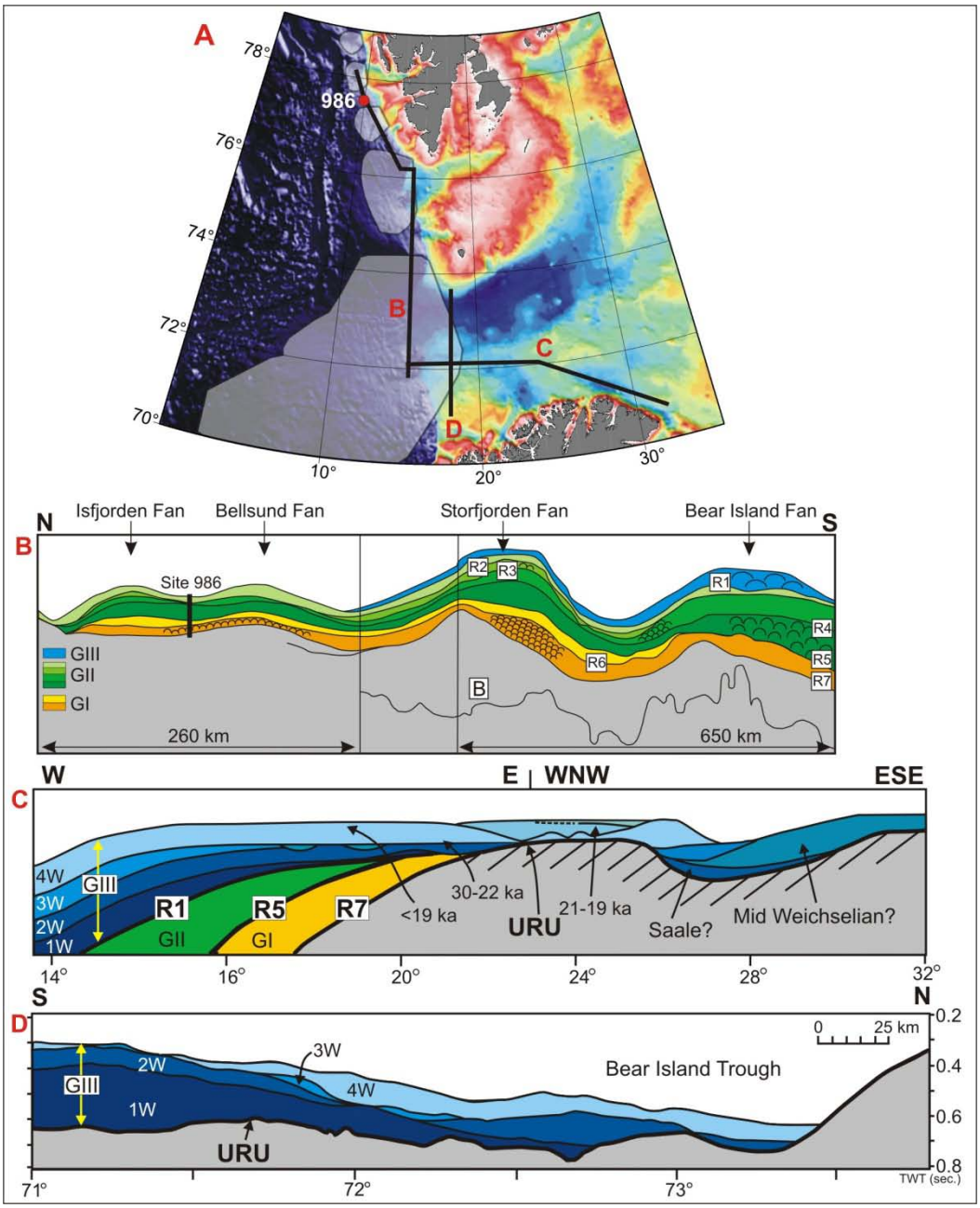

Figure 5.2. Stratigraphic relationship of the late Pliocene to Pleistocene succession in the southwestern Barents Sea. Age correlations are given in Table 5.1. Line B is from Butt *et al.* (2000). Line C is from Vorren *et al.* (1990) and western part is from Andreassen *et al.* (in prep.).

Table 5.1. Age synthesis of seismic sequences and main reflectors along the Western Barents Sea – Svalbard Margin. Reflectors R7-R1 and main sediment packages GI-GIII are from Faleide *et al.* (1996), and their age estimate from a revised interpretation of ODP Site 986 west of Svalbard (Butt *et al.* 2000). Seismic units A-H are from the Sørvestsnaget 3D and units 1W-4W are from Vorren *et al.* (1990). Age estimates of units within the upper sediment package GIII are obtained from correlation with Sættem *et al.* (1991) and Sættem *et al.* (1992). A complete correlation diagram is included in Table A1 in the appendix.

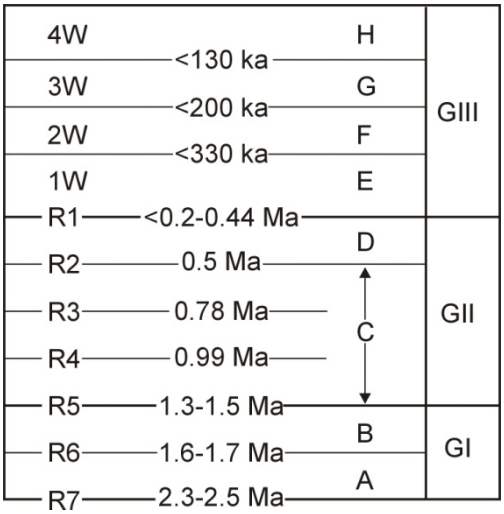

The following phases of depositional events are related to the glacial history of the Western Barents Sea – Svalbard Margin:

1) Glacially influenced deposition became dominant on the continental margin at about 2.3 Ma. This event is represented by the unconformity R7, which is also the base of the western margin trough mouth fans (Faleide *et al.* 1996). R7 marks an increase in general sedimentation rate along the entire margin. Large parts of the Barents Sea may have been emergent at this time, and fluvial systems may therefore have been an important sediment transport mechanism.
2) The first glacial advance reaching the shelf break west of Svalbard happened at R6 time (~1.6 Ma; based on results from ODP Site 986) (Butt *et al.* 2002). At the Bear Island Trough Margin the first ice streams reached the shelf break at R5 time (~1.4-1.5 Ma), probably draining out the Bear Island Trough from an ice sheet situated over Svalbard and northern Barents Sea (suggested from 3D seismic of Sørvestsnaget), model of Fig. 2.3; Middle Phase.
3) The first grounded ice draining from the Scandinavian mainland to the Bear Island Trough Margin seems, based the Sørvestsnaget 3D seismic, to have taken place at R1 time (~0.5 Ma).

The Upper Regional Unconformity (URU)

The boundary between the pre-glacial bedrock and the relatively thin cover of glacial deposits on the continental shelf is termed the Upper Regional Unconformity (URU, Solheim & Kristoffersen 1984). Although direct correlation between URU and the seismic stratigraphy defined at the margin is not straightforward, the available seismic data indicate that URU corresponds to progressively older slope reflectors from south to north along the outermost continental shelf (Faleide *et al.* 1996; Solheim *et al.* 1998). In the Bear Island Fan, URU corresponds to R1 (Fiedler & Faleide 1996), whereas it corresponds to R3 in the Storfjorden Fan (Hjelstuen *et al.* 1996), and most likely to R5 in the Isfjorden Fan (Solheim *et al.* 1996). Although URU most likely represents the erosional base for several continental shelf glaciations, the correlation between URU and R5, R3, and R1, respectively, indicate that the

last major erosion down to the level of URU at the outer shelf, occurred at a time corresponding to R5 adjacent to Svalbard, and subsequently later off the central Barents Sea (Faleide *et al.* 1996). URU represents a change from an early erosional glacial regime, to a later aggradational regime.

5.1.2. Glaciation styles – Last glaciation

The present day topography of the Barents Sea is influenced partly by the underlying bedrock and structural trends, but to a large degree also by Late Cenozoic glacial erosion and deposition.

Ice streams occupying the main troughs

The sea floor morphology of the major troughs, as seen from the sea floor shaded relief map of the southern Barents Sea and similar maps from the 3D-surveys (Fig. 5.3) is characterized by sets of elongated groove-ridge structures with an exceptionally parallel conformity within each set (Fig. 5.3; white arrows). These lineations have all the characteristics of megascale glacial lineations (Stokes & Clark 2002), and are taken as evidence for the flow of grounded ice, probably as fast-flowing ice streams with the indicated orientations. The occurrence of similar lineations have the last decade been taken as evidence for former fast-flowing ice streams (Fig. 5.4A, Clark *et al.* 2000; Stokes & Clark 2002). The best preserved set of glacial lineations, imaging a giant ice stream that flowed offshore Antarctica during the last glacial maximum is shown in Fig. 5.4B. These lineations (Fig. 5.4B), being much wider than the typical glacial lineations mapped from satellite photos from terrestrial areas (e.g. Fig. 5.4A), are called a glacial bundle structure. The lineations that can be seen in Ingøydjupet on the regional seafloor map (Fig. 5.3 main map) would also be classified as a glacial bundle structure, indicating the flow lines of an ice stream draining out Ingøydjupet from the Scandinavian mainland. The sea floor images of survey NH9605, ST9705 (Snøhvit) and that of PL229 (Goliat) provide details of the Ingøydjupet bundle structure (Fig. 5.3; white arrows). Megascale glacial lineations observed on the regional seafloor image and the outer part of the Sørvestsnaget 3D provide evidence for a major ice stream that drained out the Bear Island Trough from a Barents Sea – Svalbard ice sheet.

Well-developed sea floor glacial lineations in the easternmost 3D (Fig. 5.3; Area G) and in Djuprenna just offshore Finnmark indicate that ice streams drained north towards Nordkappbanken and the small bank-area further east, as indicated in Fig. 5.5. Correlation with the seafloor map (Fig. 5.5A) and the high-resolution seismic stratigraphy in the area (Fig. 5.5B) suggests that the Nordkappbanken Ridge is a large endmoraine of an ice stream draining north-westwards out Djuprenna, and that the sedimentwedge that laps on to Nordkappbanken Ridge is deposited at the same time, in a glacial marine setting. The small-scale sea floor morphology of the Nordkappbanken Ridge (Fig. 5.3. PL202) and the glacial marine wedge (Fig. 5.3. PL228) are characterized by iceberg plough marks.

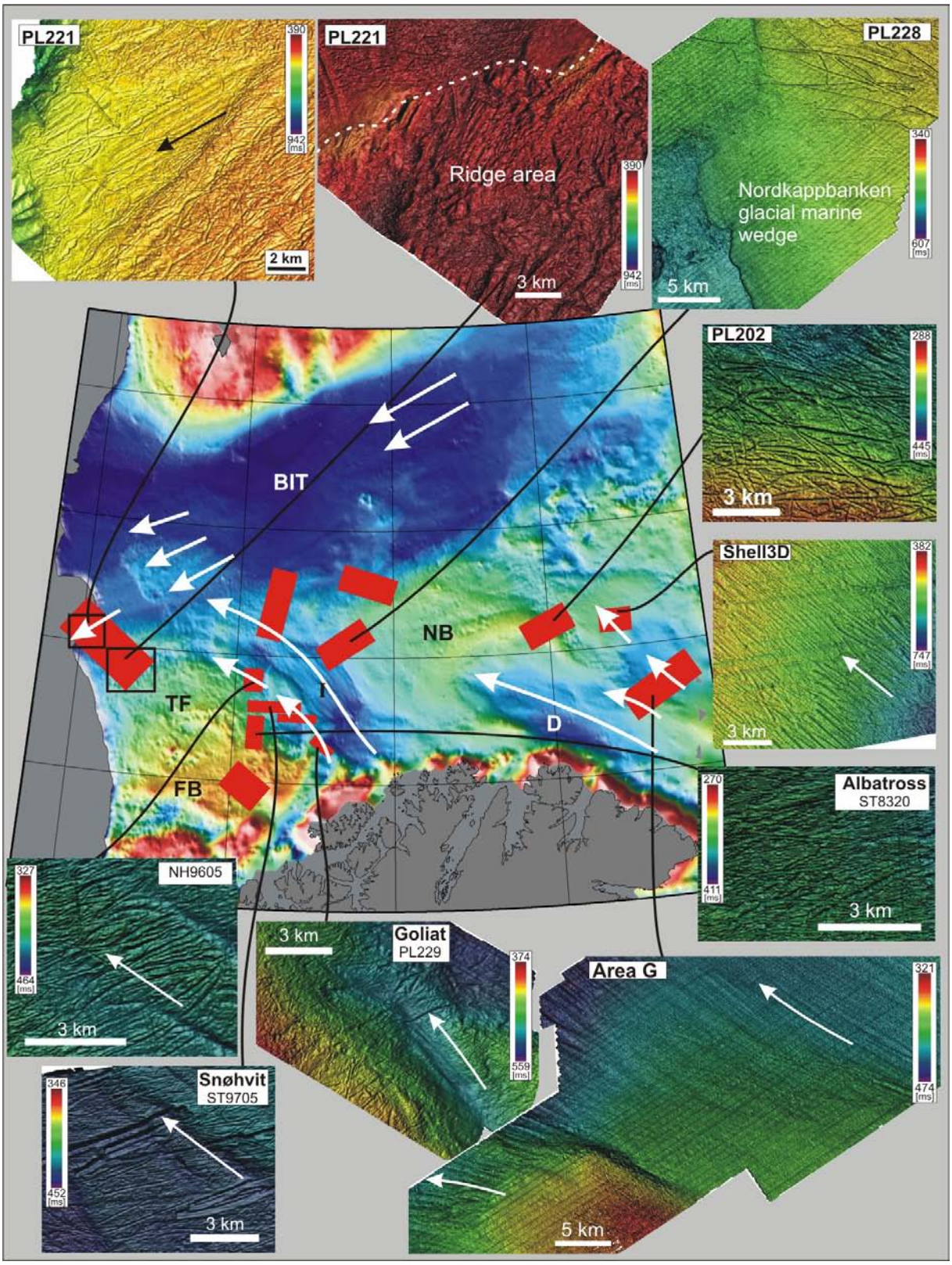

Figure 5.3. Shaded relief maps of the sea floor. BIT: Bear Island Trough; NB: Nordkappbanken; TF: Tromsøflaket; FB: Fugløybanken; I: Ingøydjupet; D: Djuprenna. The middle map is a Statoil map compiled by Mauring NGU 2003. From Andreassen *et al*. (in prep.).

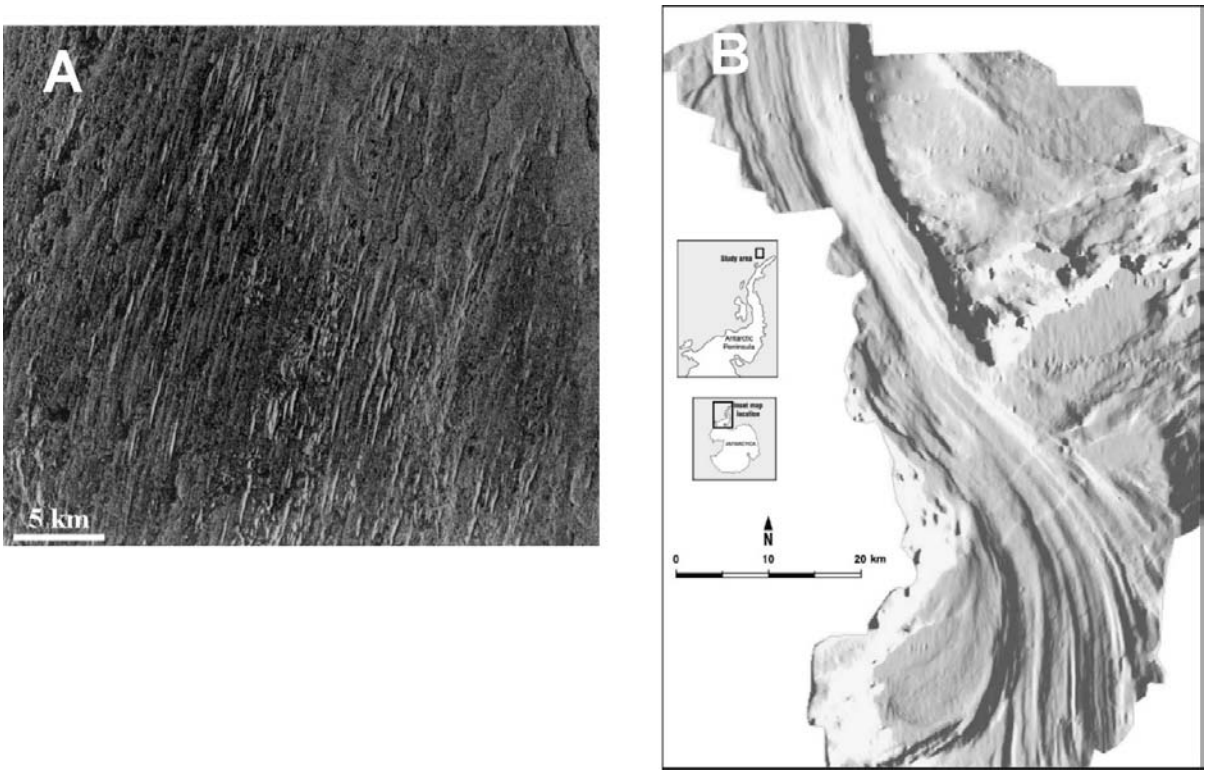

Figure 5.4. A) Appearance of glacial lineations on ERS-2 synthetic aperture radar (SAR) imagery. Note the high degree of parallel conformity of the lineaments, and overall coherence of the pattern. From Clark *et al.* (2000). **B)** Sidescan sonar image showing bundle structures consisting of glacially formed lineations beneath former ice stream in Antarctica (Canals *et al.* 2000).

Less dynamically active ice in the Tromsøflaket-Fugløybanken area

The sea floor morphology of the bank areas of Fugløybanken and Tromsøflaket shows no lineations. The last ice occupying the Tromsøflaket -Fugløybanken area is interpreted to have been of a less dynamically active type, that probably reached as far out as the southern part Sørvestsnaget, where a large area of parallel ridges are observed (Fig. 5.3; PL221). The regional seafloor image of Fig. 5.5A. suggests that these ridges are the outer end of several ridges occurring further landwards on Tromsøflaket and Nordkappbanken. Some of these ridges have been interpreted to be parts of glaciotectonic hill-hole pairs (Sættem 1990), while others have been interpreted to represent end moraines from the last glacial maximum (LGM, Vorren & Laberg 1996). It seems reasonable, from the regional picture provided by Fig. 5.5A, that the largest, southernmost moraines of Vorren and co-workers represent a deglaciation stage of the Scandinavian ice sheet, whereas the smaller of these ridges may be sub-glacially formed moraine-ridges.

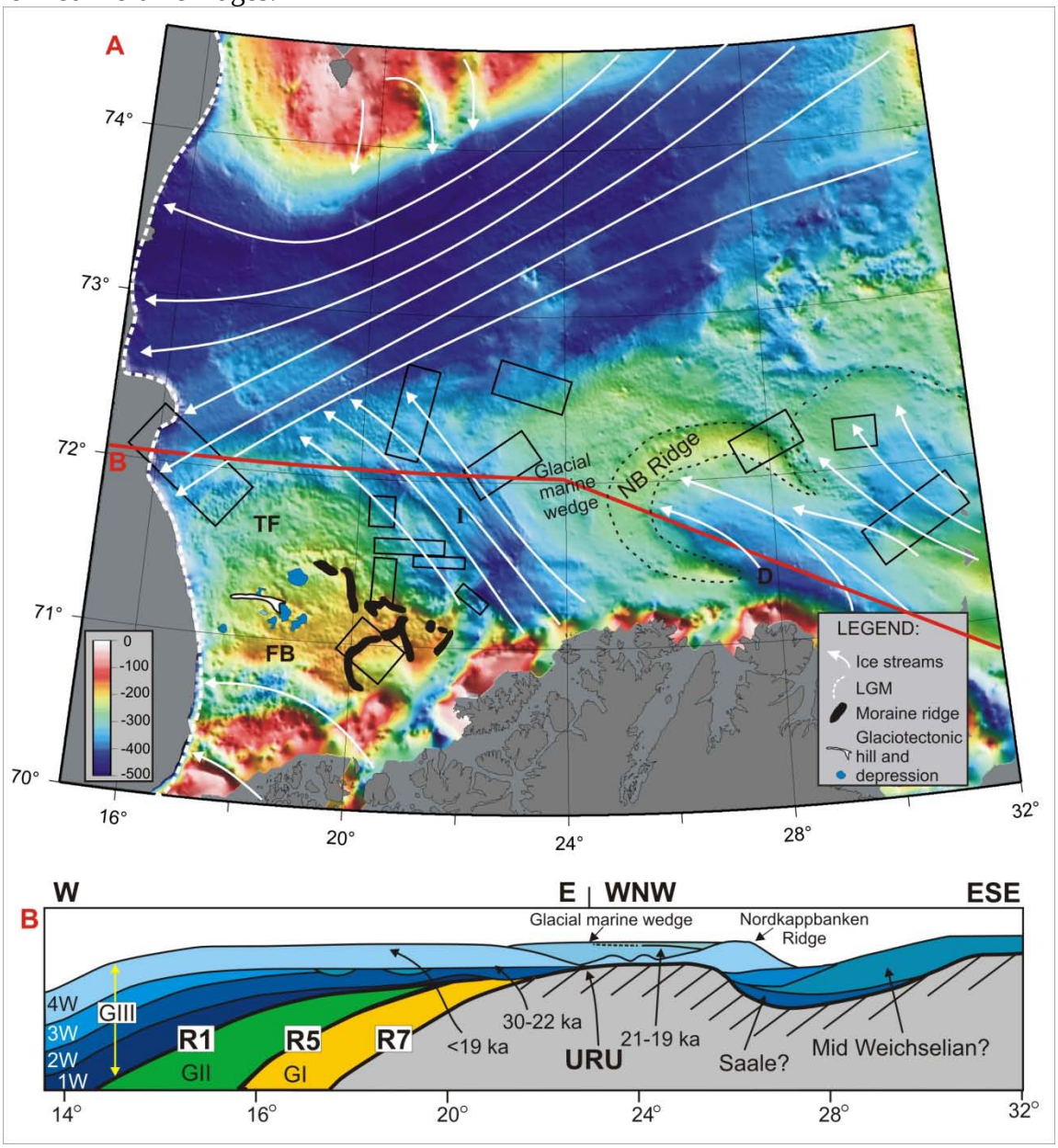

Figure 5.5. Shaded relief map showing sea floor geomorphology. Statoil map compiled by Mauring NGU 2003. The moraine ridges are from Vorren & Kristoffersen (1986) and the glaciotectonic hill-hole pairs are from Sættem (1990). NB: Nordkappbanken; TF: Tromsøflaket; FB: Fugløybanken; I: Ingøydjupet; D: Djuprenna. From Andreassen *et al*. (in prep.)

Comparison with other areas of the Scandinavian and Svalbard ice sheets

Large-scale geomorphology on the mid-Norwegian continental margin (Fig. 5.6, Ottesen *et al.* 2002) and west of Svalbard (Fig. 5.7, Landvik in prep.) indicate that fast-flowing ice streams filled major troughs also in these areas during the LGM, whereas glacier ice in the areas between was dynamically less active. Modelled velocities of ice streams in the Bear Island Trough and offshore mid Norway are shown in Fig. 5.6C.

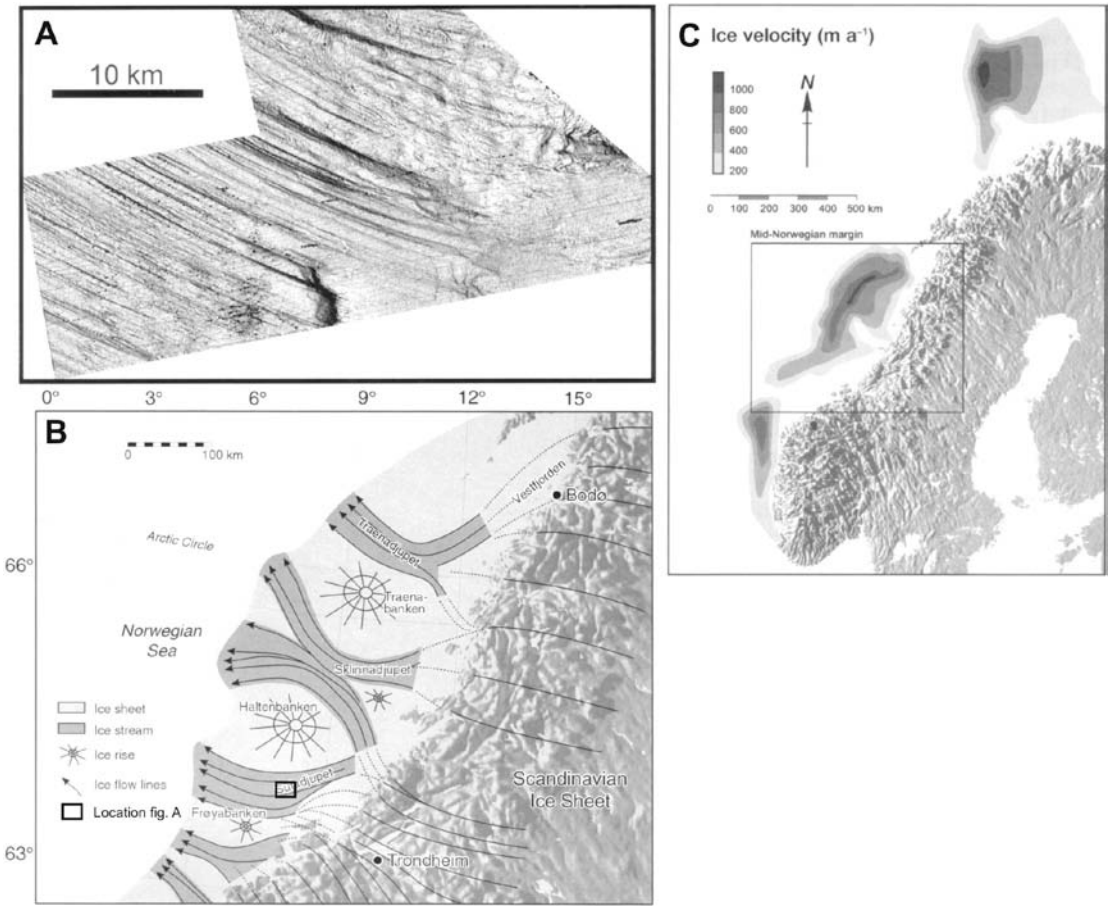

Figure 5.6. A) Shaded relief image of the sea bottom of the inner part of Trænadjupet based on 3D seismic data. **B)** Inferred ice-stream flow lines and ridges during the Late Weichselian with ice streams flowing along the main offshore depressions/troughs (Ottesen *et al.* 2002). **C)** Numerical reconstructions of ice velocities (m/year) during the last glacial maximum. From Ottesen *et al.*(2002).

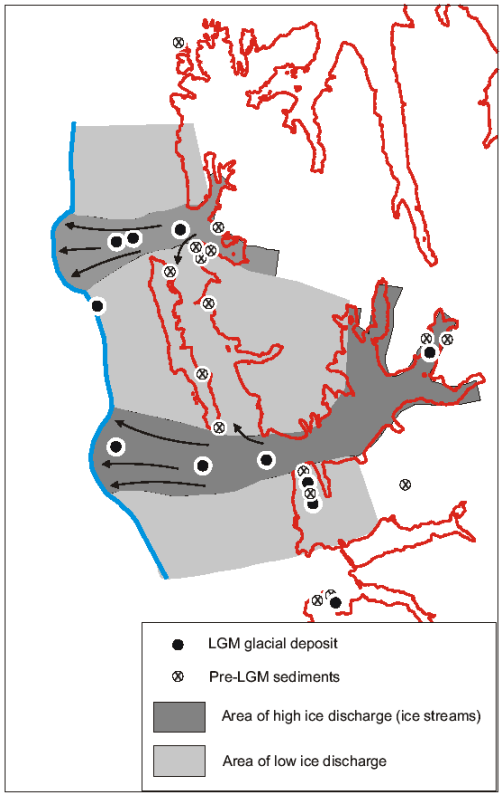

Figure 5.7. Ice streams from west of Svalbard. From Landvik (*in prep*).

5.1.3. 3D seismic at the margin – an archive of former glaciations

The Sørvestsnaget 3D area is located at the outer southern flank of the Bear Island Trough (Fig. 5.5A) and at the margin of the inferred maximum extent of ice during the Weichselian glaciation. The area is a major Cenozoic depocentre in the southwest Barents Sea. In addition to a more than 2 km long record of the Plio-Pleistocene sediments, a relatively complete pre-glacial Tertiary succession is drilled through here (Ryseth *et al.* 2003), providing a relatively continuous development through the Cenozoic.

Shaded relief maps of buried glacigenic horizons show detailed images of mega-scale glacial lineations (Fig. 5.8), providing evidence that grounded ice has extended to the shelf break in this area, probably as fast-flowing ice streams, since R5 time (~1.3-1.5 mill. years ago). The flow pattern of ice streams provided from glacial lineations has been regarded to represent a snapshot view of the bed from one single flow event. With the preservation of several hundreds of meters of till units between the glaciated horizons, we have in this area a unique possibility to study ice-stream processes over a longer period of time. The combined use of volumetric attribute maps and vertical seismic sections reveal the existence of the longest chains of megascale blocks and rafts ever described, buried in sediments between glaciated horizons, exemplified here by those of Unit F (Fig. 5.9). Seismic profiles parallel to the orientation of the block chains suggest that the sediment blocks consist of back-tilted sub-horizontal slabs that have been displaced from northeast along a series of listric shear planes (Fig. 5.10C). The blockchains of unit F are, from their location between ice-stream eroded surfaces (Fig. 5.9 B, C and D), their orientation parallel to mega-scale glacial lineations, morphology and internal structure (Fig. 5.10A and B) interpreted to be eroded, transported and deposited by an ice stream that drained out the Bear Island Trough to the shelf break. We have observed indications that many of the smaller blocks and rafts have been transported as megascale blocks and at a later stage been pulled apart from each other, partly influenced by shear zones parallel to the ice movement.

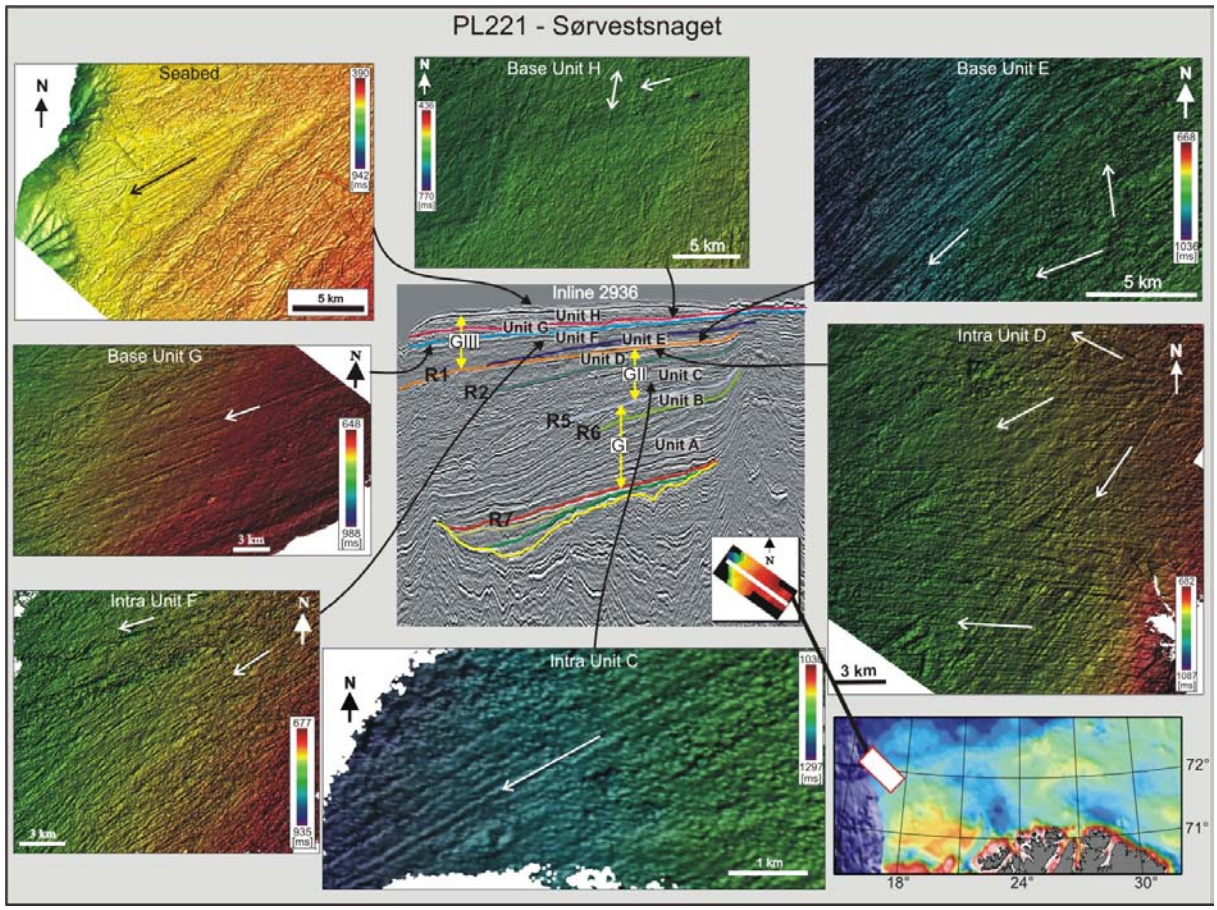

Figure 5.8. Illuminated shaded relief maps of interpreted seismic horizons in the Sørvestsnaget 3D-area, showing mega-scale glacial lineations formed sub-glacially, with orientations indicative of former ice flow.

Similar chains of sediment blocks have been identified within all the seismic units of the two upper Plio-Pleistocene sediment packages GII and GIII and some of these have been mapped (Fig. 5.11). The common occurrence of sediment blocks and rafts within the whole glacigenic sequence of the Sørvestsnaget 3D study area and increased occurrence close to the palaeo-shelf breaks, suggest that the process of glaciotectonic erosion, transportation and deposition by ice streams may account for high sediment flux from the Barents Sea to the shelf break and the Bear Island Fan during the Late Pliocene and Pleistocene. This data set documents the potential of ice streams for large–scale glaciotectonic erosion, and provides new information about the dynamics of ice streams. The lateral continuation of these sediments blocks is, however, uncertain outside of the Sørvestsnaget 3D. Do the chains of sediment blocks and rafts occur just at the *flanks* of former ice streams, or is glaciotectonic erosion a common process also away from the ice stream flanks? Inspection of 2D seismic data in the Bear Island Trough would probably answer the question.

So far, the results suggest that the till sequences of sediment package GII are deposited by ice that drained from northeast, indicating ice streams draining southwest to the Bear Island Trough shelf break from Svalbard or Central Barents Sea ice caps. The till units of sediment package GIII seem to suggest ice flowage also from the southeast, indicating ice draining from the Scandinavian mainland. So far, this is only a work-hypothesis that needs to be tested out by attribute studies of the till units to see if this pattern is consistent throughout these units. This will have important implications regarding timing and development of the Plio-Pleistocene erosion of the Barents Sea (Chapter 3.2).

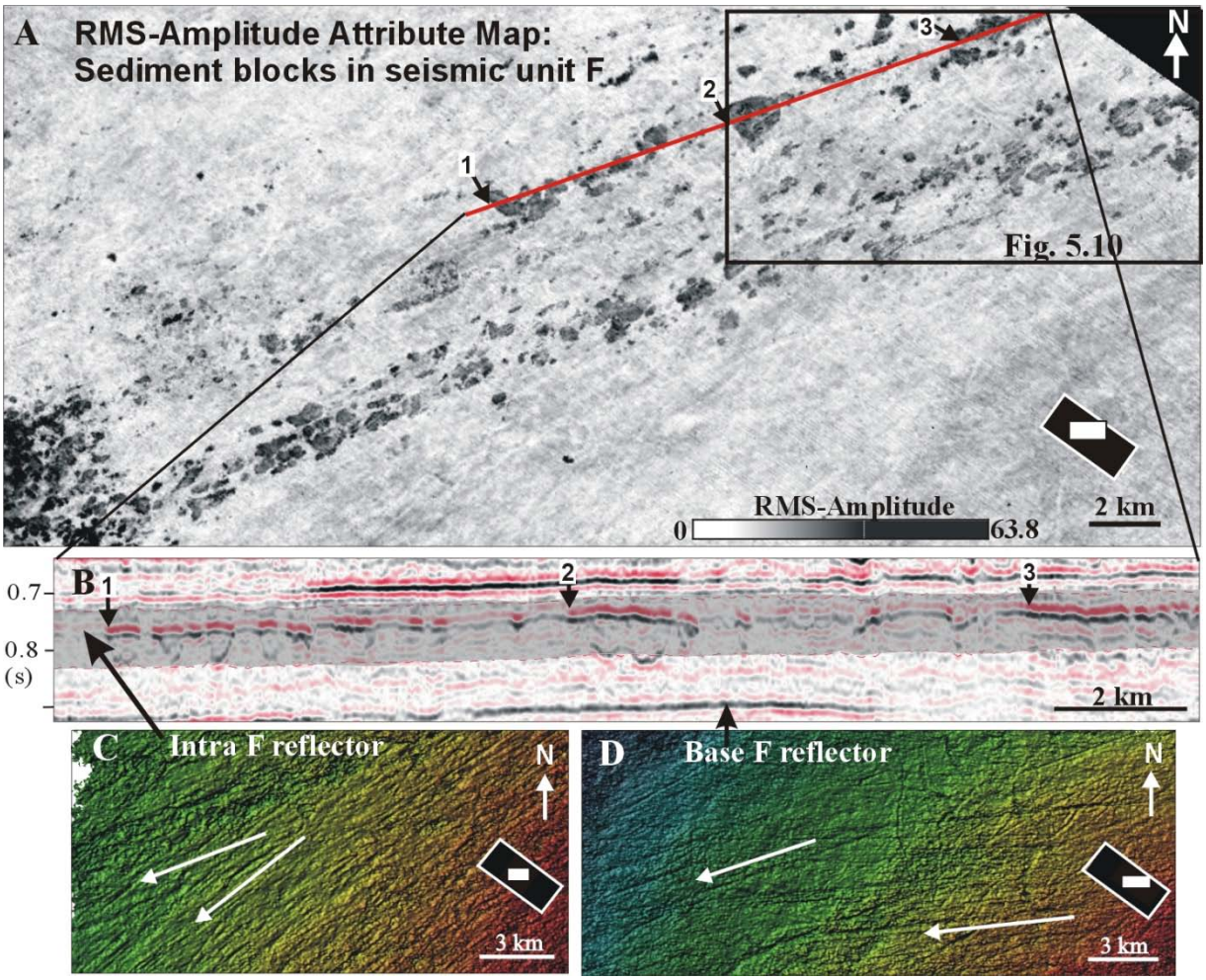

Figure 5.9. Sørvestsnaget area. **A)** RMS amplitude map of the shaded zone indicated on seismic Profile of Fig. 5.9B, showing location of sediment blocks and rafts within Unit F (dark colour on map). **B)** Seismic profile showing high-amplitude reflection segments of Unit F, location of profile is indicated in Fig. 5.9A. **C)** Shaded relief map of Intra F reflector. **D)** Shaded relief map of base F reflector. Location of the maps within the 3D-area is indicated by the small white rectangles. Stratigraphic location of Unit F is shown on the seismic profile of Fig. 5.8.

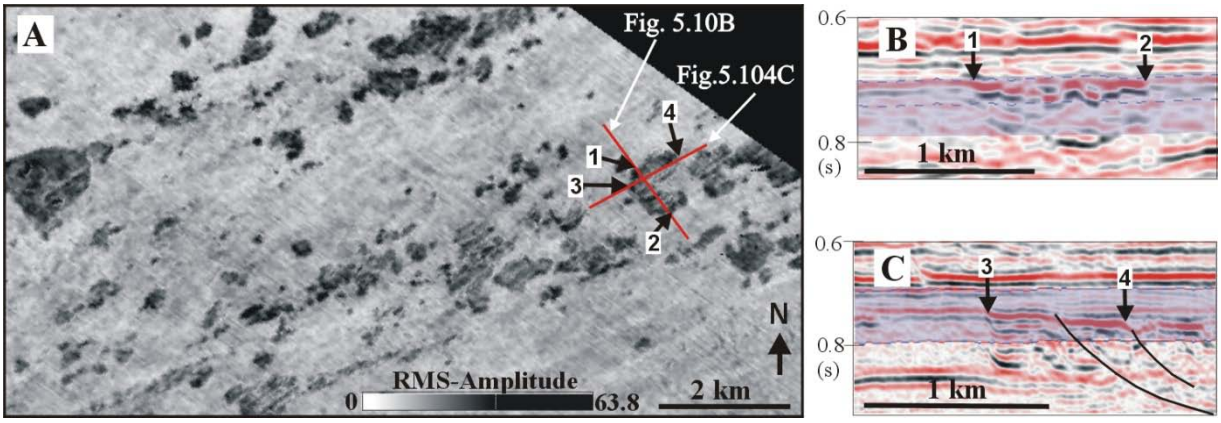

Figure 5.10. Sørvestsnaget area. **A**) Zoom in on RMS amplitude map of Fig. 5.9A, showing sediment blocks and rafts in Unit F. **B)** Seismic section perpendicular to orientation of sediment chains. **C)** Section of 2D-seismic profile (higher resolution than 3D) parallel to orientation of sediment chains. Listirc shear planes are probably of glacitectonic origin.

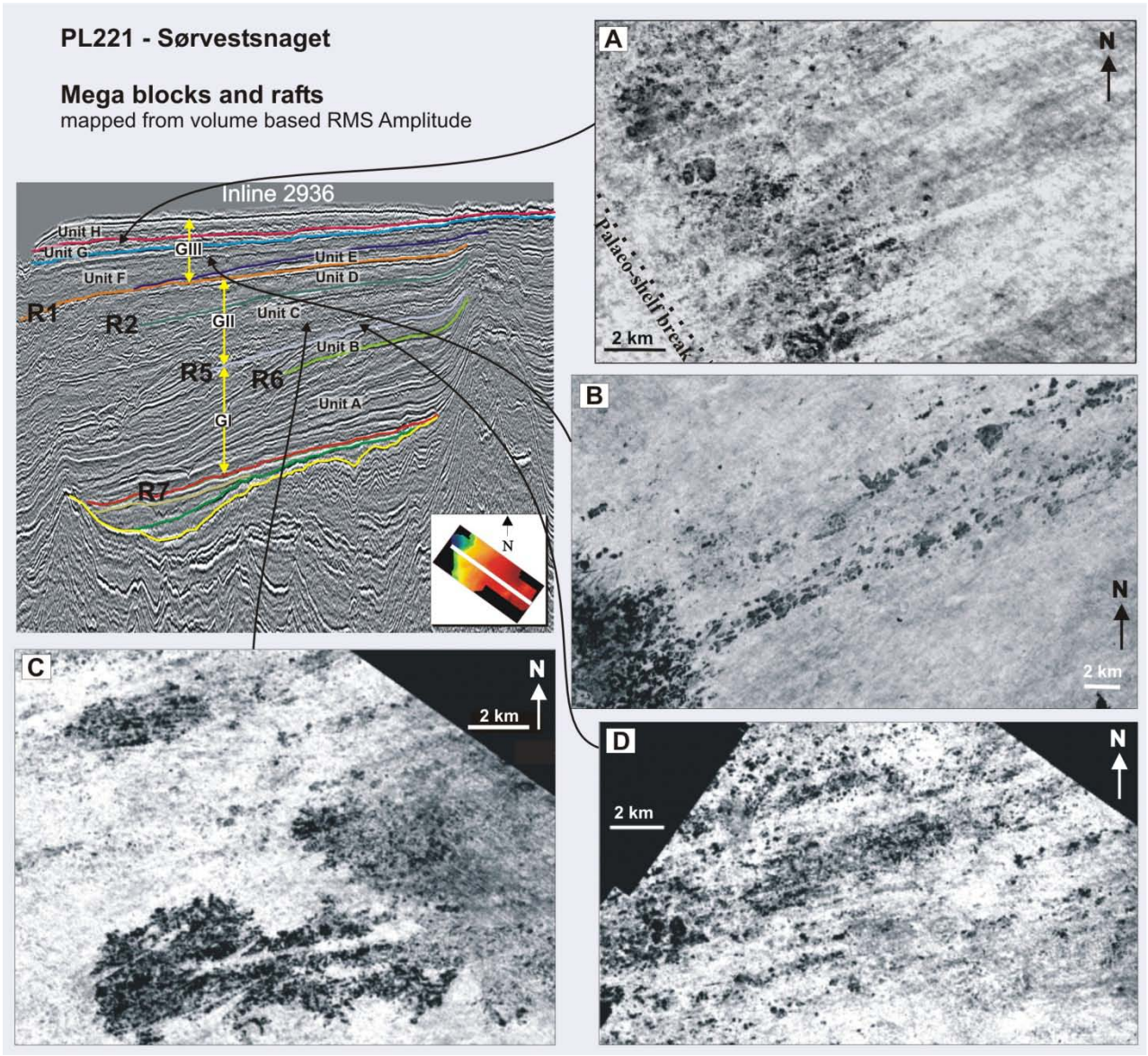

Figure 5.11. Megablocks and rafts mapped by RMS volume attribute studies in the Sørvestsnaget 3D area NH9803, where dark colour indicates high amplitude. This figure shows both older and younger units than Figs. 5.9 and 5.10. The sediment blocks displayed in Fig. 5.11C represent two stratigraphically overlying zones and show therefore two different orientations.

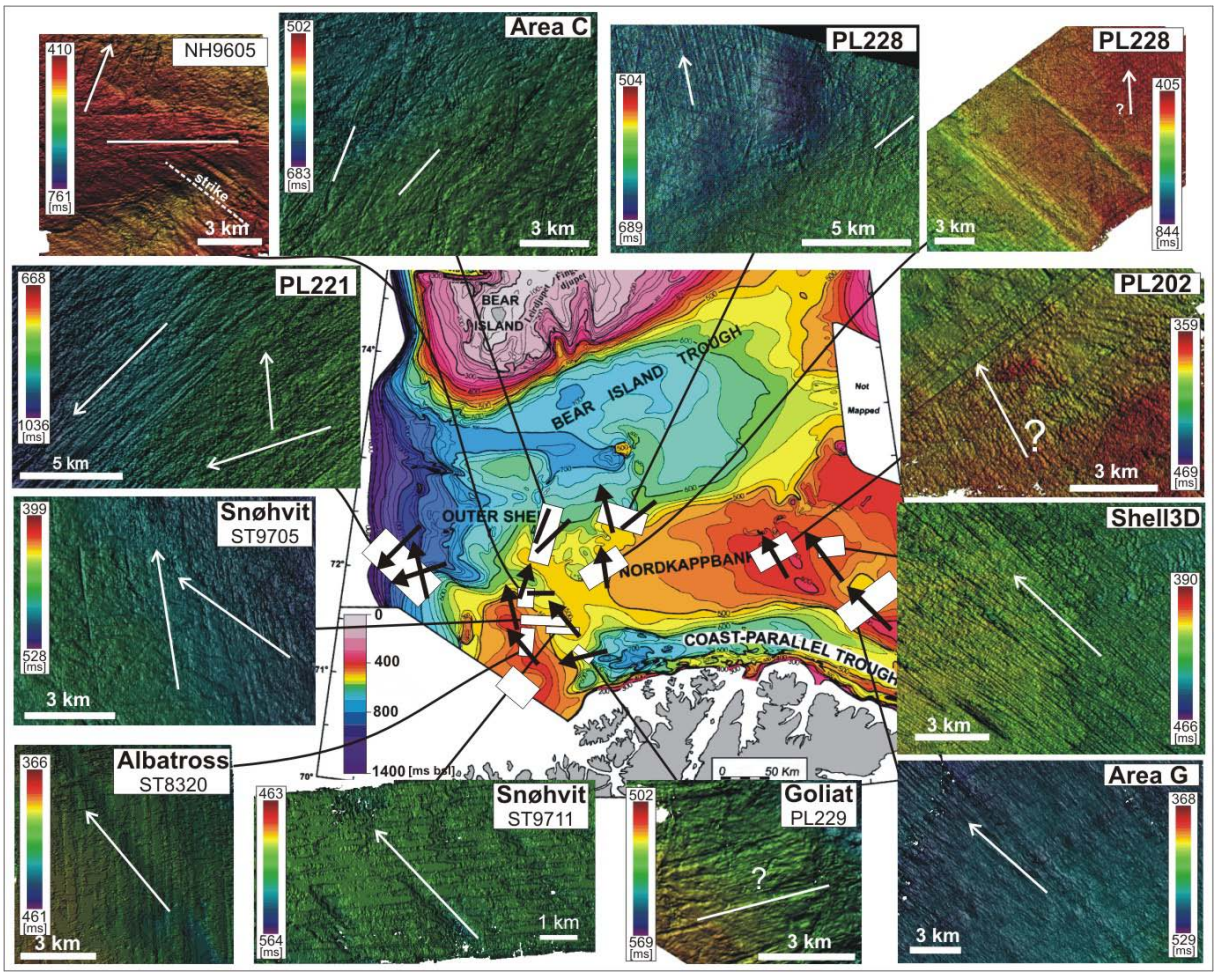

Figure 5.12. Illuminated shaded relief maps of the Upper Regional Unconformity (URU) from the different 3D surveys. The interpreted directions of ice movement from megascale glacial lineations are indicated by arrows. The time-structure map of URU in the middle of this figure is from Lebesbye (2000).

5.1.4. 3D seismic data from the southern Barents Sea and relation to prospects

The Upper Regional Unconformity (URU) is the oldest preserved glacigenic surface in the southern Barents Sea (when excluding the western margin), separating pre-glacial bedrock from overlying glacial deposits which are correlated with sediment package GIII at the western margin (Fig. 5.2). A depth map (in two-way travel time) of URU is shown in Fig. 5.12, together with illuminated shaded relief maps of this surface in the 3D surveys. The small-scale morphology of URU is characterised by mega-scale glacial lineations, suggesting erosion from fast-flowing ice. The dominant direction of the flow-lines, as inferred from the glacial lineations, is towards the north, indicating that the eroding ice sheet advanced from the Scandinavian mainland with a significant northward flow-component. A component of erosion from the east is also indicated from lineations in the NH9605 3D and in PL229 at the western end of the Coast-Parallel Trough, and may also be supported by the east-west direction of the Coast-Parallel Trough itself. Since R1 time (400-200 ka), the outer shelf in the southern Barents Sea has experienced a net accumulation and shelf aggradation. This transformation from net erosion to net accumulation, forming URU may be related to changes in glacial regime and sediment supply.

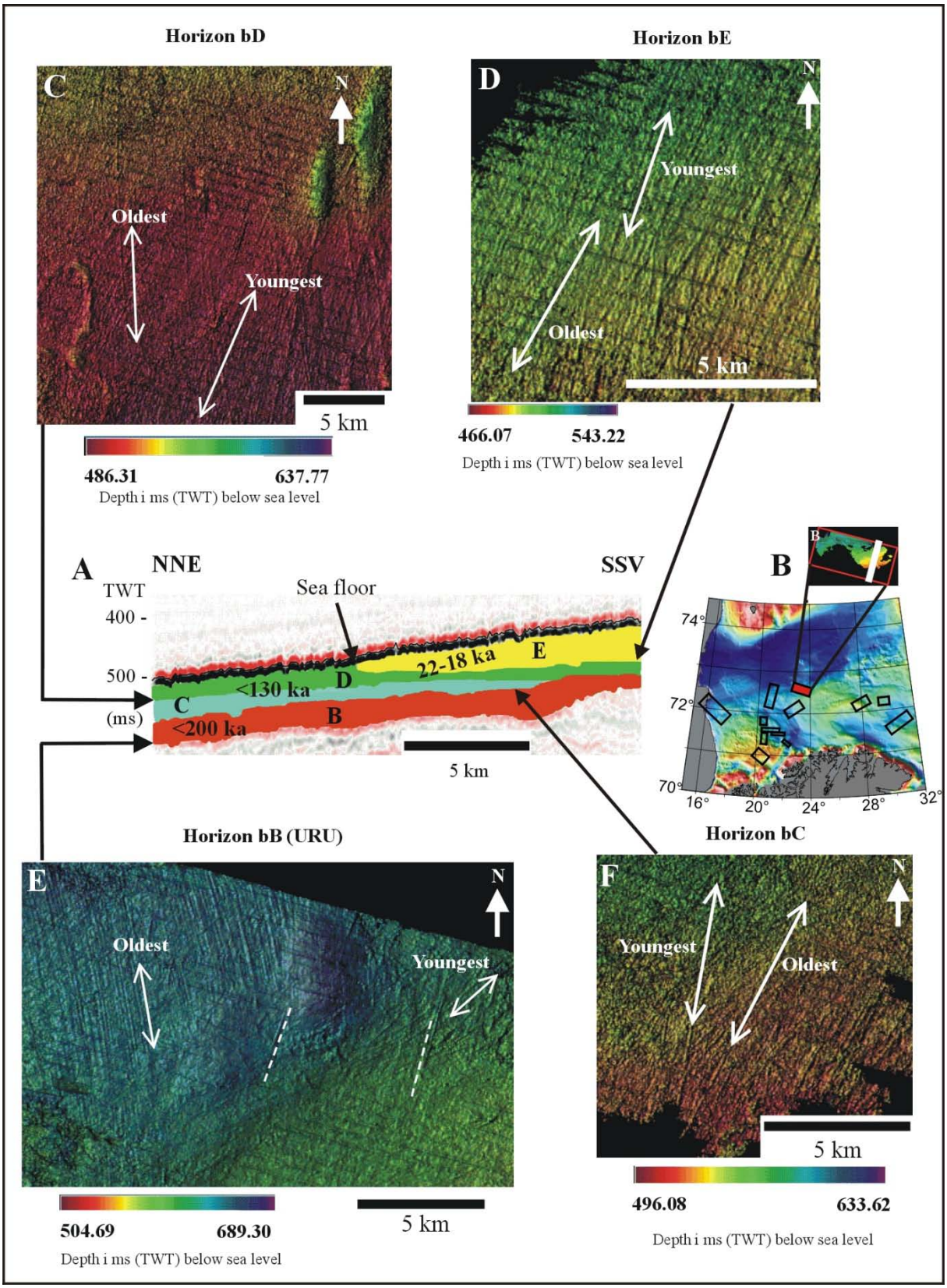

Figure 5.13. Stratigraphy from the 3D survey SG9804 in PL228, location of profile is indicated by the white line in Fig. 5.13B. (**B**) Map showing location of 3D area SG9804 (**C-F**) Illuminated shaded relief maps of the indicated seismic reflectors. Modified from Rafaelsen *et al.* (2002).

The glacigenic sequence of the southern Barents Sea has been mapped, divided in stratigraphic units (Solheim and Kristoffersen 1984; Vorren et al. 1990) and correlated to a shallow borehole (Hald et al. 1990; Sættem et al. 1992). Correlation to their work using 2D seismic is the basis for the age estimates of the stratigraphic units of the 3Ds in Area C and PL228, where Rafaelsen *et al.* (2002) identified five glacigenic units overlying sedimentary bedrock, results from PL228 are shown in Fig. 5.13. Although the 3D surveys of Rafaelsen *et al*. cover a relatively small area, they provide detailed images of interpreted stratigraphic horizons, showing flow lines of former ice sheets, and give conclusive evidence for erosion of grounded ice, whereas interpretation of glacial advances from 2D seismic data is more uncertain. The existence of mega-scale glacial lineations on four buried horizons (Fig. 5.13) that are regionally significant indicates at least four glacial advances in the southern Barents Sea.

URU can be followed basin-wide over the southern Barents Sea, whereas younger erosional events seem to have affected only part of the basin, eroding to great depth only locally (Fig. 5.5). Correlation of sea floor morphology and the stratigraphy in this area indicates that the erosion and deposition associated with ice streams at the end of the Weichselian glaciation to a large degree explains the localised distribution of the different seismic units (Fig. 5.5). We also see from the location of the 3Ds in the southern Barents Sea that erosion and deposition have been very different and had large variation over short areas, depending on location with respect to major ice streams and their associated deposits. The Bear Island Trough has been a main route for ice streams draining from the Svalbard and Barents Sea ice sheets, whereas local ice streams from the Norwegian mainland and from the east coast along Kola and Varangerhalvøya have had large effects on the shelf offshore Finnmark (Fig. 5.5).

So far, stratigraphic interpretation has been carried out only for the 3Ds of PL228 and Area G, and only as master thesis, and not with a good regional map of sea-floor morphology available. As for the other 3Ds in this area, we have just made a brief interpretation of the sea floor and URU for the 3Ds west of Ingøydjupet (Snøhvit and PL229) and offshore of Finnmark (Area G, Shell 3D and PL202), and comment in the following on different types of erosion/deposition that can be observed from the sea floor geomorphology or the geomorphology of URU.

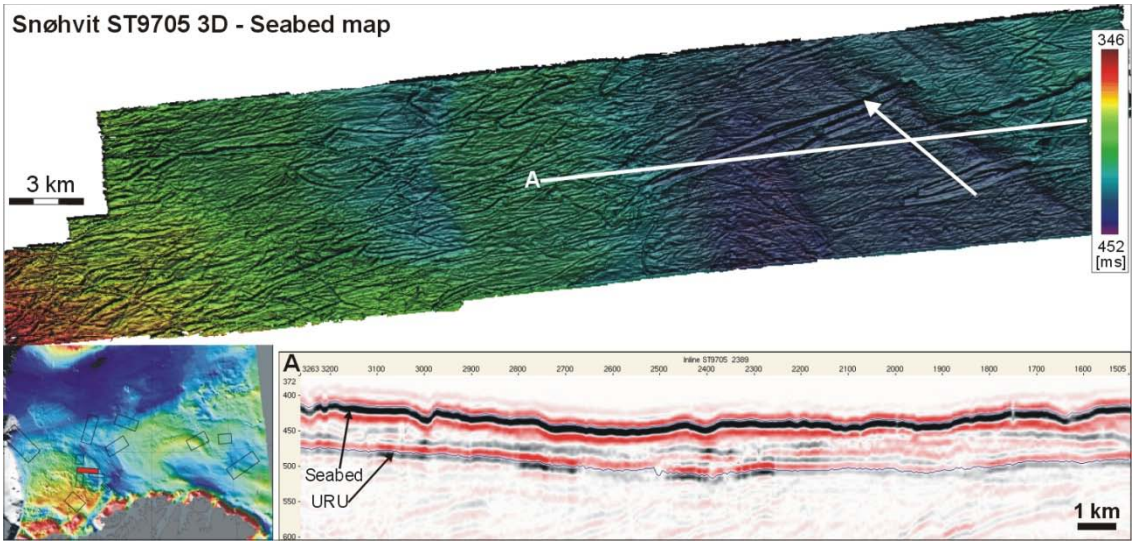

Figure 5.14. Sea floor shaded relief map from the Snøhvit area on the eastern flank of Tromsøyflaket. The white arrow indicates orientation of megascale glacial lineations.

The Snøhvit 3D area ST9705 is located at the eastern flank of Tromsøflaket. The white arrow in Fig. 5.14 indicates NNW-ESE-oriented grooves that are part of a bundle structure of glacial lineations. The regional sea floor map (Fig. 5.3) tells us that these grooves were probably eroded by an ice stream that drained out Ingøydjupet from the Norwegian mainland. Stratigraphic correlation suggests that this most likely happened at a late phase of the Last Glacial Maximum ice advance from the Scandinavian ice sheet. The westernmost part of the 3D area may not have been affected by the ice stream erosion. The grooves are disturbed by dominantly E-W oriented iceberg plough marks.

The area of SG9803 3D in **PL228** (Fig. 5.15) was also eroded by the ice stream that drained out Ingøydjupet at a late phase of the Last Glacial Maximum ice advance from the Scandinavian ice sheet. Part of a bundle structure of glacial lineations from this erosion (white arrow in Fig. 5.15) are barely visible on the sea floor shaded relief map of the 3D, but are clearly seen on the regional sea floor map (Fig. 5.5) that gives a better image of the large-scale morphological features. The north-eastern part of the area was shortly after affected by two depositional lobes that locally reached a total thickness of 70-80 m. The spill points in PL228 are extremely sensitive to tilting, and erosion and deposition of these sediment units may have influenced the spill points.

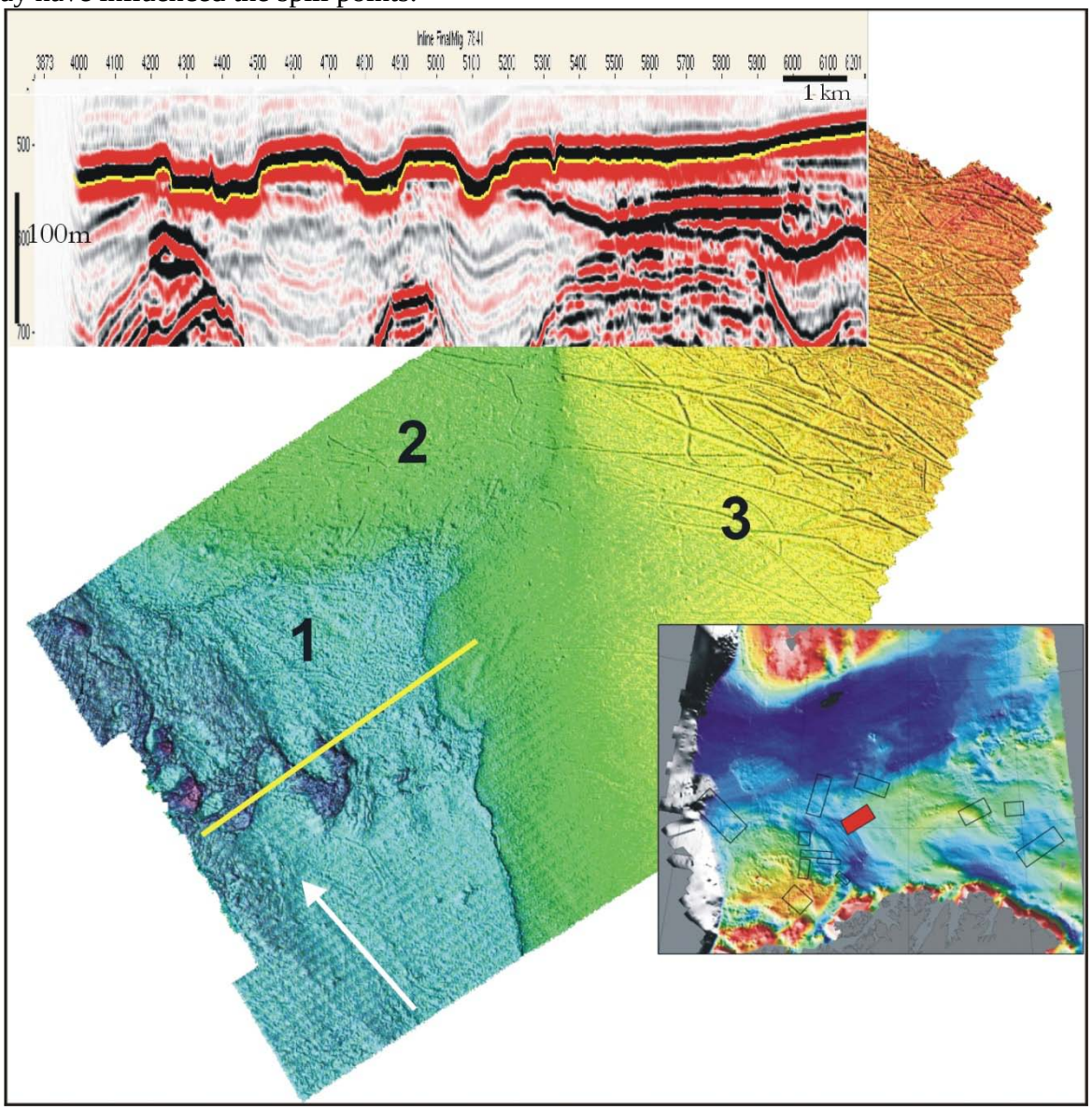

Figure 5.15. Shaded relief map of sea floor in SG9803 3D of PL 228. The white arrow indicates orientation of megascale glacial lineations (which are visualised more clearly on the regional sea floor map of Fig. 5.5A.

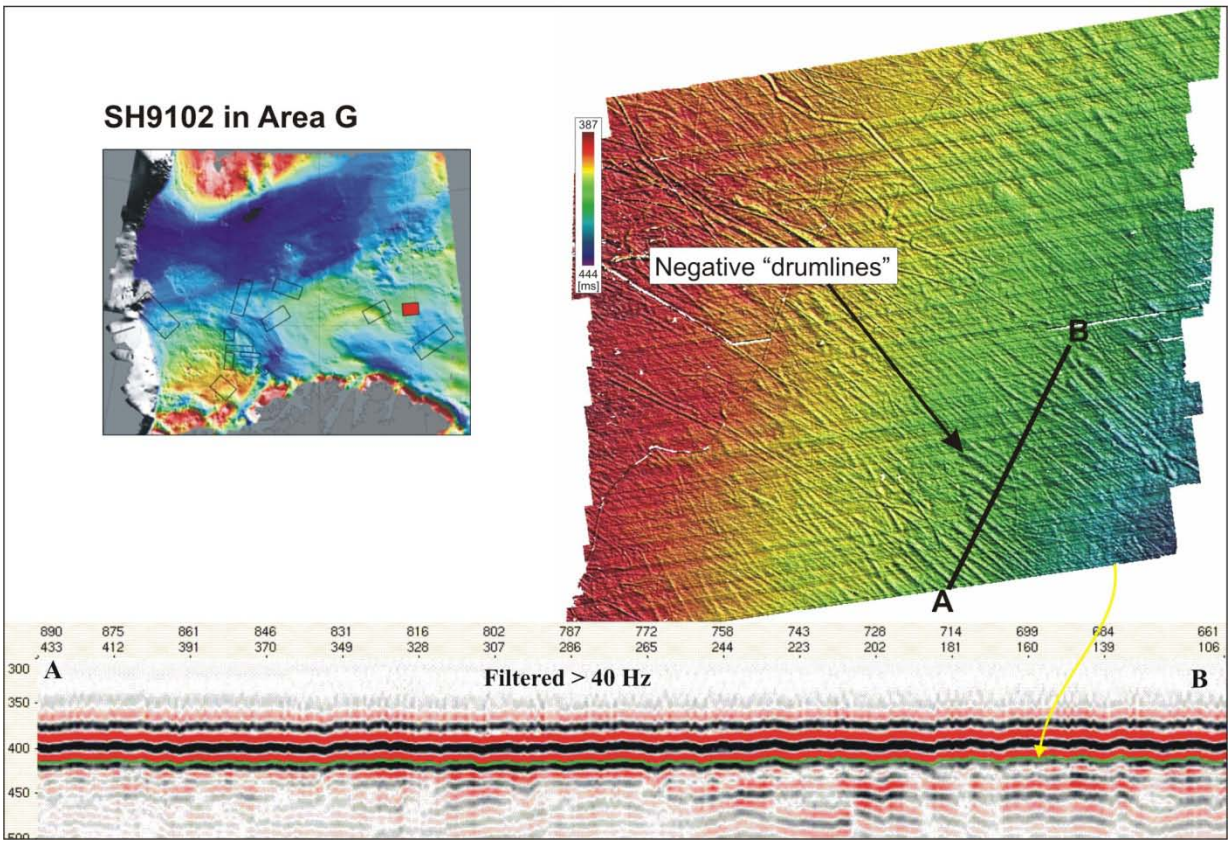

Figure 5.16. Shaded relief map of the sea floor in SH9102 in Area G. Negative "drumlines": What are they and how where they formed? SE-NW flutes but also other features are not yet understood.

The sea floor in SH9102, **Area G** (Fig. 5.16) shows SE-NW-oriented glacial flutes, indicating direction of ice flow, probably at the marginal zone of a local ice stream from south-east (Fig. 5.5A). Other features that are observed, negative "drumlins" are probably caused by glacial erosion, but similar features are not described in the literature and their formation is not understood.

The sea floor morphology of ST9802 Area G (Fig. 5.17) is totally dominated by glacial lineations, probably eroded by the same ice stream as formed the negative drumlins in SH9102. A younger sediment lobe has later buried the lineations in the south-western part of the 3D survey.

All 3Ds in the southern Barents Sea are affected by several phases of glacial erosion associated with URU, exemplified in Fig. 5.18.

A large portion of the glacigenic sequence in the 3D **SG9804 PL228** is disturbed by imbricated structures that in map view (on shaded relief maps of reflectors and on time slices) are U-shaped (Fig. 5.19 A and D). The structures cut through the whole sediment package above URU, and consist of sediment flakes that are stacked in an imbricated manner (Fig. 5.19 B and C). The imbricated structures are 200-300 m wide and can on time slices be followed as long lineations, for up to 5 km. A preliminary interpretation is that these structures are formed by glaciotectonic deformation, probably by fast-moving ice. This interpretation would fit nicely for imbrications with a dip towards the NE, suggesting an ice movement from north-east. However, since several of these structures have a dip towards SW, we must for the moment conclude that these are features that we do not understand.

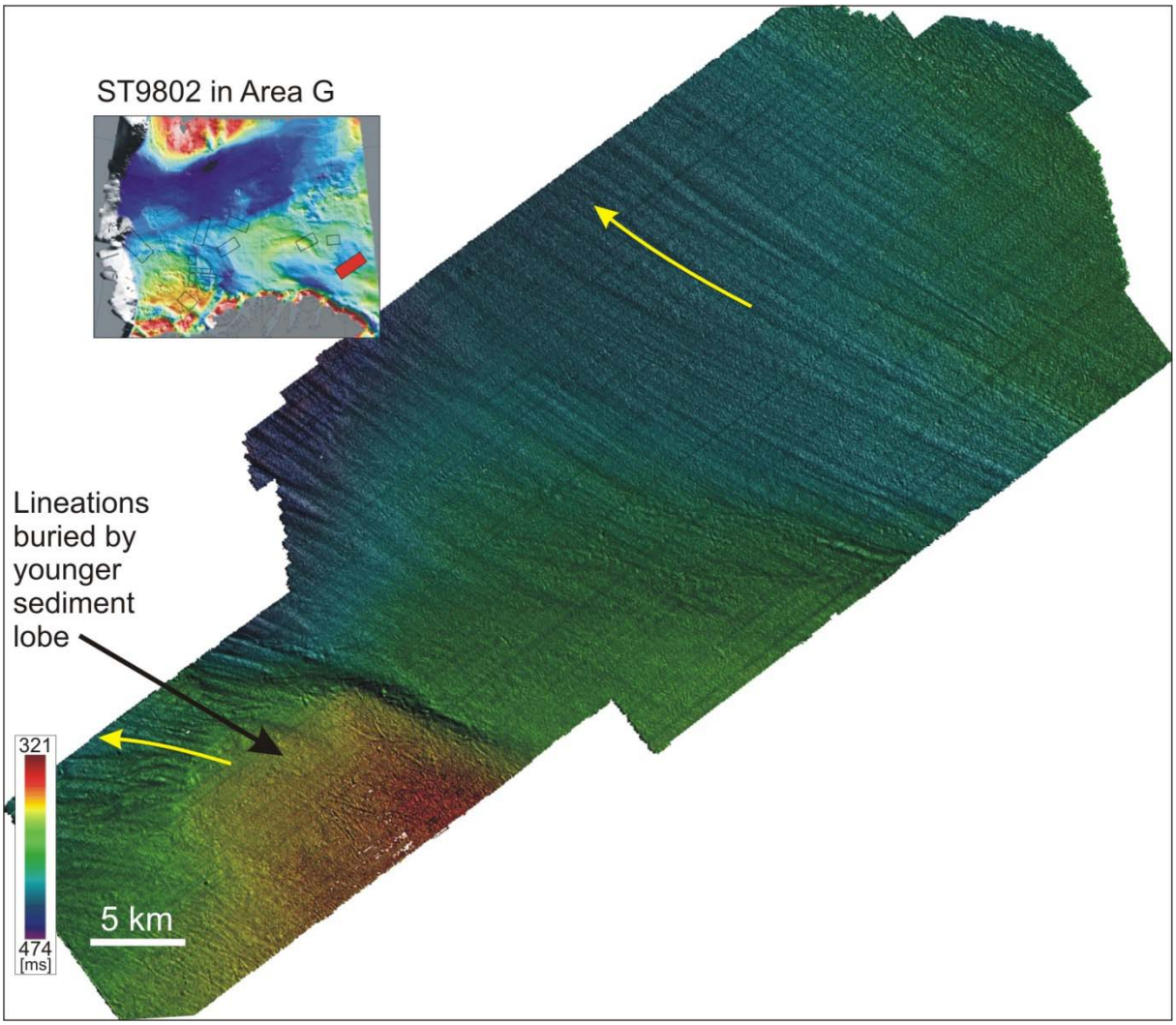

Figure 5.17. Shaded relief map of sea floor in Area G. Strong glacial lineations from a grounded ice are in the SW buried by a younger sediment lobe.

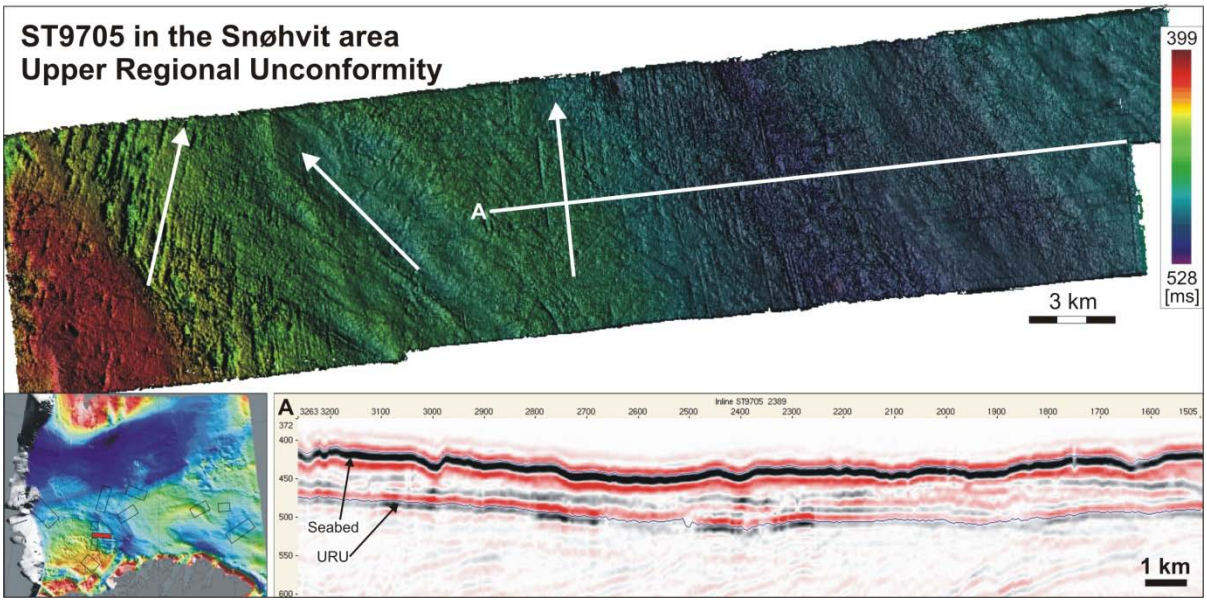

Figure 5.18. Shaded relief map of URU in the ST9705 3D in Snøhvit. White arrow indicate flow-direction of former glaciers eroding the area at R5 time (~200–440 ka).

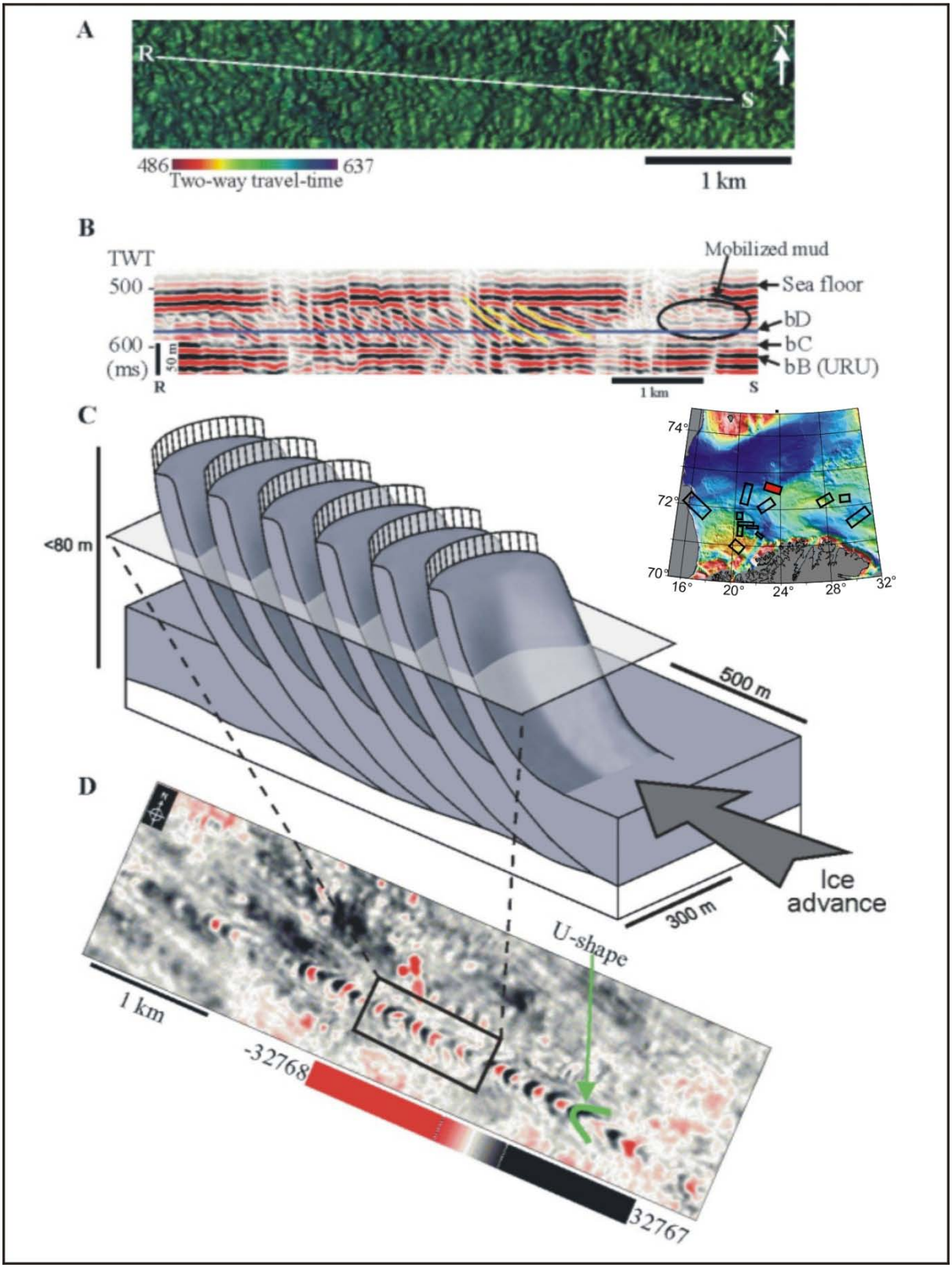

Figure 5.19. A) Interpreted horizon bC with an imbricated structure from 3D SG9804 in PL228. **B)** Seismic profile showing an imbricated structure dipping towards east with a blue line indicating where the time slice in Fig. 5.19D is taken from. Yellow lines indicate stacked flakes. **C)** Sketch showing a glaciotectonic imbricated structure in three dimensions. **D)** Time slice at 572 ms below sea level showing the imbricated structure. From Rafaelsen *et al.* (in prep).

5.2. Eastern Barents Sea and NW Russia

5.2.1. Eastern Barents Sea

We have not had any seismic data available from the Russian part of the Barents Sea, and summarize here some of the findings from the literature. Glacigenic deposits of the Central Deep (fig.5.20 A and B) is a key to the Late Quarternary evolution of the eastern Barents Sea (Gataullin *et al.* 1993). Sparker and shallow drilling data indicate that these deposits consist of basal till and glacial marine sediments deposited deposited during the last glacial cycle. Glaciotectonic features imply strong glacial erosion of Mesozoic bedrock. The generalised movement is assumed to have been from off Novaya Zemlya and it is concluded that the whole eastern Barents Sea was covered by the late Weichselian ice sheet (Gataullin *et al.* 1993).

Seismic investigations and shallow boreholes from the Pechora Sea carried out by various institutions and expeditions of the former USSR show that glaciotetonic deformation is common, in the glacigenic sediments (Fig. 5.20C) and in the underlying bedrock (Gataullin *et al.* 2001). The borings indicate that the bedrock has experienced strong shear stress from glacial flow (Gataullin *et al.* 1993; Gataullin & Polyak 1997), which appears as a strongly deformed bedrock in the 5-10 upper m. Small thrust faults, disharmonic drag and flow folds are common. On several seismic profiles, parallel dipping reflectors within the Cretaceous sequence become abruptly fractured near the bedrock surface, interpreted as the results of glaciotectonic dislocation of the pre-glacial strata. In the area with Triassic rocks, the glaciotectonic deformations are confined to this zone, usually not exceeding 1 m, whereas in the soft Cretaceous sediments the deformed zone may be as thick as 20-25 m (Gataullin *et al.* 2001). Coastal cliffs at the Kanin Peninsula commonly show glacialtectonically stacked sequences of Quaternary till and intratill sequences, suggesting that glaciotectonic deformation and transportation of sediments may be common processes in this area.

On the Kara Sea shelf, the pre-Quaternary strata appear to be widely truncated by glacial erosion (Fig. 3.3). Major ice domes were located over the Kara Sea shelf during the Late Saalian and during the Early- and Middle Weichselian, and most likely these ice sheets reached the Arctic Ocean (Svendsen *et al.* in press). The youngest till on the sea floor northeast of Severnaya Zemlya is of Middle Weichselian age, indicating a grounded ice sheet down to at least 340 m water depth (Knies *et al.* 2000).

The general absence of debris-flow lobes northeast of Severnaya Zemlya during MIS 3 suggests that there was a complete deglaciation of the eastern Kara Sea shelf following the early Middle Weichselian glaciation (Kleiber *et al.* 2000; Svendsen *et al.* in press). During the Late Weichselian the southern ice sheet limit was located on the sea floor off the Siberian mainland (Svendsen *et al.* in press). The south-eastern margin of the LGM Barents-Kara ice sheet was contained in the south-western Kara Sea east of the Novaya Zemlya Trough (Polyak *et al.* 2000).

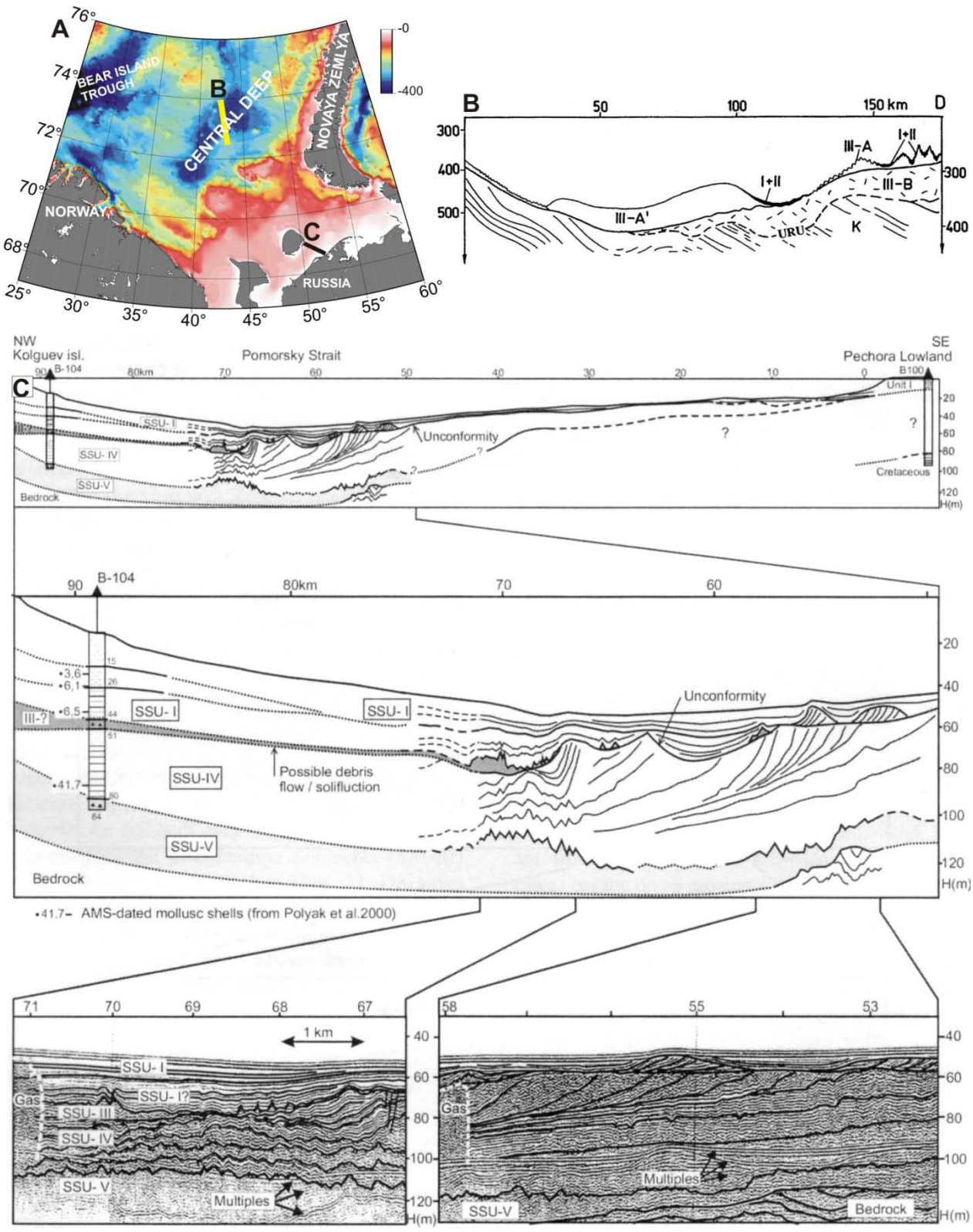

Figure 5.20. Seismic profiles and interpreted sketches from offshore Russia. Fig. 5.20 A and B are from Gataullin *et al.* (1993); C is from Gataullin *et al.* (2001).

Figure 5.21. Section at the Kanin Peninsula showing glacialtectonically stacked sequences of till and intratill sediments. The upper light bed is glaciolacustrine and not involved in thrusting. Note encircled persons for scale.

5.2.2. Northwest Russia

The northern part of Russia has been affected by major glaciations several times during the Quaternary. Ice sheets from both Scandinavia and the Barents and Kara Sea have expanded onto the mainland, but the timing and dimensions of these ice sheets have been debated (Velichko 1987; Grosswald 1993; Svendsen *et al.* in press). In the European part of Russia, the maximum Quaternary ice extent was reached by the Dnieper and Don ice lobes, which extended south to 50°N. The Don lobe may be between 400 and 600 ky old (Velichko *et al.* in press). In sections in NW Russia one often find Saalian till below Eemian marine sediments. This till sheet extends much farther south than any of the younger till beds from the last glaciation. Thus the Saalian glaciation caused considerably glacioisostatic depression leading to marine deposition up to more than 130 m above present sea level on northern Cape Kanin in the subsequent interglacial (Eemian). In a brief interval during the interglacial there was a seaway between the Gulf of Bothnia and the White Sea (Funder *et al.* 2002). It is also worth noting that all except one glacier advance during the last glaciation were followed by sea levels lower than the present, suggesting moderate glacioisostatic depression probably related to thin ice.

The Arkhangelsk region is especially important for reconstructing ice sheet variations for the last glaciation both because it was a confluence area for ice flowing from the Kara, the Barents and the Scandinavian Ice Sheets (Fig. 5.22), and because sediments are well preserved in the area (Fig. 5.23).

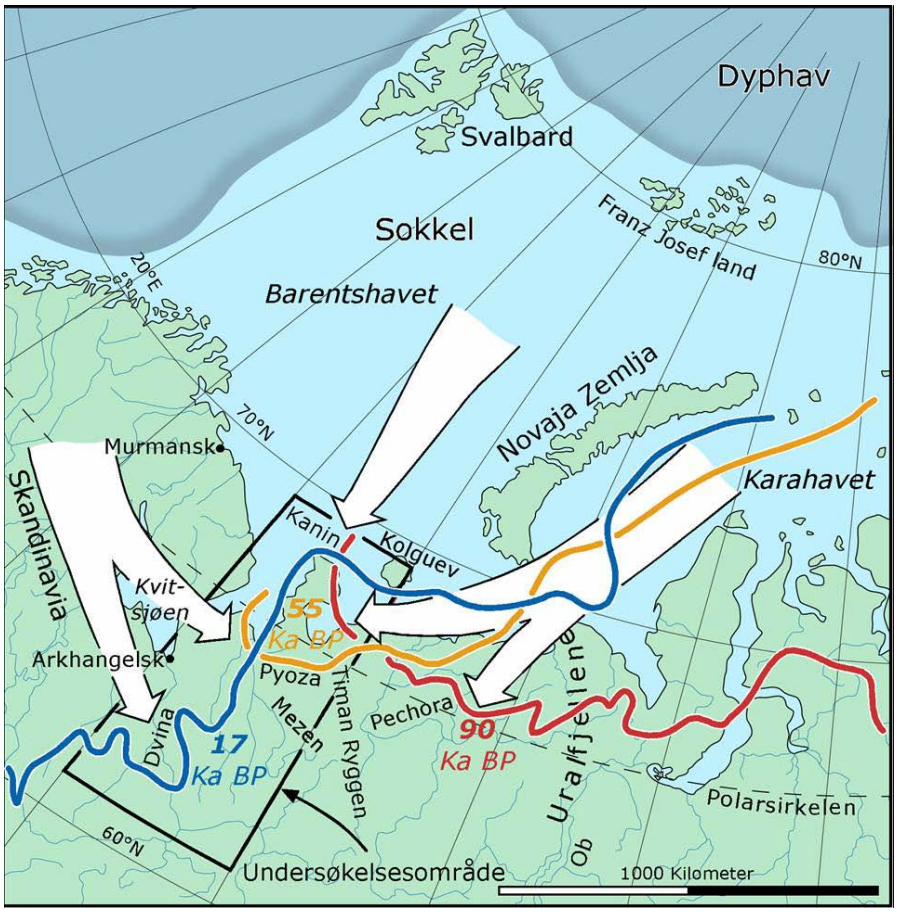

Figure 5.22. Map showing the Arkhangelsk area (framed), Weichselian maximum positions of the Kara, the Barents and the Scandinavian Ice Sheet (full lines) and main ice-flow lines for these ice sheets. Larsen *et al.* (in prep).

Numerous coastal and river sections in the Arkhangelsk region have been investigated over the last years with the main goal to reconstruct Weichselian glacier variations (Larsen *et al.* 1999a; Larsen *et al.* 1999b; Houmark-Nielsen *et al.* 2001; Kjær *et al.* 2001; Lysså *et al.* 2001; Kjær *et al.* 2003). The coastal section at Cape Tolstik (Fig. 5.23) is one of the best showing three periods of glaciation with intervening ice free periods. One of these ice-free periods (ca. 65 ky ago), is represented by tidal sediments (Fig. 5.23) evidencing a sea level approximately 50 meters above present. This high sea-level was caused by isostatic adjustment after the previous glaciation.

Figure 5.23. Part of a 4-km long section at Cape Tolstik on the SE White Sea coast. The lower till is from a local ice cap centered over the Timan ridge, the middle till was deposited by the Barents Sea Ice Sheet, and the upper till by the Kara Sea Ice Sheet (Kjær *et al.* 2003).

Figure 5.24 sums up the main paleoenvironmental results along a profile from the southwestern White Sea to the Timan ridge in the east. During the last glaciation NW Russia has been invaded by ice sheets both from Scandinavia and the Barents and Kara Sea (Fig. 5.24). It shows that the Barents and Kara Ice Sheets invaded the Russian mainland several times in Early to Middle Weichselian time. Only in Late Weichselian time did the Scandinavian Ice Sheet penetrate into Russia from the west. Between the different glacier advances there was more or less complete deglaciation with mainly fluvial and/or marine sedimentation.

Even if there are inconsistencies between the glacial records west and east of the Timan ridge (Fig. 5.25: curves c and d), it is no doubt that the Barents-/Kara ice sheets reached maximum during Early to Middle Weichselian time, whereas the Scandinavian ice sheet reached maximum in Late Weichselian time (Svendsen *et al.* in press). Thus there is an asynchroneity in size of the ice sheets through time. The oldest evidence (ca. 90 ka) of glacier advance during the last glaciation is found in the Pechora lowlands (Fig. 5.25D) (Svendsen *et al.* in press). Only weak evidence for this glacial advance is found west of the Timan ridge (Houmark-Nielsen *et al.* 2001), but it may be that the ice sheet reached the northern part of Cape Kanin (Larsen *et al.* in prep.). In Middle Weichselian time there is evidence of two advances of the Barents-/Kara ice sheet west of the Timan ridge (Kjær *et al.* 2003), but only one is found east of the Timan ridge (Svendsen *et al.* in press), cf. Figure 5.25. C and D. Between the two glacier advances of Middle Weichselian time there was a marine transgression up to some 50 m above present sea level. These glacier advances were preceded by ice centred over the Timan ridge (Houmark-Nielsen *et al.* 2001; Kjær *et al.* 2003). The Scandinavian ice sheet reached its maximum approximately 17 ky ago and only the westernmost part of Russia was affected (Larsen *et al.* 1999a). At this time the Barents-/Kara ice sheet ended north of mainland Russia. Glacier variation curves for different parts of the ice sheets (Fig. 5.25 A-E) form the foundation for constructing the spatial distribution of Weichselian glaciers (Fig. 4.3).

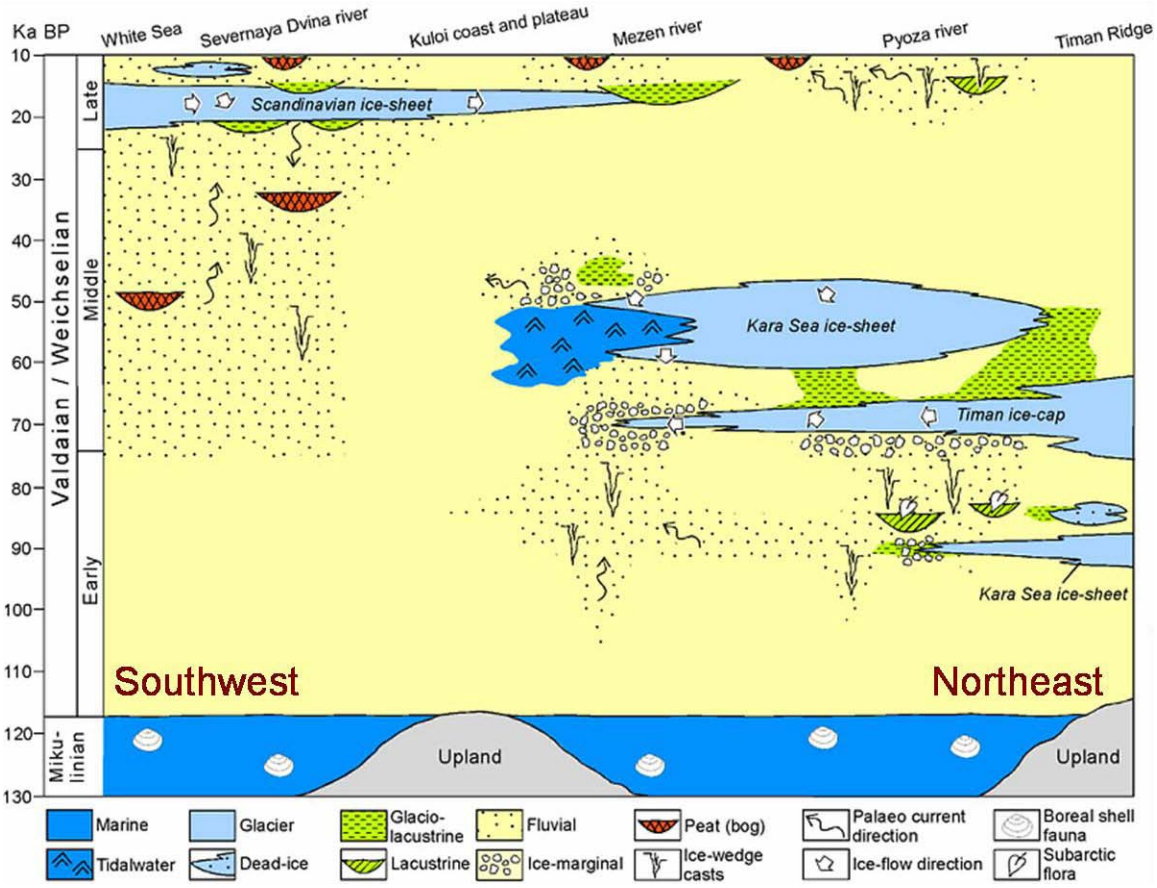

Figure 5.24. Event stratigraphy for the Arkhangelsk region illustrating both ice sheet advances and sedimentary environments through time. From Kjær (2001).

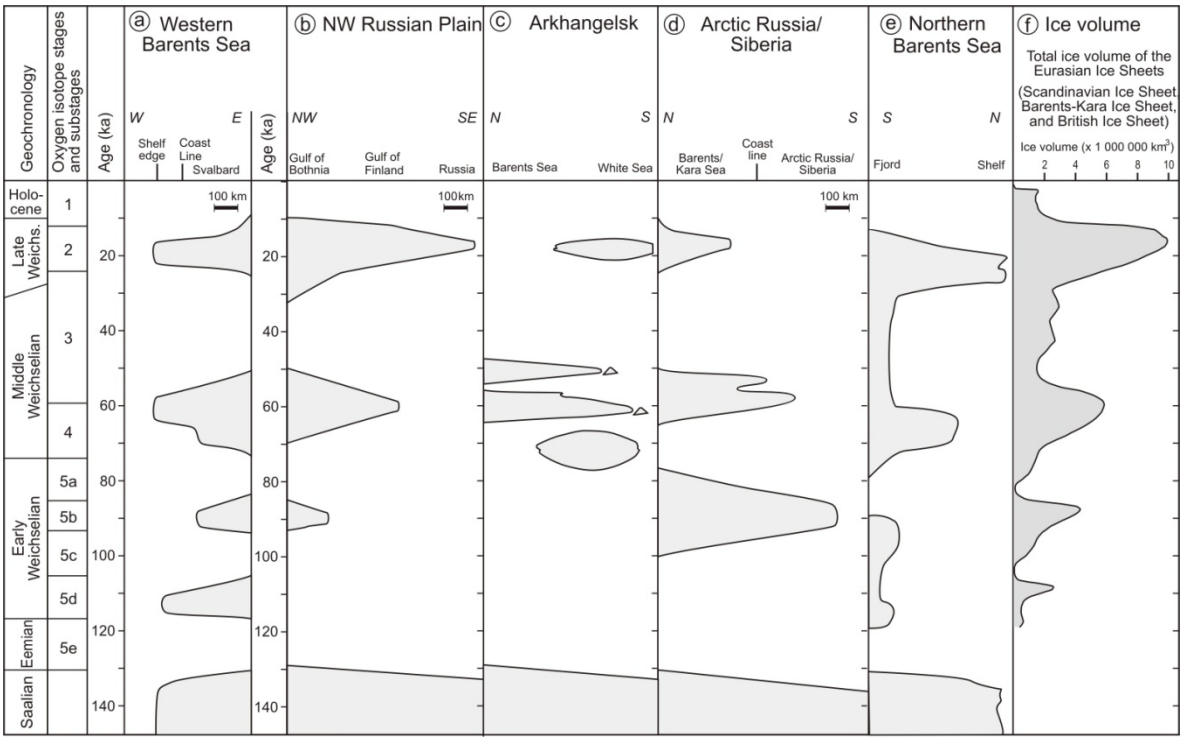

Figure 5.25. Glaciation curves from peripheral areas of the Scandinavian, the Barents Sea and the Kara Sea Ice Sheet. Compiled by Svendsen *et al.* (in press) and Larsen *et al.* (in prep.).

The Early Weichselian ice advance in the Pechora lowland (Fig. 5.25D) blocked the Pechora river and a large ice dammed lake, the Komi lake was formed in front of it (Mangerud *et al.* 2001). The shoreline elevation of Lake Komi ranges from 90 m a.s.l. in the south to 110 m in the north, reflecting a larger glacioisostatic depression near the ice margin in the north (Mangerud *et al.* 2001). Mangerud *et al.* (2001) also suggested that the Komi lake also covered a huge area west of the Timan ridge (Fig. 5.26). However, no lake sediments corresponding to the Komi lake is found west of the Timan ridge (Fig. 5.24). On the contrary, fluvial sediments show northbound drainage suggesting that at this time the rivers Mezen and Dvina were not blocked. If correct this means that there was no contact between the Scandinavian and the Barents-/Kara ice sheet in early Weichselian time (Kjær *et al.* 2003).

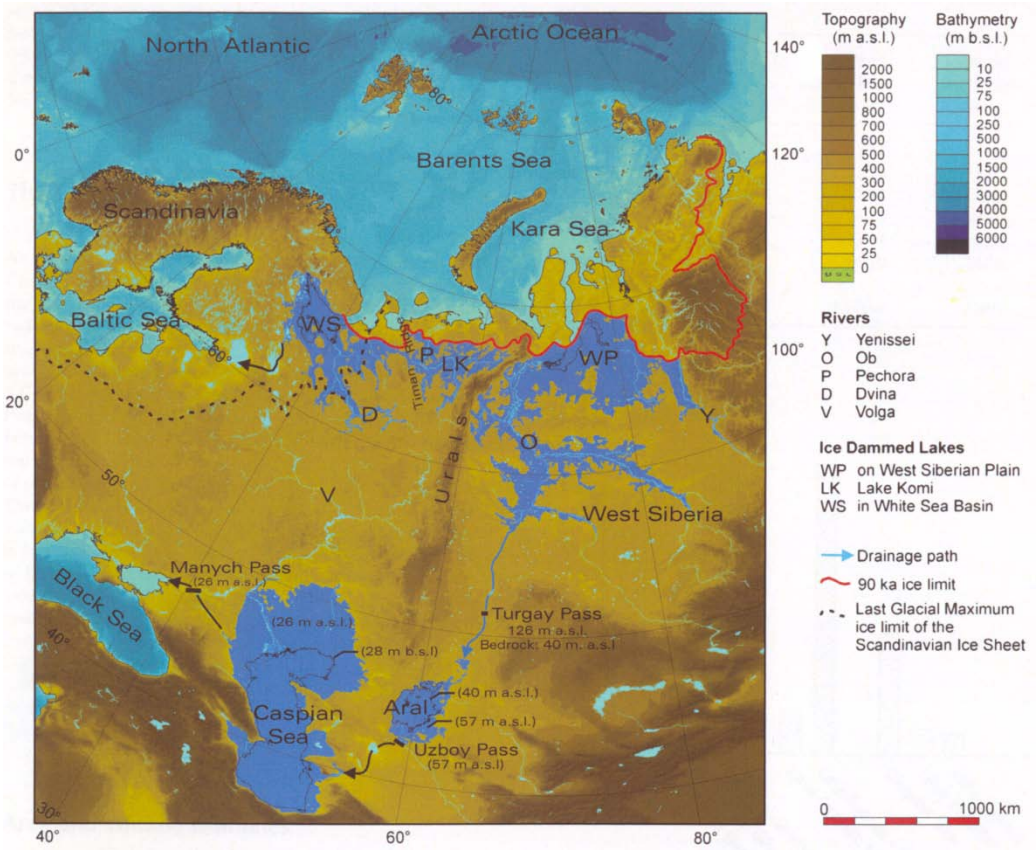

Figure 5.26. The Early Weichselian ice-dammed lake Komi in northern Russia according to Mangerud *et al.* (2001). The postulated lake west of the Timan ridge is at odd with geological data from the White Sea region.

5.2.3 Sea levels and glacioisostatic adjustment

The Saalian glaciation was much larger than any of the subsequent Weichselian glaciations (Figs. 4.2 and 4.3). Thus due to glacioisostatic depression, relative sea level in the last interglacial sea level was much higher than today, and in a short period of time during peak interglacial there was a sea-way between the Gulf of Bothnia and the White Sea (Fig. 5.27).

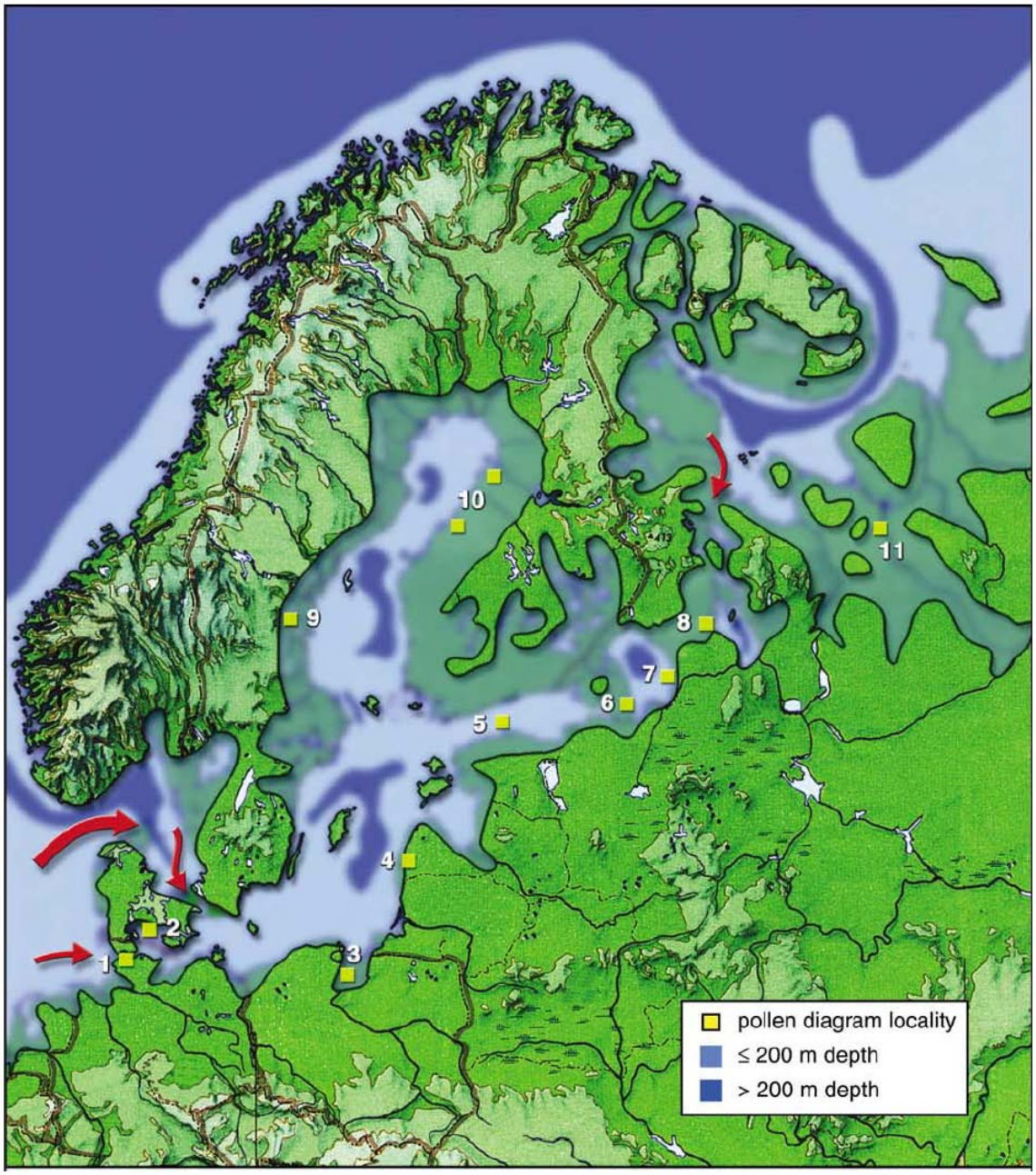

Figure 5.27. The Baltic-White Sea region at the peak of marine inundation in the Early Eemian, tentatively dated to ca. 130 ka. From Funder *et al.* (2002).

In Middle Weichselian time, ca. 65 ka, sea level was approximately 50 m above present sea level. Raised tidal sediments from this period are found at many sites in the Arkhangelsk area (cf. Figs. 5.23 and 5.24). The high sea level was caused by glacioisostatic depression due to glacial events prior to this ice free period (cf. Fig. 5.25 curve c). It is also worth noting that this is the only period in the Weichselian with a higher-than-present sea level, although there were several glacial events. This probably reflects thin ice and/or lower eustatic sea level in the other periods in question.

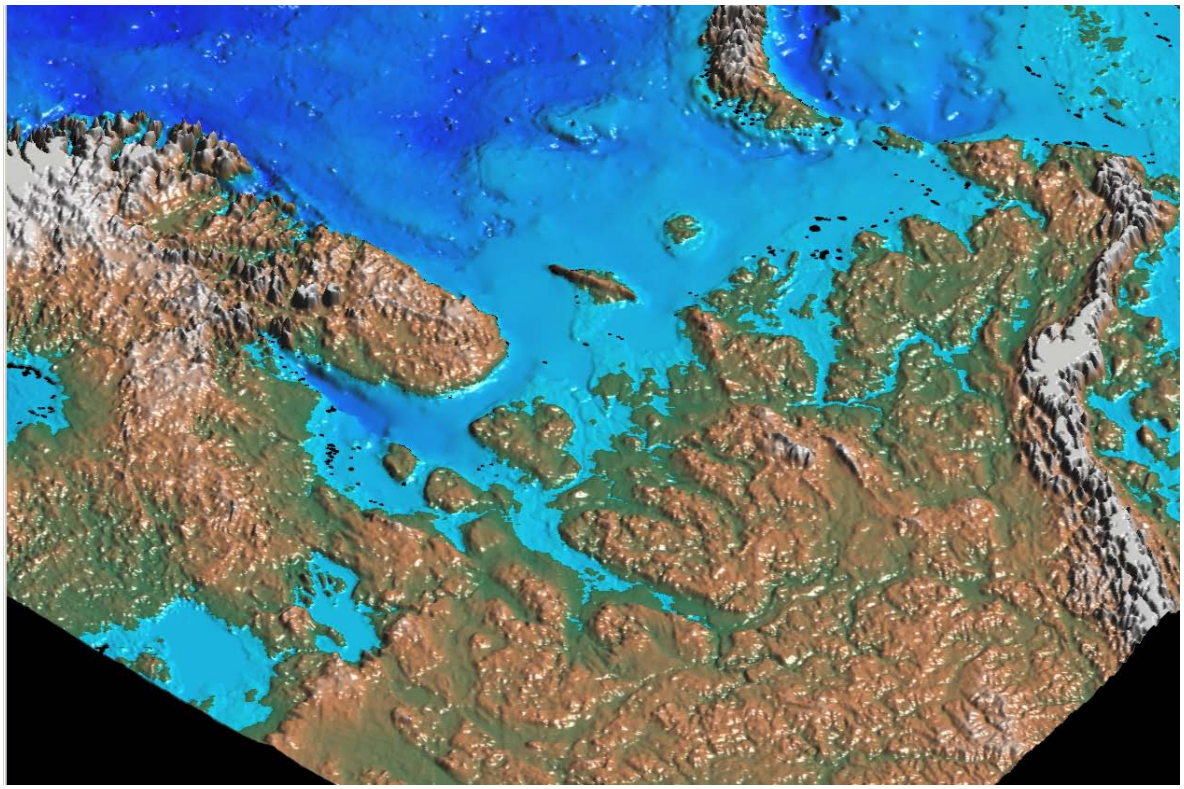

Figure 5.28. Reconstruction of a Middle Weichselian (ca. 60 ka) high sea level 50 m above present (Jensen & Larsen in prep.).

Only for the last interglacial (Fig. 5.27) and the Middle Weichselian (Fig. 5.28) in addition to the period following the last deglaciation (Fig. 4.6), there is enough information to reconstruct former sea levels. For other periods, either chronology is poor or the information is scarce. Nevertheless, Fig. 5.29 shows a compilation of sea-level information from various sites. More details are given in Table A3 in the appendix.

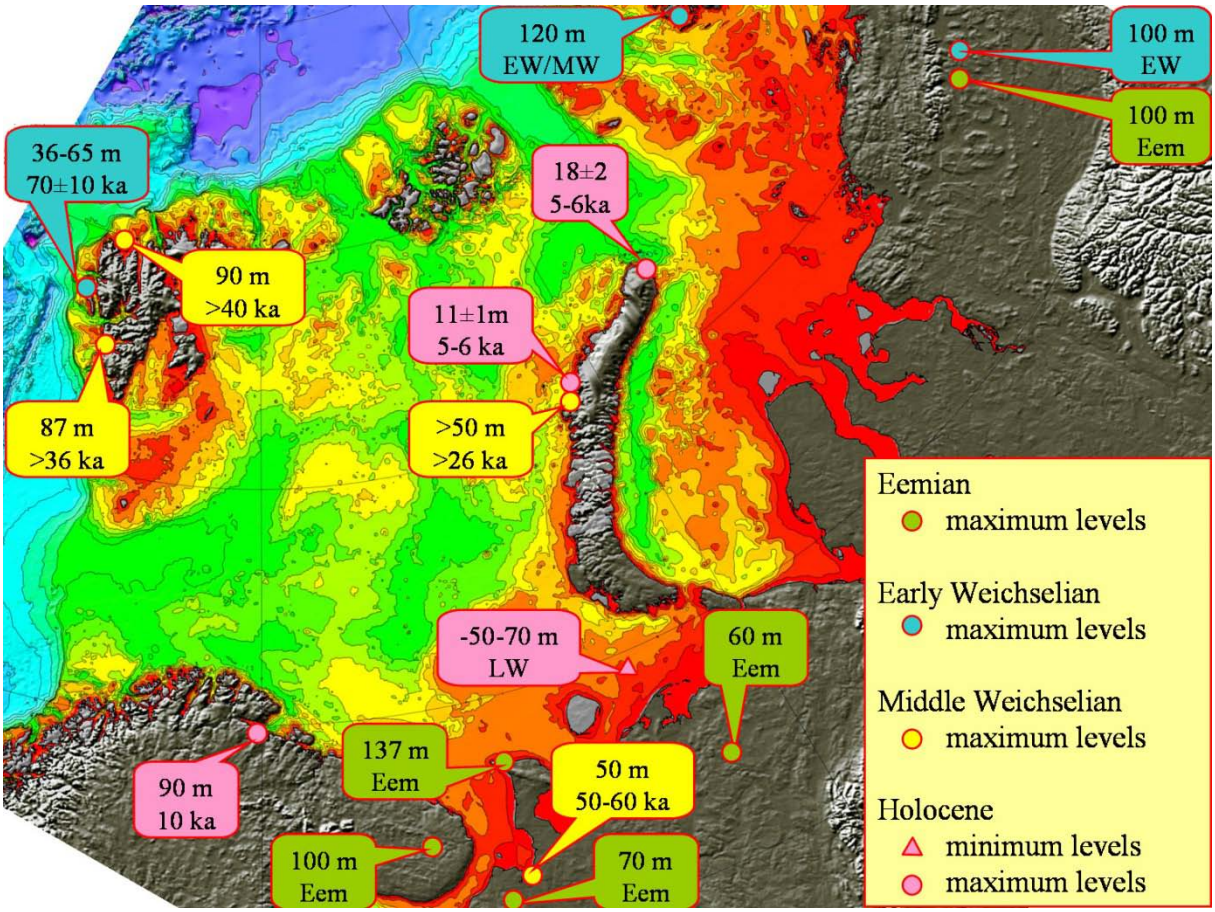

Figure 5.29. Compilation of past sea levels in the Barents Sea region. The dating of these earlier events is not as good as for the last deglaciation, and it has not been possible to construct isobase maps for these periods. The figure only gives a minimum estimate of the glacioisostatic loading at various times, as the highest sea level indicators may not have been found. Despite these difficulties, the sea level indicators give a hint about previous glaciation centres and ice thicknesses. See Table A3 in the appendix for references and further information.

The sea-level record from the southern Pechora Sea (Fig. 5.30) shows the relative, the eustatic and the isostatic component locally from that area between ca. 35 ka and the present. It may be that sea-level during the last glacial maximum was more than hundred meters lower than today (Svendsen *et al.* in press) as also suggested by Pavlidis *et al.* (2002). With more empirical data on the tidal sediments from Russia at hand (Figs. 5.23 and 5.24) it will be possible to extend the curves (Fig 5.30) back in time to 65 ka, and model the preceding glaciation.

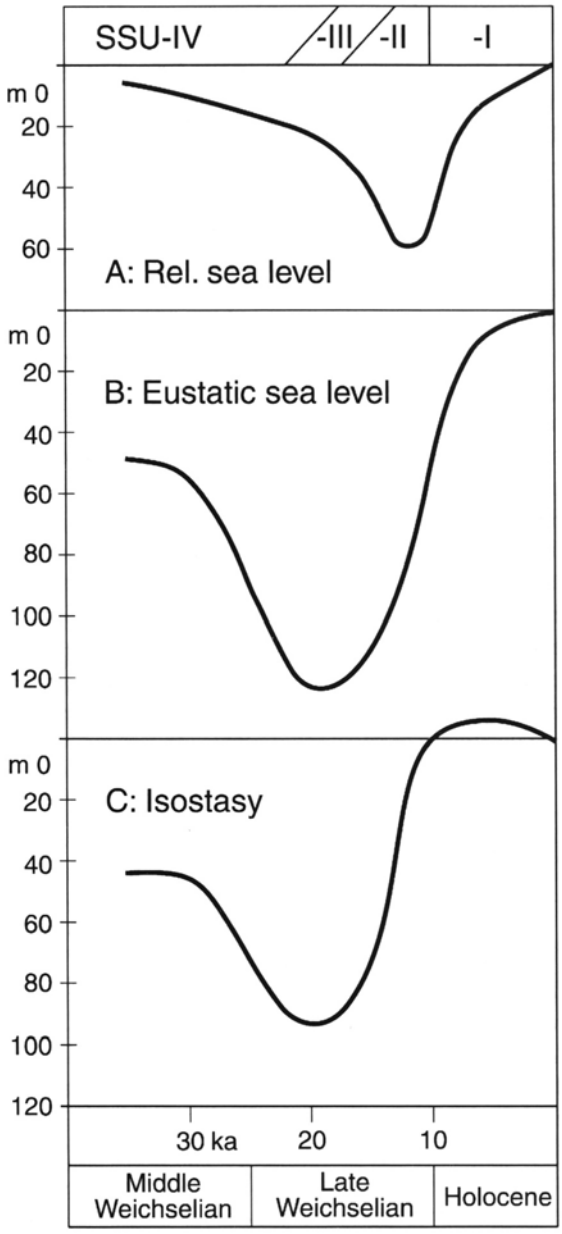

Figure 5.30. A) Inferred relative sea level curve for the southern Pechora Sea for the last 35 ka. **B)** Eustatic sea level curve, **C)** The resultant isostatic curve when B) is subtracted from A). From Gataullin *et al.* (2001).

6. Continuation of the project

Objective:

- Develop models for Pliocene - Pleistocene erosion in the Barents Sea explaining when and where erosion took place, and relative amounts through time.

Links to work in 2003:

We have developed a three-step conceptual model for the style of Plio-Pleistocene glaciations in the southwestern Barents Sea region. The model suggests that the southwestern Barents Sea was mainly influenced by glacial erosion in the youngest of the three phases (last 0.5 mill. years). The work in 2004 aims at testing and refining this conceptual model.

Proposed work in 2004:

Realizing that glacial erosion was by far the most important erosional agent, we need to develop glaciation models that span the entire Pliocene-Pleistocene in order to meet the above objective. Part of the work will be done through a joint work-shop with the Seabed Project and through interaction with modellers. The work package is listed below.

- 3D seismic interpretation, and correlations mainly through 2D seismic lines to improve glaciation models.
- Field work at three known key sites with glacially induced high sea levels to improve glaciation models.
- Synthesize available information on glaciations, including sea level variations, in the Barents Sea region.
- Include all data relevant for isostatic/flexural modelling on an ArcView platform.

References

Andersen, B. G. & Borns, H. W. 1997: *The ice age world*. 208. Scandinavian University Press, Oslo.

Andersson, T., Forman, S. L., Ingólfsson, Ó. & Manley, W. F. 1999: Late Quaternary environmental history of central Prins Karls Forland, western Svalbard. *Boreas 28*, 292-307.

Andersson, T., Forman, S. L., Ingólfsson, Ó. & Manley, W. F. 2000: Stratigraphic and morphologic constraints on the Weichselian glacial history of northern Prins Karls Forland, western Svalbard. *Geografiska Annaler 82A*, 455-470.

Bolshiyanov, D. Y. & Makeyev, V. M. 1995: *Archipelago of Severnaya Zemlya: Glaciation, Environmental History*. 216. Gidrometeoizdat, St. Petersburg.

Butt, F. A., Elverhøi, A., Solheim, A. & Forsberg, C. F. 2000: Deciphering late Cenozoic development of the western Svalbard margin from ODP Site 986 results. *Marine Geology 169*, 373-390.

Butt, F. A., Drange, H., Elverhøi, A., Otterå, O. H. & Solheim, A. 2002: Modelling late Cenozoic isostatic elevation changes in the Barents Sea and their implications for oceanic and climatic regimes; preliminary results. *Quaternary Science Reviews 21*, 1643-1660.

Canals, M., Urgeles, R. & Calafat, A. M. 2000: Deep sea-floor evidence of past ice streams off the Antarctic Peninsula. *Geology 28*, 31-34.

Channell, J. E. T., Smelror, M., Jansen, E., Higgins, S. M., Lehman, B., Eidvin, T. & Solheim, A. 1999: Age models for glacial fan deposits off east Greenland and Svalbard (Sites 986 and 987). *In* Raymo, M. E., Jansen, E., Blum, P. & Herbert, T. D. (eds.): *Proceedings of the Ocean Drilling Program, Scientific Results*, 149-166.

Clark, C. D., Knight, J. K. & Gray, J. T. 2000: Geomorphological reconstruction of the Labrador Sector of the Laurentide Ice Sheet. *Quarternary Science Reviews 19*, 1343-1366.

Corner, G. D., Yevzerov, V. Y., Kolka, V. V. & Møller, J. J. 1999: Isolation basin stratigraphy and Holocene relative sea-level change at the Norwegian-Russian border north of Nikel, Northwest Russia. *Boreas 28*, 146-166.

Dimakis, P., Braathen, B. I., Faleide, J. I., Elverhøi, A. & Gudlaugsson, S. T. 1998: Cenozoic erosion and the preglacial uplift of the Svalbard-Barents Sea region. *Tectonophysics 300*, 311-327.

Doré, A. G. & Jensen, L. N. 1996: The impact of late Cenozoic uplift and erosion on hydrocarbon exploration: offshore Norway and some other uplifted basins. *Global and Planetary Change 12*, 415-436.

Eidvin, T. & Riis, F. 1989: Nye dateringer av de tre vestligste borehullene i Barentshavet. Resultater og konsekvenser for den tertiære hevingen. *Norwegian Petroleum Directorate Contrib. 27*, 44 pp.

Eidvin, T., Jansen, E. & Riis, F. 1993: Chronology of Tertiary fan deposits off the western Barents Sea: Implications for the uplift and erosion history of the Barents Shelf. *Marine Geology 112*, 109-131.

Eidvin, T. & Nagy, J. 1999: Foraminiferal biostratigraphy of the Pliocene sequence at Site 986. *In* Raymo, M. E., Jansen, E., Blum, P. & Herbert, T. D. (eds.): *Proceedings of the Ocean Drilling Program, Scientific Results*, 3-17.

Eidvin, T., Jansen, E., Rundberg, Y., Brekke, H. & Grogan, P. 2000: The upper Cainozoic of the Norwegian continental shelf correlated with the deep sea record of the Norwegian Sea and the North Atlantic. *Marine and Petroleum Geology 17*, 579-600.

Eidvin, T. E., Goll, R. M., Grogan, P., Smelror, M. & Ulleberg, K. 1998: The Pleistocene to Middle Eocene stratigraphy and geological evolution of the western Barents Sea continental margin at well site 7316/5-1. *Norsk Geologisk Tidsskrift 78*, 99-123.

Elverhøi, A., Svendsen, J.-I., Solheim, A., Milliman, J. D., Mangerud, J. & Hooke, R. L. 1995: Late Quarternary sediment yield from the high Arctic Svalbard area. In *J. Geol.*

Faleide, J. I., Vågnes, E. & Gudlaugsson, S. T. 1993: Late Mesozoic-Cenozoic evolution of the southwestern Barents Sea. *In* Parker, J. R. (ed.): *Petroleum geology of Northwest Europe: Proceedings of the 4th conference.*, 933-950. The Geological Society of London, London, United Kingdom.

Faleide, J. I., Solheim, A., Fiedler, A., Hjelstuen, B. O., Andersen, E. S. & Vanneste, K. 1996: Late Cenozoic evolution of the western Barents Sea-Svalbard continental margin. *Global and Planetary Change 12*, 53-74.

Fiedler, A. & Faleide, J. I. 1996: Cenozoic sedimentation along the southwestern Barents Sea margin in relation to uplift and erosion of the shelf. *Global and Planetary Change 12*, 75-93.

Fjeldskaar, W. 2001: Post-glacial and Tertiary uplift 15. Rogaland Research, Stavanger.

Forman, S. L., Lubinski, D. J., Zeeberg, J. J., Polyak, L., Miller, G. H., Matishov, G. & Tarasov, G. 1999: Postglacial emergence and Late Quaternary glaciation on northern Novaya Zemlya, Arctic Russia. *Boreas 28*, 133-145.

Forsberg, C. F., Solheim, A., Elverhøi, A., Jansen, E., Channell, J. E. T. & Andersen, E. S. 1999: The depositional environment of the western Svalbard margin during the Late Pliocene and Pleistocene: Sedimentary facies changes at site 986. *In* Raymo, M. E., Jansen, E., Blum, P. & Herbert, T. D. (eds.): *Proceedings of the Ocean Drilling Program, Scientific Results*, 233-246. Friesens, Canada.

Funder, S., Demidov, I. & Yelovicheva, Y. 2002: Hydrography and mollusc faunas of the Baltic and the White Sea-North Sea seaway in the Eemian. *Palaeogeography, Palaeoclimatology, Palaeoecology 184*, 275-304.
Gabrielsen, R. H., Færseth, R. B., Jensen, L. N., Kalheim, J. E. & Riis, F. 1990: Structural elements of the Norwegian continental shelf. Part I: The Barents Sea Region. *NPD Bulletin 6*, 33 pp.
Gataullin, V., Polyak, L., Epstein, O. & Romanyuk, B. 1993: Glacigenic deposits of the Central Deep: a key to the Late Quarternary evolution of the eastern Barents Sea. *Boreas 22*, 47-58.
Gataullin, V. & Polyak, L. 1997: Morainic ridge complex, eastern Barents Sea. *In* Davies, T. A., Bell, T., Cooper Alan, K., Josenhans, H., Polyak, L., Solheim, A., Stoker, M. & Stravers, J. A. (eds.): *Glaciated continental margins: An atlas of acoustic images*, 82-83. Chapman & Hall, London.
Gataullin, V., Mangerud, J. & Svendsen, J. I. 2001: The extent of the Late Weichselian ice sheet in the southeastern Barents Sea. *Global and Planetary Change 31*, 453-474.
Grosswald, G. 1993: Extent and melting history of the Late Weichselian Ice Sheet, the Barents-Kara Continental Margin. *In* Peltier, W. R. (ed.): *Ice in the Climate System*, 1-20. Springer-Verlag, Berlin.
Grosswald, M. G. 1980: Late Weichselian ice sheet of northern Eurasia. *Quaternary Research 13*, 1-32.
Hjelstuen, B. O., Elverhøi, A. & Faleide, J. I. 1996: Cenozoic erosion and sediment yield in the drainage area of the Storfjorden Fan. *Global and Planetary change 12*, 95-117.
Houmark-Nielsen, M., Demidov, I., Funder, S., Grosfjeld, K., Kjær, K. H., Larsen, E., Lavrova, N., Lysa, A. & Nielsen, J. K. 2001: Early and middle Valdaian glaciations, ice-dammed lakes and periglacial interstadials in Northwest Russia; new evidence from the Pyoza River area. *Global and Planetary Change 31*, 215-237.
Jansen, E., Bleil, U., Henrich, R. & Slettemark, B. 1988: Paleoenvironmental changes in the Norwegian sea and the Northeast Atlantic during the last 2.8 Ma: DSDP/ODP Sites 610, 642, 643 and 644. *Paleoceanography 3*, 563-581.
Jansen, E., Raymo, M. E. & Blum, P. 1996: The Leg 162 Shipboard Scientific Party. *Proceedings of the Ocean Drilling Program, Initial Reports 162*, 1182 pp.
Kjær, K. H. 2001: Nordrusland - et krydsfelt for Istidens gletschere og nutidens kvartærgeologer. *Varv 1*,
Kjær, K. H., Demidov, I., Houmark-Nielsen, M. & Larsen, E. 2001: Distinguishing between tills from Valdaian ice sheets in the Arkhangelsk region, Northwest Russia. *Global and Planetary Change 31*, 201-214.
Kjær, K. H., Demidov, I. N., Larsen, E., Murray, A. & Nielsen, J. K. 2003: Mezen Bay - a key area for understanding Weichselian glaciations in northern Russia. *Journal of Quaternary Science 18*, 73-93.
Kleiber, H. P., Knies, J. & Niessen, F. 2000: The Late Weichselian glaciation of the Franz Victoria Trough, northern Barents Sea: ice sheet extent and timing. *Marine Geology 168*, 25-44.
Knies, J., Nowaczyk, N., Mueller, C., Vogt, C. & Stein, R. 2000: A multiproxy approach to reconstruct the environmental changes along the Eurasian continental margin over the last 150 000 years. *Marine Geology 163*, 317-344.
Knutsen, S.-M., Richardsen, G. & Vorren, T. O. 1992: Late Miocene-Pleistocene sequence stratigraphy and mass-movements on the western Barents Sea margin. *In* Vorren, T. O., Bergsaker, E., Dahl-Stamnes, Ø. A., Holter, E., Lie, E., Johansen, B. & Lund, T. B. (eds.): *Arctic Geology and Petroleum Potential*, 573-607. Elsevier, Amsterdam.
Laberg, J. S. & Vorren, T. O. 1995: The Middle and Late Pleistocene evolution of the Bear Island Trough Mouth Fan. *Global and Planetary Change 316*, 1-22.
Landvik, J. Y., Bondevik, S., Elverhøi, A., Fjeldskaar, W., Mangerud, J., Salvigsen, O., Siegert, M. J., Svendsen, J. I. & Vorren, T. O. 1998: The last glacial maximum of Svalbard and the Barents Sea area: Ice sheet extent and configuration. *Quaternary Science Reviews 17*, 43-75.
Larsen, E., Funder, S. & Thiede, J. 1999a: Late Quaternary history of northern Russia and adjacent shelves - a synopsis. *Boreas 28*, 6-11.
Larsen, E., Lysså, A., Demidov, I., Funder, S., Houmark-Nielsen, M., Kjær, K. H. & Murray, A. S. 1999b: Age and extent of the Scandinavian ice sheet in northwest Russia. *Boreas 28*, 115-132.
Lebesbye, E. 2000: *Late Cenozoic glacial history of the southwestern Barents Sea*. Doctor thesis, University of Tromsø, pp.
Lysså, A., Demidov, I., Houmark, N. M. & Larsen, E. 2001: Late Pleistocene stratigraphy and sedimentary environment of the Arkhangelsk area, Northwest Russia. *Global and Planetary Change 31*, 179-199.
Mangerud, J., Dokken, T., Hebbeln, D., Heggen, B., Ingolfsson, O., Landvik, J. Y., Mejdahl, V., Svendsen, J. I. & Vorren, T. O. 1998: Fluctuations of the Svalbard-Barents Sea Ice Sheet during the last 150 000 years. *Quaternary Science Reviews 17*, 11-42.
Mangerud, J., Astakhov, V., Jakobsson, M. & Svendsen, J. I. 2001: Huge Ice-age lakes in Russia. *Journal of Quaternary Science 16*, 773-777.
Musatov, E. E. & Romashchenko, O. G. 2003: Geomorphology; late Cenozoic evolution and neotectonics of the Novaya Zemlya shelf; implications for its oil-gas-bearing prospects. *Oceanology 43*, 276-284.

Möller, P., Bolshiyanov, D. Y. & Bergsten, H. 1999: Weichselian geology and palaeoenvironmental history of the central Taymyr Peninsula, Siberia, indicating no glaciation during the last global glacial maximum. *Boreas 28*, 92-114.

Nyland, B., Jensen, L. N., Skagen, J., Skarpnes, O. & Vorren, T. 1992: Tertiary Uplift and Erosion in the Barents Sea: Magnitude, Timing and Consequences. *In* Larsen, R. M., Brekke, H., Larsen, B. T. & Talleraas, E. (eds.): *Structural and Tectonic Modelling and its Application to Petroleum Geology*, 153-162. Elsevier, Amsterdam.

Ottesen, D., Dowdeswell, J. A., Rise, L., Rokoengen, K. & Henriksen, S. 2002: Large-scale morphological evidence for past ice-stream flow on the mid-Norwegian continental margin. *In* Dowdeswell, J. A. & Ó Cofaigh, C. (eds.): *Glacier-Influenced Sedimentation on High-Latitude Continental Margins*, 245-258. Geological Society, London, Special Publications,

Pavlidis, Y. A., Dunaev, N. N., Nikiforov, S. L. & Artem, e. A. V. 2002: Underwater terraces of the Pechora Sea. *Oceanology 42*, 845-851.

Polyak, L., Levitan, M. A., Gataullin, V., Khusid, T., Mikhailov, V. & Mukhina, V. 2000: The impact of glaciation, river-discharge and sea-level change on late Quaternary environments in the southwestern Kara Sea. *International Journal of Earth Sciences 89*, 550-562.

Rafaelsen, B., Andreassen, K., Kuilman, L. W., Lebesbye, E., Hogstad, K. & Midtbø, M. 2002: Geomorphology of buried glacigenic horizons in the Barents Sea from three-dimensional seismic data. *In* Dowdeswell, J. A. & Ó Cofaigh, C. (eds.): *Glacier-Influenced Sedimentation on High-Latitude Continental Margins*, 259-276.

Rasmussen, E. & Fjeldskaar, W. 1996: Quantification of the Pliocene-Pleistocene erosion of the Barents Sea from present-day bathymetry. *Global and Planetary Change 12*, 119-133.

Raymo, M. E., Ruddiman, W. F., Backman, J., Clement, B. M. & Martinson, D. G. 1989: Late Pliocene variation in northern hemisphere ice sheets and North Atlantic deep water ciruculation. *Paleoceanography 4*, 413-446.

Raymo, M. E. 1992: Global climate change: A three million year perspective. *In* Kukla, G. J. & Went, E. (eds.): *Start of a glaciation*, 207-223. Springer-Verlag, Berlin.

Richardsen, G., Knutsen, S.-M., Vail, P. R. & Vorren, T. O. 1992: Mid-late Miocene sedimentation on the southwestern Barents shelf margin. *In* Vorren, T. O., Bergsaker, E., Dahl-Stamnes, Ø. A., Lie, E., Johansen, B. & Lund, T. B. (eds.): *Arctic Geology and Petroleum Potential*, 539-572. Elsevier, Amsterdam.

Ruddiman, W. F., Raymo, M. E., Martinson, D. G., Clement, B. M. & Backman, J. 1989: Pleistocene evolution: Northern hemisphere ice sheets and North Atlantic Ocean. *Paleoceanography 4*, 353-412.

Ryseth, A., Augustson, J. H., Charnock, M., Haugerud, O., Knutsen, S.-M., Midbøe, P. S., Opsal, J. G. & Sundsbø, G. 2003: Cenozoic stratigraphy and evolution of the Sørvestsnaget Basin, southwestern Barents Sea. *Norwegian Journal of Geology 83*, 107-130.

Sejrup, H. P., Nagy, J. & Brigham-Grette, J. 1989: Foraminiferal stratigraphy and amino acid geochronology of interglacial and glacial sediments in the Norwegian Channel, northern North Sea. *Norsk Geologisk Tidsskrift 69*, 111-124.

Shackleton, N. J., Backman, J., Zimmerman, H., Kent, D. V., Hall, M. A., Roberts, D. G., Schnitker, D., Baldauf, J. G., Despraires, A., Homrighausen, A., Huddlestun, P., Keene, J. B., Kaltenback, A. J., Krumsiek, K. A. O., Morton, A. C., Murray, J. W. & Westberg-Smith, J. 1984: Oxygen isotope calibration of the onset of ice-rafting and history of glaciation in the North Atlantic region. *Nature 307*, 620-623.

Siegert, M. J., Dowdeswell, J. A., Hald, M. & Svendsen, J.-I. 2001: Modelling the Eurasian Ice Sheet through a full (Weichselian) glacial cycle. *Global and Planetary Change 31*, 367-385.

Siegert, M. J., Dowdeswell, J. A., Svendsen, J. I. & Elverhøi, A. 2002: The Eurasian Arctic during the last ice age. *American Scientist 90*, 32-39.

Solheim, A. & Kristoffersen, Y. 1984: The physical environment of the western Barents Sea, Map, 1:1,500,000: Sediments above the upper regional unconformity: Thickness, seismic stratigraphy and outline of the glacial history. *Nor. Polarinst. Skr. 179B*, 25 pp.

Solheim, A., Andersen, E. S., Elverhøi, A. & Fiedler, A. 1996: Late Cenozoic depositional history of the western Svalbard continental shelf, controlled by subsidence and climate. *Global and Planetary Change 12*, 135-148.

Solheim, A., Faleide, J. I., Andersen, E. S., Elverhøi, A., Forsberg, C. F., Vanneste, K., Uenzelmann-Neben, G. & Channell, J. E. T. 1998: Late Cenozoic seismic stratigraphy and glacial geological development of the East Greenland and Svalbard-Barents Sea continental margins. *Quaternary Science Reviews 17*, 155-184.

Stokes, C. R. & Clark, C. D. 2002: Are long subglacial bedforms indicative of fast ice flow? *Boreas 31*, 239-249.

Svendsen, J. I., Alexanderson, H., Astakhov, V. I., Demidov, I., Dowdeswell, J. A., Funder, S., Gataullin, V., Henriksen, M., Hjort, C., Houmark-Nielsen, M., Hubberten, H. W., Ingolfson, O., Jakobsson, M., Kjær, K. H., Larsen, E., Lokrantz, H., Lunkka, J. P., Lysså, A., Mangerud, J., Matiouchkov, A., Murray, A. S., Möller,

P., Niessen, F., Nikolskaya, O., Polyak, L., Saarnisto, M., Siegert, C., Siegert, M. J., Spielhagen, R. & Stein, R. in press: Late Quaternary ice sheet history of the northern Eurasia. *Quaternary Science Reviews*

Sættem, J. 1990: Glaciotectonic forms and structures on the Norwegian continental shelf: observations, processes and implications. *Norsk Geologisk Tidsskrift 70*, 81-94.

Sættem, J., Poole, D. A. R., Sejrup, H. P. & Ellingsen, L. 1991: Glacial geology of outer Bjørnøyrenna, western Barents Sea: preliminary results. *Norsk Geologisk Tidsskrift 71*, 173-177.

Sættem, J., Poole, D. A. R., Ellingsen, K. L. & Sejrup, H. P. 1992: Glacial geology of outer Bjørnøyrenna, southwestern Barents Sea. *Marine Geology 103*, 15-51.

Sættem, J., Bugge, T., Fanavoll, S., Goll, R. M., Mørk, A., Mørk, M. B. E., Smelror, M. & Verdenius, J. G. 1994: Cenozoic margin development and erosion of the Barents Sea: Core evidence from southwest of Bjørnøya. *Marine Geology 118*, 257-281.

Telnæs, N., Augustson, J. H., Elvebakk, G., Bugge, T. & Haugerud, O. 2002: The main petroleum systems of the southwestern Barents Sea, Murmansk.

Thiede, J., Eldholm, O. & Taylor, E. 1989: Variability of Cenozoic Norwegian-Greenland Sea paleoceanography and northern hemisphere paleoclimate. *Proceedings of the Ocean Drilling Program, Scientific Results* 1067-1118.

Velichko, A. A. 1987: The current state of the concepts of global glaciations. *Polar Geography and Geology 11*, 164-183.

Velichko, A. A., Faustova, M. A., Gribchenko, Y. N., Pisareva, V. V. & Sudakova, N. G. in press: Glaciations of the East European Plain - distribution and chronology. *In* Ehlers, J. & Gibbard, P. L. (eds.): *Quaternary Glaciations - Extent and Chronology*, Elsevier, Amsterdam.

Vorren, T. O. & Kristoffersen, Y. 1986: Late Quarternary glaciation in the south-western Barents Sea. *Boreas 15*,

Vorren, T. O., Lebesbye, E. & Larsen, K. B. 1990: Geometry and Genesis of the glacigenic sediments in the southern Barents Sea. *In* Dowdeswell, J. A. & Scourse, J. D. (eds.): *Glacimarine Environments: Processes and Sediments*, 309-328. Geol.Soc. Spec. Publ., London.

Vorren, T. O., Richardsen, G., Knutsen, S.-M. & Henriksen, E. 1991: Cenozoic erosion and sedimentation in the western Barents Sea. *Marine and Petroleum Geology 8*, 317-340.

Vorren, T. O. & Laberg, J. S. 1996: Late glacial air temperature, oceanographic and ice sheet interactions in the southern Barents Sea region. *In* Andrews, J. T., Austin, W. E. N., Bergsten, H. & Jennings, A. E. (eds.): *Late Quarternary Palaeoceanography of the North Atlantic Margins*, 303-321. Geological Society Special Publication,

Vorren, T. O. & Laberg, J. S. 1997: Trough Mouth Fans - Palaeoclimate and ice-sheet Monitors. *Quaternary Science Reviews 16*, 865-882.

Appendix

Chronology and correlations in the Barents Sea

R7 – R1

ODP Site 986 west of Svalbard (Fig. 5.2) is a key borehole for age constrains of the seismic stratigraphy of the western Barents Sea - Svalbard margin. Age estimates for this site have been made using paleomagnetic data (Channell *et al.* 1999), biostratigraphic data (Eidvin & Nagy 1999) and Sr-isotope analysis correlation (Forsberg *et al.* 1999), and from additional analysis of the data by Butt *et al.* (2000) (Table A2). It is, however, a problem that linearly interpolation between paleomagnetic data over relatively long time spans was the only means for estimating ages for several of the main seismic reflectors. Because of the debris flow origin of a major part of the sediments, however, any interpolation is very uncertain. Most likely the deposition occurred in a stepwise manner, with rapid emplacement of debris flow deposits and longer periods dominated by hemipelagic deposition, as is also indicated by the grain-size distribution record. A discrepancy between one of the biostratigraphic age-estimates and the paleomagnetic/Sr-data is not understood (Butt *et al.* 2000). All age estimates are summarised in Table A2.

Additional chronological constraints on the stratigraphy are added by biostratigraphic data from exploration wells (Eidvin *et al.* 1993; Eidvin *et al.* 1998; Eidvin *et al.* 2000; Ryseth *et al.* 2003) and information from shallow borings (Sættem *et al.* 1992; Sættem *et al.* 1994). The biostratigraphic data is often retrieved from drill cuttings, where cave-in adding younger material to the samples may be a problem. It is also problematic that the glacigenic sediments often contain large amounts of older reworked material.

R7: Interpolating linearly between the maximum age of 2.6 Ma at the base of ODP Site 986 hole and the base of the Olduvai paleomagnetic event gives a tentative age of **2.3–2.5** Ma for R7, supported by biostratigraphic and Sr. data (Butt *et al.* 2000). Although uncertain, this is compatible with age estimates of 2.3–2.5 Ma from seismic correlation to commercial wells in the southwestern Barents Sea (Faleide *et al.* 1996).

R6 and R5 are assigned interpolated ages of **1.6-1.7 Ma** and **1.3-1.5 Ma** respectively at Site 986, both supported by biostratigraphic and Sr. data (Butt *et al.* 2000). Faleide *et al.* (1996) suggested a likely age of about 1.0 Ma for R5. This sequence boundary was interpreted to represent a hiatus resulting from the most significant change in sedimentation patterns during the R7-R1 time. The erosion was suggested result from increased glacial activity on the shelf, and correlated to increased amounts of IRD and oxygen- isotope measurements showing a shift in climatic cyclicity and amplitudes in the time period 1.2-0.8 Ma (Shackleton *et al.* 1984; Jansen *et al.* 1988; Raymo *et al.* 1989; Ruddiman *et al.* 1989; Thiede *et al.* 1989).

R4 and R3 are given respective age estimates 0.99 Ma and 0.78 Ma from paleomagnetic data, whereas **R2** is assigned the interpolated, biostratigraphically supported age of **0.5 Ma**, all from ODP Site 986 data.

R1 is, based on amino acid analyses Sættem *et al.* (1992) indicated to be younger than 440 ka. Extrapolation of calculated sedimentation rates in piston cores on the Svalbard margin has given an approximate age of 200 ka in this area (Elverhøi *et al.* 1995). R1 thus has a likely age **between 440 ka and 200 ka**.

Reflectors younger than R1

Age estimates of the post R1 sequence (Table A1) from Sættem *et al.* (1992) are based on magneto-, bio-, and amino-stratigraphic mapping of borehole 7317/10-U-01, and correlation of the lower part of Unit E with Eemian sediments in the Norwegian trench (Sejrup *et al.* 1989), which provides maximum ages as the fossils may be reworked. The age estimates of Laberg & Vorren (1995) are based on uncertain correlation of debris flow on the Bear Island Fan with the deep sea stratigraphy.

Table A1. Correlation of seismic sequences along the western Barents Sea – Svalbard margin with suggested ages for the main sequence boundaries, and comparison with previously published stratigraphies.

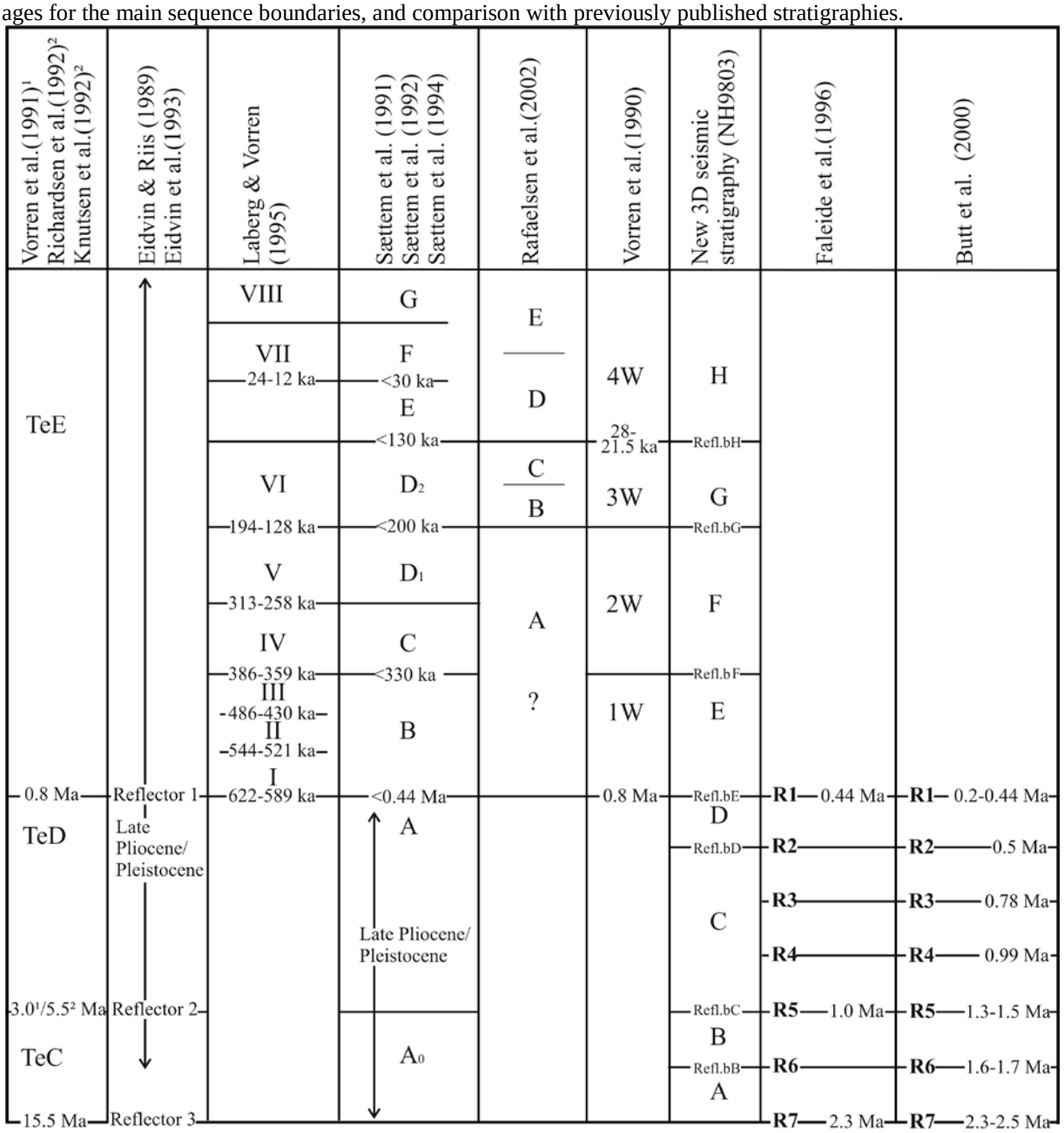

Table A2. Results from ODP Site 986 west of Svalbard. The ages assigned to reflectors R7-R1. Supporting evidence from other sources is indicated in brackets. In addition, the seismic, lithological and geotechnical subdivisions of the Site 986 succession by Jansen *et al.* (1996) are shown along with the corresponding acoustic, lithological and physical properties used for each classification. From Butt *et al.*(2000).

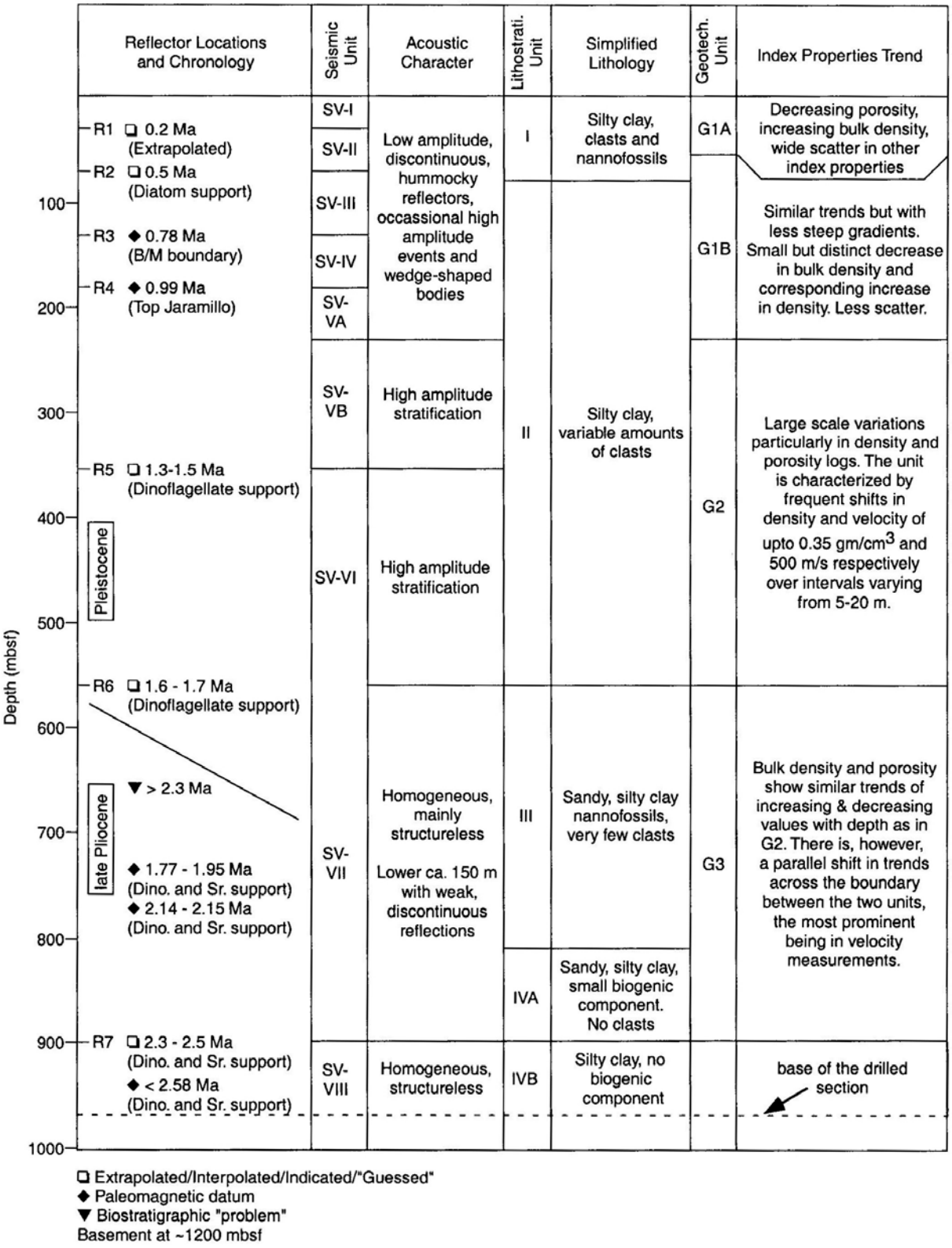

Table A3. Observed relative sea-level elevations from interglacials/interstadials older than the Last Glacial Maximum.

Previous glaciation	Location	Sea level (m a.s.l.)	Inferred age (ka)	Type	Reference
Saale	Kanin Peninsula	137	Eem	Tidal sediments	Funder (Unpublished)
Saale	Kola Peninsula	100	Eem		Svendsen *et al* (in press)
Saale	Arkhangelsk region	70	Eem		Svendsen *et al* (in press)
Saale	Pechora lowland	60	Eem		Svendsen *et al* (in press)
Saale	Central Taimyr (Siberia)	>100	Eem		Svendsen *et al* (in press)
Early Weichselian /Saalian	Central Prins Karls Forland (Svalbard)	36-65	80±10 130 ka	Beach deposits covered by till	Andersson *et al.* (1999)
Early Weichselian	Taymyr Peninsula (Siberia)	100	Early Weichselian	Delta	Möller *et al.* (1999)
Early/Middle Weichselian	Severnaya Zemlya	120	Early/Middle Weichselian	Shorelines	Bolshiyanov & Makeyev (1995)
Early Weichselian	Central Prins Karls Forland (Svalbard)	36-65	70±10	Beach deposits covered by till	Andersson *et al.* (1999)
Middle Weichselian	Linnedalen (Svalbard)	87	>36	Terrace covered by till	Mangerud *et al.* (1998)
Middle/Early Weichselian	Mezen and Chyorskaya bays (Arkhangelsk region)	50	65	Subtidal sediments	Jensen & Larsen (in prep), Kjær *et al.* (2003)
	Northern Prins Karls Forland (Svalbard)	60	Ca. 70±10	Beach deposits covered by till	Andersson *et al.* (2000)
	Nordenskiöld Bay (Novaya Zemlya)	≥50	>26	Beach deposits covered by till	Forman *et al.* (1999)
LGM	Novaya Zemlya, west coast	11±1	5-6 (Holocene)	Beach	Forman *et al.* (1999)
LGM	Novaya Zemlya, east coast	18±2	5-6 (Holocene)	Beach	Forman *et al.* (1999)
LGM	Kirkenes (Norway)	90	10 ^{14}C	Isolation-basin	Corner *et al.* (1999)